



Department of Medicine

Evans Days

October 7-8, 2021

WILKINS VISITING PROFESSOR LECTURE

Drew Weissman, MD, PhD

Professor of Medicine
Perelman School of Medicine
University of Pennsylvania
BUSM Distinguished Alumnus

“Nucleoside-modified mRNA-LNP Therapeutics.”

INGELFINGER VISITING PROFESSOR

Dale Abel, MD, PhD

Chair, Department of Medicine
Professor of Internal Medicine – Endocrinology & Metabolism
University of Iowa
Roy J. & Lucille A. Carver College of Medicine

*“(Glucose Metabolism) a Common Soil Linking Diabetes Mellitus,
Heart Failure and Cancer?”*



EVANS DEPARTMENT OF MEDICINE RESEARCH DAYS

SCHEDULE OF EVENTS

Thursday, October 7th

Oral Presentations

8:30am – 9:30am | ePosterBoards Platform

Research Poster Session

9:30am – 12:30pm | ePosterBoards Platform

Dr. Coleman interview Ingelfinger Professor, Dale Abel, MD, PhD

12:30pm – 1:00pm | ePosterBoards Platform

ARC Presentation

1:15pm – 2:15pm | ePosterBoards Platform

Wilkins Visiting Professor Lecture

3:00pm | ePosterBoards Platform

Drew Weissman, MD, PhD

Professor of Medicine, Perelman School of Medicine, University of Pennsylvania
BU Distinguished Alumnus

“Nucleoside-modified mRNA-LNP Therapeutics.”

Fireside Chats with the Distinguished Visitors

3:00pm

- Graduate Students and PostDocs meet with Dr. Weissman: [RSVP](#)
- URG Faculty and Trainees meet with Dr. Abel: [Zoom Link](#)

Friday, October 8th

Ingelfinger Visiting Professor Grand Rounds

Noon | Grand Rounds [Zoom Link](#)

Meeting ID: 945 5824 9649, Password: 447072

Dale Abel, MD, PhD

Chair, Department of Medicine, Professor of Internal Medicine – Endocrinology & Metabolism, University of Iowa
Roy J. & Lucille A Carver College of Medicine

“(Glucose Metabolism) a Common Soil Linking Diabetes Mellitus, Heart Failure and Cancer?”

EVANS DEPARTMENT OF MEDICINE RESEARCH DAYS

CHAIR AND COMMITTEE

Chair, Department of Medicine

David Coleman

Chair, Evans Days

David Salant

Blue Ribbon Panel

K. Alysandratos

Deborah Anderson

Sabrina Assoumou

Kathryn Bacon

Tracy Battaglia

Emelia Benjamin

Kimberly Bertrand

Tara Bouton

Carly Bridden

David Center

Barbara Corkey

Hollis Day

Gerald Denis

David Felson

Deepa Gopal

Valerie Gouon-Evans

Adam Gower

Elliott Hagedorn

Naomi Hamburg

Dooms Hans

Christopher Heaphy

Andrew Henderson

James Hudspeth

Christopher Heaphy

C. Robert Horsburgh, Jr.

Titi Ilori

Alice Jacobs

Yang Jin

Matthew Jones

Elizabeth Klings

Vijaya Kolachalama

Darrell Kotton

Sudhir Kumar

Gene Kwan

Rossana Lau-Ng

Anica Law

Sun Lee

Marc Lenburg

Adam Lerner

Giovanni Ligresti

Benjamin Linas

Michelle Long

Laura Lowery

Weining Lu

PJ Maglione

Sarah Mazzilli

Joseph Mizgerd

Stefano Monti

Lynn Moore

Gareth Morgan

Matthew Nayor

Julie Palmer

Vassiliki Pravodelov

Katya Ravid

Rick Ruberg

Manish Sagar

David Salant

Francesca Seta

J. Mark Sloan

Katie Steiling

Katrina Traber

Ashish Upadhyay

Kim Vanuytsel

Sushrut Waikar

Allan Walkey

Renda Weiner

Andrew Wilson

Huiping Zhang

Xiaoling Zhang

EVANS DEPARTMENT OF MEDICINE RESEARCH DAYS

HISTORY OF THE EVANS MEDICAL FOUNDATION

This year marks the 109th year of the Evans Department of Medicine. The Evans Department of Medicine began its activities in 1912. It was established by Maria Antoinette Evans, who made a series of gifts to the Massachusetts Homeopathic Hospital, now Boston Medical Center, to endow a research department of medicine, with the stipulation that research and teaching be intimately interrelated in the department. Although technically a separate research institute, the Evans Department has always functioned as an integral part of the clinical care and training programs of Boston Medical Center and the academic programs of the Department of Medicine at Boston University School of Medicine. Many of its research programs involve components at the hospital, the Medical School, and the Boston Veterans Administration Medical Center.

This year marks the 36th Evans Department of Medicine annual research celebration, which was established in 1985 to acknowledge and foster the research activities of the Evans Department of Medicine. A two-day period of academic activity will take place during which both the basic and clinical research accomplishments of the department are exhibited. In recognition of the distinguished past of the department as a training center for faculty and practitioners, we invite eminent clinical and basic scientists to share their scholarship and enlighten present trainees and faculty.

Poster presentations of ongoing research demonstrate our vigorous present and future. The two-day event features Distinguished Clinical and Basic Science Lectures (Ingelfinger Visiting Professor and Wilkins Visiting Professor respectively), which serve as touchstones of the excellence to which we all aspire.

EVANS DEPARTMENT OF MEDICINE RESEARCH DAYS SPEAKERS 1992-2021

	Ingelfinger Visiting Professor	Wilkins Visiting Professor
1992	Lawrence G. Raisz, MD	J. Michael Bishop, MD
1993	William G. Couser, MD	Robert J. Lefkowitz, MD
1994	Sheldon Greenfield, MD	Philip Leder, MD
1995	Marcia Angell, MD	Thomas P. Stossel, MD
1996	Jeffrey Glassroth, MD	Harold Varmus, MD
1997	Lee Goldman, MD	Phillip A. Sharp, PhD
1998	Andrew I. Schafer, MD	Mark Ptashne, PhD
1999	Jerome P. Kassirer, MD	Leroy Hood, MD, PhD
2000	Harold C. Sox, Jr., MD	James Wilson, MD, PhD
2001	Edward J. Benz, Jr., MD	Andrew Wyllie, FRS
2002	Ralph Horwitz, MD	Eric N. Olson, PhD
2003	Martin J. Blaser, MD	Stuart H. Orkin, MD
2004	Robert Moellering Jr., MD	Marc Kirschner, PhD
2005	Alan Fogelman, MD	Craig C. Mello, PhD
2006	Bradford C. Berk, MD, PhD	Richard P. Lifton, MD, PhD
2007	Nicholas F. LaRusso, MD	Elizabeth G. Nabel, MD
2008	Christine K. Cassel, MD	Stephen O’Rahilly, MD, FRS
2009	Talmadge E. King Jr., MD	David A. Flockhart, MD, PhD
2010	Richard Shannon, MD	Cynthia Kenyon, PhD
2011	William Bremner, MD, PhD	Richard Mulligan, PhD
2012	Joseph Loscalzo, MD, PhD	Aram Chobanian, MD
2013	Wendy Levinson, MD	Orian Shirihai, MD, PhD
2014	Christine A. Sinsky, MD, FACP	David A. Schwartz, MD
2015	David Johnson, MD, MACP, FASCO	Jennifer Lippincott-Schwartz, PhD
2016	John M. Carethers, MD	Glenn Dranoff, MD
2017	Nancy J. Cox, PhD	Katrina Armstrong, MD
2018	Gary V. Desir, MD	Gregg L. Semenza, MD, PhD
2019	Nancy Brown, MD	Aviv Regev, PhD
2020	Nakela Cook, MD, MPH	Elaine Fuchs, PhD
2021	Dale Abel, MD, PhD	Drew Weissman, MD, PhD

EVANS DEPARTMENT OF MEDICINE RESEARCH DAYS

CENTERS

Evans Center for Interdisciplinary Biomedical Research (ECIBR)

Boston University Interdisciplinary Biomedical Research Office (BU IBRO; www.bu.edu/research/ibro) creates opportunities for new interdisciplinary approaches to biomedical research and, in so doing, enhances the training experience at BU. It builds on the success of the Evans Center for Interdisciplinary Biomedical Research (ECIBR) at the Medical Campus, and was established under the auspices of the office of BU Vice President and Associate Provost for Research and the Department of Medicine.

Under the leadership of Katya Ravid, professor of medicine, biochemistry, biology and health sciences, IBRO and ECIBR collaborate with the Clinical & Translational Science Institute (CTS) to facilitate interdisciplinary basic research discovery across campuses. IBRO maintains mechanisms developed by the ECIBR, including grant support of Affinity Research Collaboratives (ARCs), workshops, and seminars aimed at creating innovative, interdisciplinary team science research.

How It All Fits Together: ECIBR (www.bumc.bu.edu/evanscenteribr) began on the Medical Campus, providing the groundwork and tools to facilitate biomedical team science. IBRO expands the reach of those efforts to the Charles River Campus, encouraging more robust collaboration across the University and inspiring initiatives that are larger in scope. ECIBR focused on investigator-initiated research topics within the medical campus, while IBRO develops cross-campus programs around research strengths at BU with the potential to develop into university-wide research initiatives and programs.

Center for Integrative Transdisciplinary Epidemiology (CITE)

The vision of CTE is to harness contemporary integrative epidemiological tools to better elucidate the multilevel determinants of health and disease in diverse populations in the community, in clinical setting and at the individual level, evaluate strategies for promoting and maintaining health and preventing and treating disease and strengthen teaching and building capacity in population health and epidemiological research.

The mission of CTE is to expand, refine and innovate the epidemiological methods and quantitative analysis of health measures to improve people's lives and to reduce inequalities in health.

We hope to achieve this transformative vision and mission by developing and facilitating highly collaborative translational and interdisciplinary epidemiological research that leverages and integrates large populations and well-defined clinical studies with high dimensional data via *methodological innovation and analysis, in part by combining cohort-based genomic, proteomic and other Omics research with personalized behaviorome and exposome and the phenome.*

EVANS DEPARTMENT OF MEDICINE RESEARCH DAYS

In addition, the CITE will provide education and practical hands-on training in integrative epidemiology and quantitative health sciences methods *to train the public health workforce and clinical investigators of the future* using its resident databases, clinical trials and cohort studies.

Leveraging our expertise in planning, recruiting cohorts and establishing an infrastructure for surveillance (of cohorts, registries, crowd-sourced patient groups) we hope to contribute to *new and future observational cohort studies and clinical trials at BUSM*.

The CITE will make initial investments in creating a valued resource in five thematic areas leveraging resources at BUSM and focusing on methodological innovation:

1. *Life course epidemiology creating supercohorts with extant and new data*
2. *Integrative approaches for personalized and public health epidemiology*
3. *Novel epidemiological designs and analytical methods suited for supercohorts*
4. *Designing synthetic and pragmatic clinical trials in key areas of disease burden*
5. *Health disparities research incorporating aforementioned themes*

Evans Center for Implementation and Improvement Sciences (CIIS)

The Boston University Department of Medicine Center for Implementation and Improvement Sciences (CIIS) is a methodological hub for the scientific evaluation of efforts to improve healthcare delivery that integrates key components of implementation and improvement sciences with a focus on care within safety net systems, especially including Boston Medical Center.

What are Implementation and Improvement Sciences?

- Implementation science seeks to understand the process of evidence uptake into clinical practice. Did people perform the new endeavor? Why or why not?
- Improvement science seeks to rigorously measure outcomes of efforts to improve healthcare delivery. Did the new endeavor measurably improve desirable outcomes?

Combining Implementation and Improvement Sciences allows CIIS to assist in the development and rigorous evaluation of endeavors that seek to improve the quality of healthcare, particularly related to care for the underserved. CIIS serves as a conduit to the free flow of ideas between clinicians, administrators and health services researchers in the Boston University community and beyond to facilitate improvement in care that not only measures internal program adherence, but also produces inferential and generalizable evaluations of healthcare delivery.

Specific objectives of CIIS are to:

1. Guide, support, and innovate design of projects that rigorously evaluate the effectiveness of efforts to implement healthcare system change.
2. Identify factors and strategies that accelerate the adoption and promote sustainability of effective healthcare interventions in safety net systems.
3. Educate faculty and trainees in Implementation and Improvement Sciences.
4. For more information, please visit our website: <http://sites.bu.edu/ciis/>

EVANS DEPARTMENT OF MEDICINE RESEARCH DAYS
TABLE OF CONTENTS

S Session 1 – Floor 1 Thursday 10/7 9:30 – 10:30 a.m.

- 90 METABOLIC REPROGRAMMING OF THE HEART BY SGLT2 INHIBITION**
Jordan Chambers, Dominique Croteau, Fuzhong Qin, Ivan Luptak, David Pimentel, Wilson Colucci.
Station # 1
- 80 DOWNREGULATED FLI1 IN SCLERODERMA MYELOID CELLS MAY CONTRIBUTE TO CARDIAC FIBROSIS VIA A GALECTIN-3/M-TOR DEPENDENT PATHWAY**
Fatima El adili, Mortada Najem, Maria Trojanowska, Andreea Bujor.
Station # 2
- 153 ANTI-B1 INTEGRIN ANTIBODY THERAPY FOR JAK2^{V617F+} MYELOPROLIFERATIVE NEOPLASMS**
Xiaosheng Yang, Katya Ravid, Shinobu Matsuura.
Station # 3
- 77 THE EFFECT OF SARS-COV-2 ON HEART MUSCLE CELLS: COMPARISON OF CULTURED CARDIOMYOCYTES AND SERUM OF COVID-19 PATIENTS**
Allyson Zheng, Dr. James Hamilton, PhD, Dr. Nasi Huang, MD, Dr. Mohsan Saeed, PhD, Dr. Manish Sagar, MD.
Station # 4
- 93 NEUTROPHILS PLAY A PIVOTAL ROLE IN OBESOGENIC DIET-INDUCED NON-ALCOHOLIC STEATOHEPATITIS**
Qiong Zhou, Youhua Wang, Michael Rigor, Indeevar Beeram, Zhen Jiang.
Station # 5
- 119 COMPARATIVE ANALYSIS OF CEREBROSPINAL FLUID MARKERS AND MULTIMODAL IMAGING IN PREDICTING ALZHEIMER'S DISEASE PROGRESSION**
Akshara Balachandra, Michael Romano, Xiao Zhou, Michalina Jadick, Shangran Qiu, Diya Nijhawan, Sang Chin, Rhoda Au, Vijaya Kolachalama.
Station # 6
- 44 GSTP1 AS A MEDIATOR OF IMMUNE RESPONSE IN BRONCHIAL PREMALIGNANT LESIONS**
Julia Camassola Breda, Carter Merenstein, Christopher Stevenson, Mary Reid, Avrum Spira, Marc Lenburg, Sarah Mazzilli, Jennifer Beane, Eric Burks.
Station # 7
- 88 SINGLE-NUCLEUS RNA-SEQ REVEALS CELLULAR HETEROGENEITY IN RARE LUNG CANCER HISTOLOGIES**
Darren Chiu, Morgan Thompson, Elizabeth Duffy, Eric Burks, Joshua Campbell, Sarah Mazzilli, Jennifer Beane.
Station # 8
- 105 BATCH EFFECT CORRECTION OF METAGENOMIC DATA USING COMBAT-SEQ**
Howard Fan, William Johnson, Jessica Petrick, Julie Palmer.
Station # 9

- 122 BAYESIAN STRUCTURE LEARNING FOR HIERARCHICAL REGULATORY NETWORKS**
Anthony Federico.
Station # 10
- 17 MULTI-MODAL MODELS FOR MUTATIONAL SIGNATURES**
Kelly Geyer, Masanao Yajima, Jonathan Huggins, Joshua Campbell.
Station # 11
- 75 CONAN:DIFFERENTIAL NETWORK CONNECTIVITY ANALYSIS**
Lina Kroehling, Oluwatosin Olayinka, Samantha Clayton, Anthony Federico,
Eric Reed, Gary Benson, Stefano Monti.
Station # 12
- 167 HEMATOPOIETIC MOSAIC CHROMOSOMAL ALTERATIONS IN THE NEW ENGLAND CENTENARIAN STUDY.**
Anastasia Leshchik.
Station # 13
- 103 DIFFERENTIAL REGULATION ANALYSIS QUANTIFIES MIRNA REGULATORY ROLES AND MOLECULAR SUBTYPE-SPECIFIC TARGETS**
Boting Ning, Jennifer Beane, Marc Lenburg.
Station # 14
- 84 ANALYSIS OF LONGITUDINAL NASOPHARYNGEAL MICROBIOME PATTERNS IN MATERNALLY HIV-EXPOSED AND UNEXPOSED INFANTS IN ZAMBIA**
Aubrey Odom.
Station # 15

Session 1 – Floor 2 Thursday 10/7 9:30 – 10:30 a.m.

- 97 IL-23 SIGNALING IN EARLY STAGE LUNG CANCERS**
Roxana Pfefferkorn, Emily Green, Eric Burks, Jennifer Beane, Sarah Mazzilli.
Station # 1
- 132 IMMUNE CHARACTERIZATION IN BRONCHIAL PREMALIGNANT LESIONS USING SCRNASQ**
Conor Shea, Ipsita Dey-Guha, Avrum Spira, Mary Reid, Marc Lenburg, Sam Janes, Jennifer Beane, Sarah Mazzilli, Joshua Campbell.
Station # 2
- 127 USING DEEP LEARNING TO CHARACTERIZE PATHOLOGY IMAGES OF BRONCHIAL PREMALIGNANT LESIONS**
Divya Venkatraman, Rushin Gindra, Emily Green, Sarah Mazzilli, Eric Burks, Vijaya Kolachalama, Jennifer Beane.
Station # 3
- 134 INTERACTIVE ANALYSIS OF SINGLE-CELL RNA-SEQUENCING DATA WITH SINGLE-CELL TOOLKIT (SCTK)**
Yichen Wang.
Station # 4
- 23 IMMUNOPHENOTYPING EARLY STAGE LUNG ADENOCARCINOMAS(LUAD) USING IMAGING MASS CYTOMETRY**
Zhanhao Xi, Roxana Pfefferkorn, Eric Burks, Jennifer Beane, Sarah Mazzilli.
Station # 5

- 20 DETECTION OF DEMENTIA ON RAW VOICE RECORDINGS USING DEEP LEARNING**
Chonghua Xue, Cody Karjadi, Ioannis Paschalidis, Rhoda Au, Vijaya Kolachalama.
Station # 6
- 69 AN INDUCED PLURIPOTENT STEM CELL BASED MODEL TO STUDY LUNG MESENCHYME DEVELOPMENT AND DISEASE**
Andrea Alber, Liang Ma, Hector Marquez, Carlos Villacorta-Martin, Jonathan Lindstrom-Vautrin, Laertis Ikonou, Darrell Kotton.
Station # 7
- 140 PATIENT-SPECIFIC IPSCS CARRYING AN *SFTPC* MUTATION REVEAL THE INTRINSIC ALVEOLAR EPITHELIAL DYSFUNCTION AT THE INCEPTION OF INTERSTITIAL LUNG DISEASE**
Konstantinos Alysandratos, Scott Russo, Anton Petcherski, Evan Taddeo, Rebeca Acín-Pérez, Carlos Villacorta-Martin, J. C. Jean, Surafel Mulugeta, Luis Rodriguez, Benjamin Blum, Ryan Hekman, Olivia Hix, Kasey Minakin, Marall Vedaie, Seunghyi Kook, Andrew Tilston-Lunel, Xaralabos Varelas, Jennifer Wambach, F. Cole, Aaron Hamvas, Lisa Young, Marc Liesa, Andrew Emili, Susan Guttentag, Orian Shirihai, Michael Beers, Darrell Kotton.
Station # 8
- 89 A MULTIMODAL IPSC PLATFORM FOR CYSTIC FIBROSIS DRUG TESTING**
Andrew Berical.
Station # 9
- 39 GENERATION OF HUMAN ALVEOLAR EPITHELIAL TYPE I CELLS FROM PLURIPOTENT STEM CELLS**
Claire Burgess, Carlos Villacorta-Martin, Xaralabos Varelas, Darrell Kotton.
Station # 10
- 101 MULTI-MODAL CHARACTERIZATION OF THE PERIPHERAL BLOOD OF CENTENARIANS AT SINGLE CELL RESOLUTION REVEALS A DISTINCT IMMUNE CELL TYPE COMPOSITION AND TRANSCRIPTIONAL SIGNATURE OF EXTREME LONGEVITY**
Todd Dowrey, Tanya Karagiannis, Carlos Villacorta Martin, Paola Sebastiani, Stefano Monti, Thomas Perls, George Murphy.
Station # 11
- 52 HORMONE THERAPY TO ACCELERATE REGENERATION FROM SEXUALLY DIMORPHIC ACETAMINOPHEN-INDUCED LIVER INJURY**
Elissa Everton, Carlos Villacorta-Martin, Jonathan Lindstrom-Vautrin, Fatima Rizvi, Valerie Guon-Evans.
Station # 12
- 151 PSC-DERIVED ORGANOID BASED MODEL OF INTESTINAL FILOVIRUS INFECTION**
Elizabeth Yvonne Flores, Elke Mühlberger, Gustavo Mostoslavsky.
Station # 13

135 HIPSC-DERIVED NEURONS FROM CJD INDIVIDUALS WITH THE E200K MUTATION RECAPITULATE PATHOLOGICAL HALLMARKERS OF THE DISEASE

Aldana Gojanovich, Nhat Le, Robert Mercer, David Harris, Gustavo Mostoslavsky.
Station # 14

141 NOTCH ACTIVATION DURING MESODERM INDUCTION MODULATES EMERGENCE OF THE T/NK CELL LINEAGE FROM HUMAN IPSC.

Dar Heinze, Seonmi Park, Andrew McCracken, Mona Haratianfar, Jonathan Lindstrom-Vautrin, Carlos Villacorta-Martin, Aditya Mithal, George Murphy, Gustavo Mostoslavsky.
Station # 15

Session 1 – Floor 3 Thursday 10/7 9:30 – 10:30 a.m.

70 TRANSPLANTATION OF MURINE PLURIPOTENT STEM CELL DERIVED DISTAL TIP-LIKE CELLS INTO IMMUNOCOMPETENT MICE

Michael Herriges, Carlos Villacorta-Martin, Darrell Kotton.
Station # 1

60 MECHANISMS OF SELF-RENEWAL OF IPSC-DERIVED ALVEOLAR EPITHELIAL TYPE 2 CELLS

Jessie Huang, Carlos Villacorta-Martin, Darrell Kotton.
Station # 2

157 CHARACTERIZING AATD ASSOCIATED METABOLIC DYSREGULATION IN SYNGENEIC PATIENT IPSCS

Joseph Kaserman, Feiya Wang, Jonathan Lindstrom-Vautrin, Carlos Villacorta-Martin, Andrew Wilson.
Station # 3

115 UTILIZING THE IPSC DIRECTED DIFFERENTIATION PLATFORM TO IDENTIFY DOSE AND STAGE DEPENDENT ROLES OF BMP, TGF- β AND RETINOIC ACID SIGNALING IN LUNG PROGENITOR SPECIFICATION

Jake Le Suer.
Station # 4

45 REGENERATION OF MOUSE TRACHEAL EPITHELIUM VIA SYNGENEIC TRANSPLANTATION OF PLURIPOTENT STEM CELL-DERIVED BASAL-LIKE CELLS

Liang Ma, Bibek Thapa, Michael Herriges, Jonathan Lindstrom-Vautrin, Carlos Villacorta-Martin, Darrell Kotton.
Station # 5

146 DEFINING NKX2-1-DEPENDENT TRANSCRIPTOMIC SIGNATURES IN LUNG DEVELOPMENT

Taylor Matte, Mary Lou Beermann, JC Jean, Jonathan Lindstrom-Vautrin, Jonathan Lindstrom-Vautrin, Carlos Villacorta Martin, Jake LeSuer, Andrew Berical, Darrell Kotton, Finn Hawkins.
Station # 6

- 117 DERIVATION OF THYROID PROGENITORS FROM HUMAN INDUCED PLURIPOTENT STEM CELLS**
Alberto Posabella, Hendrik Undeutsch, Andrea Alber, Anita Kurmann, Anthony Hollenberg, Darrell Kotton.
Station # 7
- 59 VEGFA INDUCES CHOLANGIOCYTE DRIVEN LIVER REGENERATION IN MOUSE MODELS OF LIVER INJURY**
Fatima Rizvi, Elissa Everton, Valerie Gouon Evans.
Station # 8
- 148 MODELING COLORECTAL CANCER INITIATION USING HUMAN IPSC-DERIVED INTESTINAL ORGANOIDS**
Victor Schingo, Andrew McCracken, Dar Heinze, Aditya Mithal, Gustavo Mostoslavsky.
Station # 9
- 47 MULTIMODULAR APPROACH TO IMPROVE HEPATOCYTE TRANSPLANTATION TO TREAT ALPHA-1 ANTITRYPSIN DEFICIENCY ASSOCIATED LIVER DISEASE**
Anna Smith, Hua Liu, Valerie Gouon-Evans.
Station # 10
- 43 UNDERSTANDING CELL STATE CHANGES IN MURINE ADULT LUNG FOLLOWING PNEUMONECTOMY INJURY**
Bibek Thapa, Jason Rock, Darrell Kotton.
Station # 11
- 99 MULTI-MODAL PROFILING OF HUMAN FETAL LIVER HEMATOPOIETIC STEM CELLS REVEALS THE MOLECULAR SIGNATURE OF ENGRAFTMENT**
Kim Vanuytsel, Carlos Villacorta-Martin, Jonathan Lindstrom-Vautrin, Zhe Wang, Wilfredo Garcia-Beltran, Vladimir Vbranac, Dylan Parsons, Evan Lam, Taylor Matte, Todd Dowrey, Sara Kumar, Mengze Li, Gustavo Mostoslavsky, Ruben Dries, Joshua Campbell, Anna Belkina, Alejandro Balazs, George Murphy.
Station # 12
- 79 APPLYING CRISPR IN IPSC-DERIVED ALVEOLAR EPITHELIAL CELLS TO INTERROGATE COPD GWAS**
Rhiannon Werder, Michael Cho, Xiaobo Zhou, Darrell Kotton, Andrew Wilson.
Station # 13
- 109 DE NOVO HEMATOPOIESIS FROM THE FETAL LUNG**
Anthony Yeung, Carlos Villacorta-Martin, Jonathan Lindstrom-Vautrin, Anna Belkina, Kim Vanuytsel, Vladimir Vbranac, Alejandro Balazs, George Murphy.
Station # 14
- 142 IDENTIFYING BIOMARKERS FOR INFLAMMATORY BOWEL DISEASE USING EXTRACELLULAR VESICLES**
Kanchana Ayyar, Ria Shah, Alan Moss.
Station # 15

Session 1 – Floor 4 Thursday 10/7 9:30 – 10:30 a.m.

- 50 THE CROSS-SECTIONAL ASSOCIATION BETWEEN HEPATIC STEATOSIS AND SARCOPENIA: THE FRAMINGHAM HEART STUDY**
Max Rosenthaler, Sarah Altajar, Na Wang, Joanne Murabito, Michelle Long.
Station # 1

- 197 PURIFICATION OF EXOSOMES FROM INTRALUMINAL FLUIDS FOR THE STUDY OF IBD**
Sarah Watanabe, Alan Moss, Carla Mazzeo.
Station # 2
- 191 ASSOCIATION BETWEEN HEAVY ALCOHOL CONSUMPTION AND TRIMETHYLAMINE N-OXIDE**
Samuel Mensah, Debbie Cheng, Matthew Freiberg, Vladimir Palatkin, Gregory Patts, Sally Bendiks, Elena Blokhina, Natalia Gnatienco, Hilary Tindle, Sonam Tandon, Dmitry Lioznov, Jeffrey Samet, Kaku So-Armah.
Station # 3
- 184 REDUCED ALCOHOL CONSUMPTION AND CHANGE IN RELATIVE ABUNDANCE OF *BUTYRATE KINASE (BUK)* GENE IN GUT MICROBIOME OF PEOPLE WITH HIV (PWH)**
Sonam Tandon, Richa Singhal, Shirish Barve, Gregory Patts, Samuel Mensah, Matthew Freiberg, Jeffrey Samet, Kaku So-Armah.
Station # 4
- 166 ASSEMBLING 2D SLICES INTO 3D SPATIAL TRANSCRIPTOMICS DATASETS**
George Chen, Liam Murray, Ruben Dries.
Station # 5
- 169 ENDOTHELIAL SCAVENGER RECEPTORS IN THE HEMATOPOIETIC NICHE**
Khaliun Enkhbayar, Justine Wagaman, Dana Ragoonanan, Helen Wang, Emily Henault, Elliott Hagedorn.
Station # 6
- 173 PATHWAY ANALYSIS OF IMMUNE CHECKPOINT GENE REGULATION AS ALTERED IN TYPE 2 DIABETES: IMPLICATIONS FOR BREAST CANCER PATIENTS TREATED WITH CHECKPOINT INHIBITORS**
Christina Ennis, Pablo LLevenes, Manohar Kolla, Naser Jafari, Anna Belkina, Gerald Denis.
Station # 7
- 100 PHOTOACOUSTIC STIMULATION OF PRIMARY EMBRYONIC NEURONS IN *XENOPUS LAEVIS***
Gavin Rosen, Mackenzie Hulme, Linli Shi, Chen Yang, Laura Lowery.
Station # 8
- 58 INVESTIGATING THE ROLE OF THE COREST REPRESSOR COMPLEX IN MELANOMA METASTASIS IN VIVO**
Ainsley Hutchison, Mackenzie Hulme, Bengisu Gur, Joe Ebbert, Rhoda Alani, Laura Lowery.
Station # 9
- 171 ADIPOCYTE-ORIGIN EXOSOMES REGULATE BREAST CANCER AGGRESSIVENESS IN OBESITY AND METABOLIC DISEASE**
Naser Jafari, Manohar Kolla, Tova Meshulam, Jordan Shafran, Yuhan Qiu, Allison Casey, Gerald Denis.
Station # 10

- 78 ESTABLISHING A SINGLE-CELL RNA-SEQ PIPELINE FOR TREATMENT NAIVE TRIPLE NEGATIVE BREAST CANCER BIOPSIES**
Emma Kelley, George Chen, Yibing Wei, Christina Ennis, Ruben Dries.
Station # 11
- 160 EXOSOMES PRODUCED BY ADIPOCYTES INDUCE EMT, IMMUNE EXHAUSTION & TUMOR METASTASIS, IN BOTH *IN VIVO* & *IN VITRO* MODELS OF TNBC**
Yuhan Qiu, Conor Ross, Naser Jafari, Manohar Kolla, Isabella Pompa, Pablo Llevenes, Carla Mazzeo, Kiana Mahdavian, Naomi Ko, Gerald Denis.
Station # 12
- 19 THE FETAL HEMATOPOIETIC NICHE IS DISPENSABLE UNDER STEADY STATE CONDITIONS**
Dana Ragoonanan, Helen Wang, Khaliun Enkhbayar, Emily Henault, Serine Avagyan, Rebecca Freeman, Elliott Hagedorn.
Station # 13
- 87 CELLULAR CHARACTERIZATION OF PROSTATE CANCER CELLS WITH FUNCTIONAL LOSS OF *ATRX* OR *DAXX***
Marija Stojanova, Elizabeth Nelson, Mindy Graham, Alan Meeker, Christopher Heaphy.
Station # 14
- 164 DEVELOPMENT OF AN *IN VITRO* 3D CO-CULTURE MULTIPLEXING STRATEGY FOR A SYSTEMATIC RECAPITULATION OF THE HETEROGENOUS AND DYNAMIC BREAST TUMOR MICROENVIRONMENT**
Yibing Wei, Rose Zhao, Emma Kelley, Jiaji Chen, Kylor Lachut, Clare Melley, Ruben Dries, Ph.D..
Station # 15

Session 2 – Floor 5 Thursday 10/7 10:30 – 11:30 a.m.

- 159 DOMAIN-SPECIFIC COGNITIVE FUNCTIONS PREDICT NEUROPATHOLOGICAL TRAITS IN FRAMINGHAM HEART STUDY**
Donghe Li.
Station # 1
- 107 CHRONIC ACTIVATION OF THE ARYL HYDROCARBON RECEPTOR LEADS TO IMMUNE SUPPRESSION AND TUMOR FORMATION IN BOTH ORAL AND LUNG CANCERS**
Megan Snyder, Brian Lara, Jessica Kenison-White, Zhongyan Wang, Kangkang Yang, David Sherr.
Station # 2
- 55 PULMONARY TUBERCULOSIS IS ASSOCIATED WITH THE DEVELOPMENT OF BROAD AND POTENT NEUTRALIZING ANTIBODIES IN CHRONIC HIV-1**
Bukola Adeoye, Alex Olson, Yvetane Moreau, Manish Sagar.
Station # 3
- 83 EPIDEMIOLOGICAL FACTORS AND HUMORAL IMMUNE RESPONSES ASSOCIATED WITH SARS-COV-2 RE-INFECTION OR PROLONGED SHEDDING**
David Bean, Janet Monroe, Manish Sagar.
Station # 4

- 110 INTEGRASE STRAND TRANSFER INHIBITORS ALTER ADIPOKINE PROFILES AND METABOLIC ACTIVITY OF ADIPOCYTES IN-VITRO**
R. Taylor Pickering, Kaitlin Soden, Archana Asundi, Nina Lin.
Station # 5
- 71 SMALL MOLECULES THAT CORRECT ABERRANT TNF RESPONSE INCREASE INNATE RESISTANCE TO TUBERCULOSIS**
Shivraj Yabaji, Sujoy Chatterjee, Igor Kramnik.
Station # 6
- 46 A NOVEL RODENT MODEL OF CENTRAL VENOUS STENOSIS**
Nagla EL ZINAD, Saran Lotofollahzadeh, CONNOR KIM, Meng wei Zhang, JOSEPHINE Orrick, Murad Elsadawi, Vipul C Chitalia.
Station # 7
- 54 QUANTIFICATION OF CELLULAR COMPONENTS OF AVF EXPLANTS**
Connor Kim, John Le, Yichi Zhang, Wenqing Yin, Mostafa Belghasem, Mengwei Zhang, Saran Lotfollahzadeh, Josephine Orrick, Nagla Elzinad, Vijaya Kolachalama, Vipul Chitalia.
Station # 8
- 68 ZEB2 CONTROLS KIDNEY STROMAL PROGENITOR DIFFERENTIATION AND INHIBITS ABNORMAL MYOFIBROBLAST EXPANSION AND KIDNEY FIBROSIS**
Sudhir Kumar, Xueping Fan, Hila Milo Rasouly, Richa Sharma, David J. Salant, Weining Lu.
Station # 9
- 102 ROLE OF PIP COMPLEX IN PODOCYTES INDICATED BY PODOCYTE-SPECIFIC KNOCKOUT OF INTEGRIN-LINKED KINASE (ILK)**
Aksel Laudon, Sudhir Kumar, Weining Lu.
Station # 10
- 35 PHARMACOLOGICAL MANIPULATION OF LSF SUPPRESSES WNT SIGNALING IN COLON CANCER CELLS AND INHIBITS COLON TUMOR GROWTH IN MICE**
Saran Lotfollahzadeh, Dominic Lo, Meng Wei Zhang, Nagla Elzinad, Josephine Orrick, Kim Connor, Scott Schaus, Ulla Hansen, Vipul Chitalia.
Station # 11
- 40 SUBCELLULAR LOCALIZATION OF ORF9B, A MYSTERIOUS SARS-COV-2 PROTEIN IN ENDOTHELIAL CELLS**
Josephine Orrick, Marc Napoleon, Winnie Zhang, Connor Kim, Nagla Elzinad, Saran Lotfollahzadeh, Jena Goodman, Michael Kirber, Ali Munawar, Vipul Chitalia.
Station # 12
- 32 OXIDATIVE STRESS AND HYPOXIA DOWNREGULATE TMIGD1 IN CALPAIN 2-DEPENDENT MANNER TO MODULATE RENAL TUBULE CELL SURVIVAL**
Mengwei Zhang, Wenqing Yin, John Le, Josephine Orrick, Connor Kim, Nagla Elzinad, Saran Lotfollahzadeh, Nader Rahimi, Vipul Chitalia.
Station # 13

106 LYSYL OXIDASE LIKE-2 IN CHONDROPROGENITOR FUNCTION AND OSTEOARTHRITIS

Faiza Ali, Manish Bais.
Station # 14

14 NOVEL COCRYSTALLIZATION OF APOLIPOPROTEIN A-I WITH BUTYRIC ACID

Grace Ferri.
Station # 15

Session 2 – Floor 6 Thursday 10/7 10:30 – 11:30 a.m.

172 PULMONARY LYMPHATIC VESSEL REMODELING IN RESPONSE TO INFLUENZA INFECTION

Senegal Carty, Erin Crossey, MD, PhD, Fengzhi Shao, Alexandra Ysasi, Michelle Zeng, Jin Yuan, MD, PhD, Jhonatan Henao-Vasquez, Anne Hinds, Alan Fine, MD, Matthew Jones, PhD.
Station # 1

143 ERG DEFICIENCY CONTRIBUTES TO PULMONARY FIBROSIS VIA AFFECTING TISSUE LYMPHANGIOGENESIS

Adri Chakraborty, Grace Marden, Vrinda DAMBAL, Ashna Panchmatia, Yashasvi Tharani, Maria Trojanowska.
Station # 2

112 A ROLE FOR DISTINCT LYMPHATIC ENDOTHELIAL CELL SUBSETS IN PULMONARY LYMPHANGIOGENESIS

Erin Crossey, Senegal Carty, Matt Jones, Alan Fine.
Station # 3

178 LUNG B CELL DYNAMICS DURING RESPIRATORY INFECTION

Neelou Etesami, Kimberly Barker, Anukul Shenoy, Carolina Lyon De Ana, Wesley Goltry, Anna Belkina, Joseph Mizgerd.
Station # 4

30 INDUCED PLURIPOTENT STEM CELL MODELING OF COMMON VARIABLE IMMUNE DEFICIENCY-ASSOCIATED *NFKB1* MUTATIONS

Kevin Hayes, Aditya Mithal, Gustavo Mostoslavsky, PJ Maglione.
Station # 5

61 AIRWAY MULTICILIATED CELL HETEROGENEITY IN RESPONSE TO INFLUENZA INFECTION

Jhonatan Henao Vasquez, Jin Yuan, Senegal Carty, Erin Crossey, Fengzhi Shao, Lee Quinton, Katrina Traber, Joseph Mizgerd, Alan Fine, Matthew Jones.
Station # 6

12 A MOUSE SINGLE-CELL LUNG ATLAS OF COMPLEMENT GENE EXPRESSION

Archana Jayaraman, Neha Chaudhary, Joseph Mizgerd, Joshua Campbell, Markus Bosmann.
Station # 7

72 HETEROGENEITY OF CD4⁺T CELLS IN PNEUMOCOCCAL PNEUMONIA

Carolina Lyon De Ana, Anukul Shenoy, Kimberly Barker, Emad Arafa, Neelou Etesami, Ian Martin, Anna Belkina, Brian Tilton, Wesley Goltry, Matthew Jones, Lee Quinton, Joseph Mizgerd.
Station # 8

- 136 ASSOCIATIONS OF PLASMA BAFF AND SOLUBLE BAFF WITH AUTOIMMUNE AND LYMPHOPROLIFERATIVE COMPLICATIONS IN COVID**
Erik Matson, Paul Maglione.
Station # 9
- 67 LIF-MEDIATED TISSUE INJURY AND APOPTOSIS DURING PNEUMONIA**
Elim Na, Filiz Korkmaz, Christine Odom, Lillia Baird, Matthew Jones, Joseph Mizgerd, Katrina Traber, Xaralabos Varelas, Lee Quinton.
Station # 10
- 124 LIVER ACTIVITY MODULATES THE LUNG DURING ENDOTOXEMIA AND PNEUMONIA**
Christine Odom, Yuri Kim, Filiz Korkmaz, Elim Na, Lillia Baird, Matthew Jones, Joseph Mizgerd, Katrina Traber, Lee Quinton.
Station # 11
- 42 PLATFORM TO INVESTIGATE NEUTROPHIL HETEROGENEITY AND DIFFERENTIATION IN MURINE LUNG**
Riley Pihl, Nia Shaw, Katrina Traber.
Station # 12
- 76 MOUSE MODEL OF LATE-ONSET NEUTROPHILIC ASTHMA REVEALS NOVEL CELLULAR AND MOLECULAR CIRCUITS UNDERLYING DESTRUCTIVE AIRWAY NEUTROPHILIA.**
Anukul Shenoy, Filiz Korkmaz, Carolina Lyon De Ana, Christine Odom, Kimberly Barker, Wesley Goltry, Ian Martin, Feng-Zhi Shao, Matthew Jones, Lee Quinton, Felicia Chen, Anna Belkina, Joseph Mizgerd.
Station # 13
- 139 LUNG MESENCHYMAL CELL RESPONSES TO PNEUMONIA**
Alicia Soucy, Joshua Campbell, Tianmu Hu, Filiz Korkmaz, Anukul Shenoy, Wesley Goltry, Ian Martin, Katrina Traber, Matthew Jones, Lee Quinton, Joseph Mizgerd.
Station # 14
- 138 DOUBLE DELETION OF C5AR1 AND C5AR2 DURING STREPTOCOCCAL PNEUMONIA**
Sarah Walachowski, Markus Dudek, Leonid Eshkind, Vanessa Tansi, Joseph Mizgerd, Markus Bosmann.
Station # 15
-

Session 2 – Floor 7 Thursday 10/7 10:30 – 11:30 a.m.

- 16 AIRWAY MULTICILIATED CELL MIW12 AND INFLUENZA PATHOGENESIS**
JIN YUAN, Carty Senegal, Erin Crossey, Jhonatan Henao Vasquez, Fengzhi Shao, Joseph Mizgerd, Matthew Jones, Alan Fine.
Station # 1
- 156 DYSFUNCTIONAL ERG SIGNALING DRIVES PULMONARY VASCULAR AGING AND PROGRESSIVE FIBROSIS**
Jisu Lee, Nunzia Caporarello, Tho Pham, Dakota Jones, Jiazhen Guan, Jefferey Meridew, Grace Marden, Takashi Yamashita, Daniel Tschumperlin, Maria Trojanowska, Giovanni Ligresti.
Station # 2

- 81 COMPARATIVE TRANSCRIPTIONAL ANALYSIS OF LUNG FIBROBLASTS FROM YOUNG AND AGED MICE IDENTIFIES PIMI/NFATC1 AXIS AS A DRIVER OF PERSISTENT FIBROSIS**
 Tho Pham, Jisu Lee, Jaizhen Guan, Nunzia Caporarello, Dakota Jones, Jeffrey Meridew, Qi Tan, Steven Huang, Daniel Tschumperlin, Giovanni Ligresti.
 Station # 3
- 196 REDOX REGULATION OF SIRT1 IN AORTIC ANEURYSM IN MARFAN'S SYNDROME**
 Enkhjargal Budbazar, Sandra Sulser Ponce de Leon, Jena Brooke Goodman, Yu Wang, Yuko Tsukahara, Jingyan Han, Francesca Seta.
 Station # 4
- 73 A NOVEL OXALATE-CURCUMIN-BASED IMAGING PROBE: ENABLING TO VISUALIZE REACTIVE OXYGEN SPECIES IN ATHEROSCLEROSIS**
 Fangzhou Cheng.
 Station # 5
- 183 ELUCIDATING THE ROLE OF BCL11B IN AORTIC ANEURYSM DEVELOPMENT**
 Jena Goodman, Jeff Valisno, Lisia Vargas, Steven Tabor, Michael Kirber, Francesca Seta.
 Station # 6
- 180 UTILIZING THE COMPARATIVE TOXICOGENOMIC DATABASE TO DISCOVER NOVEL PATHWAYS CONNECTING CHRONIC BINGE DRINKING TO ATHEROSCLEROSIS**
 Rebecca Johnson.
 Station # 7
- 137 THE EFFECTS OF POD-BASED E-LIQUIDS ON VASCULAR ENDOTHELIAL CELL FUNCTION**
 Sana Majid, Robert Weisbrod, Jessica Fetterman, Naomi Hamburg.
 Station # 8
- 121 ALCOHOL BINGE DRINKING SELECTIVELY STIMULATES PROTEIN S-GLUTATHIONYLATION IN AORTA AND LIVER OF APOE^{-/-} MICE**
 Kerstin Seidel, Xueping Wan, Mo Zhang, Yuxiang Zhou, Mengwei Zang, Jingyan Han.
 Station # 9
- 114 REDOX REGULATION OF VASCULAR SMOOTH MUSCLE SIRTUIN-1 IN AORTIC ANEURYSMS**
 Sandra Sulser Ponce de Leon, Enkhjargal Budbazar, Yuhao Huangfu, Hanxiao Liu, Francesca Seta.
 Station # 10
- 162 GLUTAREDOXIN-1 IN ENDOTHELIAL CELLS ATTENUATES STEATOSIS IN NON-ALCOHOLIC STEATOHEPATITIS (NASH)**
 Yuko Tsukahara, Beatriz Ferran, Brian Chong, Erika Minetti, Jingyan Han, Francesca Seta, Valerie Gouon-Evans, Reiko Matsui.
 Station # 11

- 189 INUCTION OF VASCULAR PROTEIN S-GLUTATHIONLATION IMPAIRS UNFOLDED PROTEIN RESPONSE IN AGING**
Xueping Wan, Yuxiang Zhou, Tomoko Mori, Fangzhou Cheng, Kerstin Seidel, Jingyan Han.
Station # 12
- 85 ALPHA-1 ANTITRYPSIN DEFICIENCY ADULT CLINICAL AND GENETIC LINKAGE STUDY**
Mark Dodge, Michelle Higgins, Nora Lee, Erica Menino, Grace (Qing) Zhao, Joseph Kaserman, Danielle Zimmerman, Andrew Wilson.
Station # 13
- 194 ENDOCRINOLOGISTS' EXPERIENCES WITH TELEHEALTH: ORGANIZATIONAL AND LOGISTICAL ISSUES WITH IMPLEMENTATION**
Denise Wong, Kailyn Sitter, Rendelle Bolton, Varsha Vimalananda.
Station # 14

Session 2 – Floor 8 Thursday 10/7 10:30 – 11:30 a.m.

- 170 TRANSCRIPTOME-WIDE ANALYSIS OF DIFFERENT DEMENTIA TYPES IN HUMAN HIPPOCAMPUS**
Oluwatosin Olayinka, Junming Hu, Nicholas O'Neill, Xiaoling Zhang, Irene Simkin, Thor Stein, Lindsay Farrer.
Station # 1
- 113 USE OF A STANDARDIZED DISCHARGE TEMPLATE MAY IMPROVE POST-DISCHARGE TRANSITIONS OF CARE FOR DIALYSIS PATIENTS**
Sophie Claudel, Christopher Valente, Hope Serafin, Mohamed Hassan Kamel, Sandeep Ghai.
Station # 2
- 193 ROLE OF INTRAVASCULAR ULTRASOUND (IVUS) IN DETECTION AND CHARACTERIZATION OF VASCULAR STENOSIS IN PATIENTS WITH DIALYSIS ACCESS MALFUNCTION**
Najia Idrees, Wenqing Yin, Joanna Mangio, Kevin Daley, Suvarnu Ganghuly, Jeffrey Syracuse, Alik Farber, Vipul Chitalia.
Station # 3
- 163 THE USE OF PLASMA BIOMARKER-DERIVED CLUSTERS FOR CLINICOPATHOLOGIC PHENOTYPING**
Insa Schmidt, Prasad Patil, Steele Myrick, Ingrid Onul, Isaac Stillman, Anand Srivastava, Ragnar Palsson, Helmut Rennke, Sushrut Waikar.
Station # 4
- 129 DIETARY SATURATED AND UNSATURATED FATS AND CARDIOMETABOLIC RISK IN THE FRAMINGHAM OFFSPRING STUDY**
Ioanna Yiannakou, Mengjie Yuan, Martha Singer, Lynn Moore.
Station # 5
- 144 YOGURT INTAKE, WEIGHT GAIN, AND OBESITY RISK DURING THE MENOPAUSAL TRANSITION**
Mengjie Yuan, Yanping Li, Howard Cabral, Frank Hu, Lynn Moore.
Station # 6

- 108 INTERSECTION OF STRUCTURAL, INSTRUMENTAL, AND SYMBOLIC STIGMA AMONG PEOPLE WITH HIV WHO INJECT DRUGS: A QUALITATIVE STUDY IN ST. PETERSBURG, RUSSIA**
Molly Zhao, Marina Vetrova, Olga Toussova, Olga Toussova, Nakul Vyas, Sarah Rossi, Elena Blokhina, Karsten Lunze.
Station # 7
-

Session 3 – Floor 1 Thursday 10/7 11:30 a.m. – 12:30 p.m.

- 92 UTILIZATION OF TECHNETIUM-99M PYROPHOSPHATE IMAGING FOR THE DIAGNOSIS OF TRANSTHYRETIN AMYLOID CARDIOMYOPATHY (ATTR-CM): A MULTI-CENTER, COMMUNITY HOSPITAL-BASED STUDY**
Rabah Alreshq, Steven Sigman, Catherine Marti, Andrew Darlington, Arun Krishnamoorthy, Benjamin DeMoss, Frederick Ruberg.
Station # 1
- 182 FACILITATORS AND BARRIERS TO CHRONIC CARE AMONG PATIENTS WITH HEART FAILURE IN RURAL HAITI A QUALITATIVE STUDY**
Elizabeth Basow, Gene Kwan, Benito Isaac, Darius Fenelon, Evyrna Toussaint, Dawson Calixte, Michel Ibrahim, Lisa Hirschhorn, Mari-Lynn Drainoni, Alma Adler, Gene Bukhman.
Station # 2
- 15 EVALUATING FOR EQUITY AT A SAFTEY NET HOSPITAL-SOCIOECONOMIC STATUS, ADHERENCE, AND OUTCOMES IN CARDIAC REHABILITATION**
Joshua Gilman, Tulani Washington-Plasket, Na Wang, Stephanie Zombeck, Gary Balady.
Station # 3
- 96 ABNORMAL LIGHT-CHAIN TESTING AND DIAGNOSIS OF TRANSTHYRETIN AMYLOID CARDIOMYOPATHY (ATTR-CM) AMONG PATIENTS REFERRED FOR TECHNETIUM-99M PYROPHOSPHATE IMAGING**
Matthew Cozzolino, Rabah Alreshq, Brian Lilleness, Alexandra Pipilas, Varsha Muralidhar, Eric Guardino, John Berk, Omar Siddiqi, Deepa Gopal, Vaishali Sanchorawala, Frederick Ruberg.
Station # 4
- 133 EVALUATION OF DIFFERENTIAL MICRO RNA EXPRESSION IN PERIPHERAL ARTERY DISEASE**
Syed Husain Mustafa Rizvi, Rosa Bretón Romero, Robert M. Weisbrod, Naomi M. Hamburg.
Station # 5
- 95 LONG-TERM MORTALITY ASSOCIATED WITH USE OF CARVEDILOL VS METOPROLOL IN HEART FAILURE PATIENTS WITH AND WITHOUT TYPE 2 DIABETES- A DANISH NATIONWIDE COHORT STUDY**
Brian Schwartz, Colin Pierce, Christian Madelaire, Morten Schou, Søren Lund Kristensen, Gunnar Gislason, Lars Køber, Christian Torp-Pedersen, Charlotte Andersson.
Station # 6

- 125 THE SHORT PHYSICAL PERFORMANCE BATTERY SCORE IS ASSOCIATED WITH QUALITY OF LIFE IN BLACK AND HISPANIC OUTPATIENTS WITH STABLE CONGESTIVE HEART FAILURE**
Christopher Valente, Cody Chiuzan, Rabah Alreshq, Tori Blot, Denise Fine, Stephen Helmke, Carlos Rodriguez, Natalia Sabogal, Sergio Teruya, Morgan Winburn, Mathew Maurer, Frederick Ruberg.
Station # 7
- 13 CONTEMPORARY INCIDENCE AND OUTCOMES OF AORTIC DISSECTION DURING PREGNANCY AND PUERPERIUM IN THE UNITED STATES**
Yunda (George) Wang, Kanhua Yin, Karl Karlson, Niloo Edwards, Nikola Dobrilovic.
Station # 8
- 86 UTILIZING GENOMIC MARKERS OF BRONCHIAL PREMALIGNANT LESION SEVERITY AND PROGRESSION TO PREDICT CANCER STATUS OF INDETERMINATE PULMONARY NODULES**
Kelley Anderson, Gang Liu, Ehab Billatos, Marc Lenburg, Jennifer Beane.
Station # 9
- 62 PREDICTING MALIGNANCY IN INDETERMINATE PULMONARY NODULES USING MODELS INTEGRATING QUANTITATIVE CT IMAGING AND NASAL GENE EXPRESSION**
Kate Bloch.
Station # 10
- 94 ENHANCED DECONVOLUTION AND PREDICTION OF MUTATIONAL SIGNATURES**
Aaron Chevalier.
Station # 11
- 118 SUBCHONDRAL BONE LENGTH: A DEEP LEARNING DRIVEN IMAGING MEASURE FOR KNEE OSTEOARTHRITIS**
Ray Jhun, Gary Chang, Lisa Park, Nina Le, Tejus Surendran, Joseph Lai, Hojoon Seo, Nuwapa Promchotchai, Grace Yoon, Jonathan Scalera, Terence Capellini, David Felson, Vijaya Kolachalama.
Station # 12
- 25 CHARACTERIZING TRANSCRIPTOMIC PROFILES AND MICROBIAL ABUNDANCE OF ORAL POTENTIALLY MALIGNANT DISORDERS**
Mohammed Muzamil Khan, JENNIFER FRUSTINO, ALESSANDRO VILLA, BACH-CUC NGUYEN, SOOK-BIN WOO, XARALABOS VARELAS, MARIA KUKURUZINSKA, STEFANO MONTI.
Station # 13
- 66 VALIDATION OF BRONCHIAL GENE EXPRESSION ASSOCIATED WITH COPD IN BRONCHIAL AND NASAL BRUSHINGS PROFILED BY RNA-SEQ**
Yusuke Koga, Melody Morris, Margaret Fleming, Joshua Campbell, Ehab Billatos, Marc Lenburg.
Station # 14

145 IMMUNOPHENOTYPING OF PREMALIGNANCY IN A MURINE MODEL OF LUNG SQUAMOUS CELL CARCINOMA VIA IMAGING MASS CYTOMETRY

Tachira Pichardo, Roxanna Pfefferkorn, Chris Husted, Jennifer Beane, Sarah Mazzilli.
Station # 15

Session 3 – Floor 2 Thursday 10/7 11:30 a.m. – 12:30 p.m.

82 GENE EXPRESSION ASSOCIATED WITH VASCULAR INVASION IS PREDICTIVE OF TUMOR AGGRESSIVENESS IN STAGE I LUNG ADENOCARCINOMA

Dylan Steiner, Jiarui Zhang, Gang Liu, Avrum Spira, Eric Burks, Jennifer Beane, Marc Lenburg.
Station # 1

155 POST-TRAUMATIC STRESS DISORDER IN COMBAT-EXPOSED VETERANS IS NOT ASSOCIATED WITH IRRITABLE BOWEL SYNDROME AND FUNCTIONAL DYSPEPSIA BUT GASTROESOPHAGEAL REFLUX DISEASE

Abishek Arokiadoss, Kelly Harper, Hassen Abdulkерim, Brian Marx, Terence Keane, Christian Weber.
Station # 2

188 RISK FACTORS ASSOCIATED WITH DELAY IN DIAGNOSIS OF EARLY-ONSET COLORECTAL CANCER IN A SAFETY-NET HOSPITAL POPULATION

Laura Chiu, Kevin Huang, Xixi Xu, Rubiya Rahman, Paul Schroy.
Station # 3

120 PLANNING FOR THE FUTURE: DETECTING MISSED HIGH-RISK ADENOMAS AND COLORECTAL CANCERS DUE TO THE COVID-19 PANDEMIC

James Connolly, Heidi Ahmed, Enoch Chung, Howard Cabral, Arpan Mohanty.
Station # 4

26 VACCINE HESITANCY TOWARDS COVID VACCINATION IN IBD PATIENTS IN A DIVERSE SAFETY NET HOSPITAL PATIENT POPULATION

Howard Herman, Max Rosenthaler, Venkata Satyam, Sharmeel Wasan.
Station # 5

37 THE PERFORMANCE OF FRACTURE RISK SCORES IN PATIENTS WITH IBD

Helen Lyo, Matthew Custodio, Alan Moss.
Station # 6

179 PATTERNS OF ALCOHOL USE AND LIVER FIBROSIS IN THE FRAMINGHAM HEART STUDY

Brooke Rice, Michelle Long.
Station # 7

150 LAXATIVE USE FOR PATIENTS WITH BOTH IMPAIRED COLONIC WAKE RESPONSE AND SLOW TRANSIT CONSTIPATION IS ASSOCIATED WITH IMPROVED CONSTIPATION SEVERITY SCORES BUT NOT LOWER ABDOMINAL PAIN OR DISCOMFORT

Brian Surjanhata, Ingrid Guerrero López, Jack Semler, Brad Kuo.
Station # 8

- 49 INTERPROFESSIONAL COLLABORATION BETWEEN MINDFULNESS INSTRUCTORS AND PRIMARY CARE PROVIDERS**
Dhanesh Binda, Janice Weinberg, Natalia Morone.
Station # 9
- 165 METASTATIC MALIGNANT INSULINOMA WITH FAILURE OF INITIAL OCTREOTIDE THERAPY: A RARE MANAGEMENT COMPLICATION**
Laura Burns.
Station # 10
- 21 ASSOCIATION BETWEEN CHANGE IN ALCOHOL CONSUMPTION AND D-DIMER OVER TIME AMONG PLHIV**
Alexis Kiyanda, Samuel Mensah, Gregory Patts, Debbie Cheng, Wenqing Jiang, Jeffrey Samet, Kaku So-Armah.
Station # 11
- 190 EFFECT OF ALCOHOL CONSUMPTION ON CD4 RECOVERY AFTER ANTIRETROVIRAL THERAPY (ART) INITIATION IN PEOPLE LIVING WITH HIV (PLWH)**
A McLaughlin, N Lin, W Jiang, S Lodi, D Lioznov, G Patts, N Gnatienco, E Blokhina, S Bendiks, M Freiberg, H Tindle, E Krupitsky, J Samet, K So-Armah.
Station # 12
- 24 COVID-19 PANDEMIC-RELATED STRESS AND SUBSTANCE USE BEHAVIORS AMONG PEOPLE WITH HIV IN ST. PETERSBURG, RUSSIA**
Sarah Rossi, Dmitry Lioznov, Debbie Cheng, Ve Truong, Sally Bendiks, Natalia Gnatienco, Sara Lodi, Elena Blokhina, Anita Raj, Lindsey Rateau, Yuliia Sereda, Evgeny Krupitsky, Jeffrey Samet, Karsten Lunze.
Station # 13
- 91 THE ASSOCIATION OF PRESCRIBED OPIOIDS AND INCIDENT CARDIOVASCULAR DISEASE IN THE VETERANS AGING COHORT STUDY**
Kaku So-Armah, Minhee Sung, Svetlana Eden, Chung-Chou Chang, Meredith Duncan, Suman Kundu, Kirsha Gordon, Robert Kerns, Steve Crystal, William Becker, Matthew Freiberg, Jennifer Edelman, Jennifer Edelman.
Station # 14
- 154 DIFFERENCES IN TREATMENT DELAY AMONG BREAST CANCER PATIENTS WITH ALCOHOL AND MARIJUANA COMPARED TO NARCOTIC SUBSTANCE USE DISORDERS**
Anne Buck, Haley Urbach, Naomi Ko.
Station # 15

Session 3 – Floor 3 Thursday 10/7 11:30 a.m. – 12:30 p.m.

- 131 PERIPHERAL BLOOD MONOCYTE COUNT IS A DYNAMIC PROGNOSTIC MARKER FOR RISK STRATIFICATION IN MULTIPLE MYELOMA**
Camille Edwards, Hamza Hassan, Grace Ferri, Karina Verma, Cenk Yildirim, Nathanael Fillmore, Nikhil Munshi.
Station # 1

- 175 DEVELOPMENT OF A CLINICAL INFORMATION AND BIOSPECIMEN DATABASE IN THE HEMATOLOGY/ONCOLOGY OUTPATIENT CLINICS**
Adrian Ilinski, Kiana Mahdavian, David Li, Nina Modanlo, Casey Simon-Plumb, Matthew Kulke.
Station # 2
- 177 ASSESSMENT OF TRYPTOPHAN METABOLITES AS POTENTIAL BIOMARKERS OF RESPONSE TO IMMUNE CHECKPOINT INHIBITORS**
David Li, Kiana Mahdavian, Lucas Schiffer, Nina Modanlo, Casey Simon-Plumb, Adrian Ilinski, Stephen Whelan, Norman Lee, Evan Johnson.
Station # 3
- 9 RACIAL DISPARITIES IN MYELOMA CLINICAL TRIALS: A SYSTEMATIC REVIEW AND POOLED ANALYSIS**
Charles Milrod, David Hughes, Frances Blevins, J. Mark Sloan.
Station # 4
- 152 THE IMPACT OF DIABETES AND HYPERTENSION ON BREAST CANCER RECURRENCE IN PATIENTS AT BOSTON MEDICAL CENTER**
Arthi Palani, Muhammad Qureshi, Naomi Ko, Tsion Fikre, Ariel Hirsch.
Station # 5
- 185 TREATMENT DELAYS IN BREAST CANCER PATIENTS WITH SUBSTANCE USE DISORDER**
Haley Urbach, Anne Buck, Naomi Ko.
Station # 6
- 198 IMPACT OF MASSHEALTH ON BREAST CANCER SURVIVORSHIP CARE DISPARITIES BETWEEN BLACK AND WHITE SURVIVORS AT AN URBAN SAFETY NET HOSPITAL**
Preetha Velu, Tsion Fikre, Alexandra Fischman Han, Naomi Ko.
Station # 7
- 64 RARE CASE OF HYPERAMMONEMIC ENCEPHALOPATHY IN NON-SECRETORY MULTIPLE MYELOMA**
Karina Verma, Tina Zhang, David Mueller, Andrew Staron.
Station # 8
- 123 A MIXED-METHODS STUDY OF MINORITY ENROLLMENT IN CANCER BIOSPECIMEN RESEARCH**
Tina Zhang, Nina Modanlo, David Li, Kiana Mahdavian, Anish Parekh, Adrian Ilinski, Naomi Ko.
Station # 9
- 168 INVESTIGATION OF EFFECT OF CHRONIC OPIOID MISUSE ON HIV PATHOGENESIS AND LATENCY ESTABLISHMENT**
Binita Basukala.
Station # 10
- 8 BARRIERS TO ACCESSING TREATMENT FOR OPIOID USE DISORDER AFTER INPATIENT MANAGED WITHDRAWAL PROGRAM (DETOX): A QUALITATIVE STUDY**
Allison David, Carlos Sian, Benjamin Linas, Jeffrey Samet, Judith Bernstein, Sabrina Assoumou.
Station # 11

- 98 RISK FACTORS AND CARDIOMETABOLIC IMPLICATIONS OF INTEGRASE INHIBITORS AMONG PEOPLE LIVING WITH HIV**
Alex Olson, Archana Asundi, Carrie Coote, Wenqing Jiang, Laura White, Swati Patel, Manish Sagar, Nina Lin.
Station # 12
- 11 CARDIAC MANIFESTATIONS OF CHAGAS DISEASE PATIENTS IDENTIFIED THROUGH COMMUNITY HEALTH SCREENING AND SEEN AT BOSTON MEDICAL CENTER TRAVEL MEDICINE CLINIC**
Katherine Reifler, Samantha Hall, Davidson Hamer, Natasha Hochberg.
Station # 13
- 104 THE IMPACTS OF THE COVID-19 PANDEMIC ON THE WELLBEING OF SYRINGE SERVICE PROGRAM STAFF**
Andrea Wang, Raagini Jawa, Connor Buchholz, Angela Bazzi.
Station # 14
- 174 ALKYLRESORCINOL, A BIOMARKER FOR WHOLE GRAIN INTAKE, IS NOT ASSOCIATION WITH OSTEOARTHRITIS: THE MOST STUDY**
Juan-Pablo Zertuche, Gabriela Rabasa, Alice Lichtenstein, Nirupa Matthan, Michael Nevitt, James Torner, Cora Lewis, Devyani Misra, David Felson.
Station # 15

Session 3 – Floor 4 Thursday 10/7 11:30 a.m. – 12:30 p.m.

- 176 QUANTITATIVE PUPILLOMETRY FOLLOWING ANALGO-SEDATIVE ADMINISTRATION IN CRITICALLY ILL PATIENTS WITH NEUROLOGIC EMERGENCIES**
Wang Pong Chan, Brenton Prescott, Emelia Benjamin, Stelios Smirnakis, Josee Dupuis, David Greer, Charlene Ong.
Station # 1
- 41 EVALUATION OF LIPOSOMAL BUPIVACAINE INFILTRATION AT RECONSTRUCTIVE SKIN GRAFT DONOR SITES IN OLDER PEDIATRIC AND YOUNG ADULT BURN PATIENTS: A RETROSPECTIVE ANALYSIS**
Matthew DePamphilis, Farzin Sadeq, Robert Dabek, Branko Bojovic, Gennadiy Fuzaylov, Daniel Driscoll.
Station # 2
- 158 EPITRANSCRIPTOMIC AND TRANSCRIPTOMIC CHANGES IN POSTMORTEM NUCLEUS ACCUMBENS OF SUBJECTS WITH ALCOHOL USE DISORDER, A PILOT STUDY**
Yashrajsinh Jadeja, Yolpanhchana Lim, Huiping Zhang.
Station # 3
- 18 VALIDATION OF A CRISIS STANDARDS OF CARE MODEL FOR PRIORITIZATION OF LIMITED RESOURCES DURING THE CORONAVIRUS DISEASE 2019 CRISIS IN AN URBAN, SAFETY-NET, ACADEMIC MEDICAL CENTER**
Albert Nadjarian, Jessica LeClair, Taylor Mahoney, Eric Awtry, Jsvinder Bhatia, Lisa Caruso, Alexis Clay, David Greer, Karan Hingorani, Lucas Horta, Michel Ibrahim, Michael Ieong, Thea James, Matthew Kulke, Remington Lim, Robert Lowe, James Moses, Jaime Murphy, Ala Nozari, Anuj Patel, Brent Silver, Arthur Theodore, Ryan Wang, Ellen Weinstein, Stephen Wilson, Anna Cervantes-Arslanian.
Station # 4

- 187 ASSOCIATION BETWEEN CHANGE IN ALCOHOL USE AND CHANGE IN SCD14 IN PEOPLE WITH HIV (PWH)**
Victoria Ontiveros.
Station # 5
- 29 BLOOD TRANSFUSION AT A HEMOGLOBIN THRESHOLD OF SEVEN G/DL IN CRITICALLY ILL PATIENTS: A TARGET TRIAL EMULATION**
Nicholas Bosch.
Station # 6
- 63 PREVALENCE OF LUNG-RADS S CLASSIFICATIONS IN A NATIONAL COHORT OF US VETERANS SCREENED FOR LUNG CANCER**
Caitlin Butler, Eduardo Nunez, Tanner Caverly, Sanqian Zhang, Mark Glickman, Shirley Qian, Jacqueline Boudreau, Donald Miller, Renda Wiener.
Station # 7
- 74 VARIATION IN USE OF REPURPOSED MEDICATIONS AMONG PATIENTS WITH COVID-19**
Michael Garcia, Shelsey Johnson, Nicholas Bosch, Emily Sisson, Christopher Sheldrick, Vishakha Kumar, Karen Boman, Scott Bolesta, Vikas Bansal, Neha Deo, Juan Domecq, Amos Lal, Ognjen Gajic, Rahul Kashyap, Allan Walkey.
Station # 8
- 56 HOSPITAL VARIATION IN MANAGEMENT OF ACUTE RESPIRATORY DISTRESS SYNDROME (ARDS) DUE TO CORONAVIRUS DISEASE-2019 (COVID-19) AND ASSOCIATED MORTALITY**
Shelsey Johnson, Michael Garcia, Emily Sisson, Christopher Sheldrick, Vishakha Kumar, Karen Boman, Scott Bolesta, Juan Pablo Domecq Garces, Amos Lal, Ognjen Gajic, Rahul Kashyap, Allan Walkey.
Station # 9
- 57 UNDERSTANDING VA SPECIALTY AND PRIMARY CARE CLINICIANS' PERSPECTIVES ON E-CONSULT REQUESTS**
Ariella Krones, Ekaterina Anderson, Varsha Vimalananda, Sarah Cutrona, Jay Orlander, Judith Strymish, Seppo Rinne.
Station # 10
- 22 A CLASSIFICATION AND REGRESSION TREE MODEL FOR RISK STRATIFYING PATIENTS FOR RIGHT HEART CATHETERIZATION IN SYSTEMIC SCLEROSIS**
Justin Lui, Ruchika Sangani, Deepa Gopal, Marcin Trojanowski, Andreea Bujor, Michael LaValley, Renda Soylemez Wiener, Elizabeth Klings.
Station # 11
- 126 FACTORS ASSOCIATED WITH DECLINING LUNG CANCER SCREENING AFTER SHARED DECISION MAKING IN A NATIONAL COHORT OF VETERANS**
Eduardo Nunez, Tanner Caverly, Sanqian Zhang, Mark Glickman, Shirley Qian, Jacqueline Boudreau, Donald Miller, Renda Soylemez Wiener.
Station # 12

**130 VARIATION IN THE INITIAL SEDATION GOAL FOR
MECHANICALLY VENTILATED PATIENTS ACROSS UNITED
STATES HOSPITALS**

Justin Rucci, Nicholas Bosch, Wei Wang, Michael Harhay, Allan Walkey.
Station # 13

**36 THE IMPACT OF INTERSTITIAL LUNG DISEASE SEVERITY ON
CLINICAL OUTCOMES IN SYSTEMIC SCLEROSIS-RELATED
PULMONARY HYPERTENSION**

Ruchika Sangani, Justin Lui, Kari Gillmeyer, Marcin Trojanowski, Andreea
Bujor, Michael LaValley, Elizabeth Klings.
Station # 14

EVANS DEPARTMENT OF MEDICINE RESEARCH DAYS

ABSTRACTS

Session 1 – Floor 1 Thursday 10/7 9:30 am - 10:30 am

90 METABOLIC REPROGRAMMING OF THE HEART BY SGLT2 INHIBITION

Jordan Chambers, Dominique Croteau, Fuzhong Qin, Ivan Luptak, David Pimentel, Wilson Colucci.

Station # 1

Objectives: SGLT2 inhibitors, designed to treat type 2 diabetes, cause dramatic improvement in outcomes in patients with heart failure, independent of diabetes. The mechanism responsible is unknown. We recently showed in mice that SGLT2 inhibition with ertugliflozin (ERTU) markedly increased myocardial gene sets associated with oxidative phosphorylation and fatty acid metabolism, independent of diabetes. We now test whether metabolic reprogramming contributes to the beneficial effect of SGLT2 inhibition on cardiac phenotype in non-diabetic mice with cardiac-specific *Gαq* overexpression.

Methods: Gq mice were treated with ERTU for 16 wks, beginning at 4 wks of age.

Results: Gq mice developed heart failure by 20 wks of age, with dilation of the left ventricle and impaired contractility, associated with cardiac mitochondrial dysfunction reflected by an 8% decrease in ATP production and a 26% increase in reactive oxygen species production. In Gq mice, RNA sequencing revealed marked downregulation of myocardial gene sets for oxidative phosphorylation and fatty acid metabolism at 4 wks of age. In Gq mice, ERTU prevented the development of LV hypertrophy ($p < 0.0001$) and the decrease in systolic function ($p < 0.0001$).

Conclusion: Pending RNA seq and mitochondrial studies will elucidate whether these improvements in cardiac structure and function are associated with metabolic reprogramming and correction of mitochondrial dysfunction. Our data show that SGLT2 inhibition prevents the development of heart failure in non-diabetic mice and will test the role of metabolic reprogramming in the heart.

80 DOWNREGULATED Fli1 IN SCLERODERMA MYELOID CELLS MAY CONTRIBUTE TO CARDIAC FIBROSIS VIA A GALECTIN-3/M-TOR DEPENDENT PATHWAY

Fatima El adili, Mortada Najem, Maria Trojanowska, Andreea Bujor.

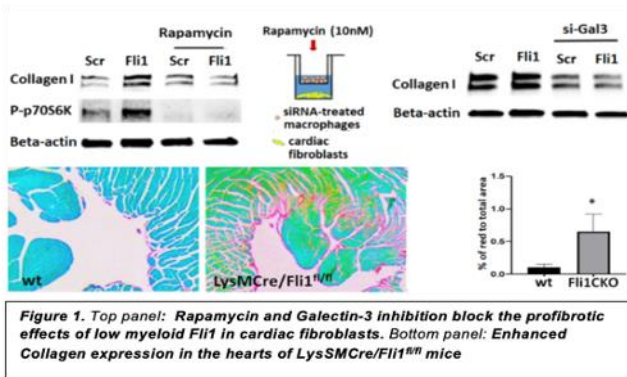
Station # 2

Objectives: Cardiomyopathy is a common complication in scleroderma (SSc). We have shown that Fli1 is decreased in SSc myeloid cells which has a profibrotic effect. We aim to evaluate the contribution of myeloid Fli1 to cardiac fibrosis.

Methods: Primary human cardiac fibroblasts were co-cultured with macrophages and treated with Rapamycin. Collagen deposition in hearts from mice with conditional deletion of Fli1 in macrophages (*LysMCre/Fli1^{fl/fl}*) was assessed by picrosirius red.

Results: Co-culture of human cardiac fibroblasts and Fli1 depleted macrophages resulted in induction of galectin-3 expression by macrophages and activation of the mTOR/p70S6K pathway with enhanced collagen I deposition by fibroblasts. These effects were blocked by Rapamycin, and by treatment of macrophages with siRNA against galectin-3. Deletion of Fli1 in macrophages via Cre-mediated recombination using *LysMCre* mice predisposed mice to develop cardiac fibrosis.

Conclusion: These findings suggest that Fli1 deficiency in macrophages may contribute to SSc cardiac fibrosis and that Rapamycin may be a potential therapeutic option.



153 ANTI- $\beta 1$ INTEGRIN ANTIBODY THERAPY FOR $JAK2^{V617F+}$ MYELOPROLIFERATIVE NEOPLASMS

Xiaosheng Yang, Katya Ravid, Shinobu Matsuura.

Station # 3

Objectives: Evaluate the efficacy of $\beta 1$ integrin inhibition for reduction of megakaryocytosis in a mouse model of $JAK2^{V617F+}$ primary myelofibrosis (PMF). Megakaryocytosis, or abnormally elevated megakaryocyte number in bone marrow, is a prominent feature in PMF, responsible for the release of fibrogenic factors which contribute to myelofibrosis by inducing stromal cells to produce excessive amounts of extracellular matrix (ECM).

Methods: As part of pre-clinical studies, primary bone marrow cells from $Vav1$ - $JAK2^{V617F}$ -transgenic mice were incubated with mouse-specific anti- $\beta 1$ integrin antibodies HMb1-1 and KMI6 *in vitro* for three days, after which total number of cells, expression of CD41 megakaryocyte markers, and expression of Annexin V/propidium iodide apoptosis markers were evaluated.

Results: Both anti- $\beta 1$ integrin antibodies (HMb1-1 and KMI6) demonstrated a strong ability to lower megakaryocyte number in $Vav1$ - $JAK2^{V617F}$ cultures, roughly to a similar level as in WT samples. This result is in line with our finding that $\beta 1$ integrin is activated in $JAK2^{V617F+}$ megakaryocytes, and it contributes to increased adhesion of these cells to fibronectin, compared to controls.

Conclusion: Anti- $\beta 1$ integrin antibody therapy is a promising approach for reducing the burden of megakaryocytosis in $JAK2^{V617F+}$ PMF. This finding opens possibilities for an *in vivo* antibody therapy for PMF, considering that anti- $\beta 1$ integrin was employed before in clinical trials for other diseases.

77 THE EFFECT OF SARS-COV-2 ON HEART MUSCLE CELLS: COMPARISON OF CULTURED CARDIOMYOCYTES AND SERUM OF COVID-19 PATIENTS

Allyson Zheng, Dr. James Hamilton, PhD, Dr. Nasi Huang, MD, Dr. Mohsan Saeed, PhD, Dr. Manish Sagar, MD.

Station # 4

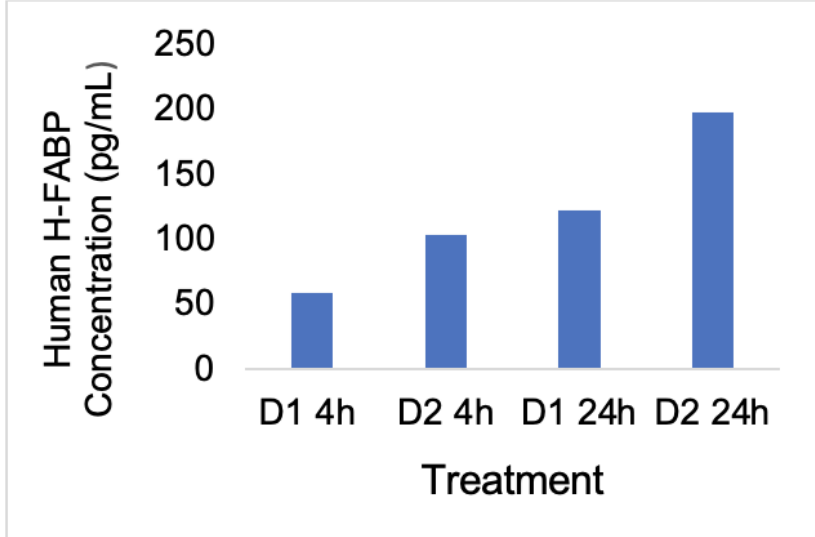
Objectives: Identify optimal blood biomarkers for monitoring cardiovascular comorbidities that lead to prolonged hospitalization and heart failure in COVID-19 patients.

Methods: We tested our hypothesis that the highly specific biomarkers Heart-Fatty Acid Binding Protein (H-FABP) and Cardiac Troponin-T are released from the cytoplasm after cardiomyocyte membrane damage. We compared cultured cardiomyocytes after exposure to lipopolysaccharide (LPS) and SARS-CoV-2. We assayed serum samples from SARS-CoV-2-infected and non-infected patients.

Results: Figure 1 shows increased H-FABP in the cell supernatant with increasing LPS dose and incubation time. Troponin T assays showed a similar trend. Biomarker concentrations in the serum were higher in the SARS-CoV-2-infected samples than controls, indicating higher leakage of these proteins.

Conclusion: With increasing comorbidities in COVID-19 patients and new SARS-CoV-2

variants, this assay will optimize treatment for individuals' medical needs upon hospitalization and guide therapeutics, proving to be an essential tool for the most effective patient care.



93 NEUTROPHILS PLAY A PIVOTAL ROLE IN OBESOGENIC DIET-INDUCED NON-ALCOHOLIC STEATOHEPATITIS

Qiong Zhou, Youhua Wang, Michael Rigor, Indeevar Beeram, Zhen Jiang.

Station # 5

Objectives: Lipid deposition, inflammatory damage, and fibrotic remodel are the hallmarks of non-alcoholic steatohepatitis (NASH). However, the molecular and cellular mechanisms by which obesogenic diet-induced progression from steatosis to NASH remains elusive. Here, we report that neutrophils play a significant role in mediating NASH in the liver.

Methods: Liver tissues from different diets fed mice were examined by immunohistochemistry, Western Blot and real-time PCR methods. Isolated mouse liver cells from different diets fed mice have been studied by flow cytometer method.

Results: Remarkably, high-fat high-fructose diet (HFHFD) feeding increased expression of chemokines in the liver leading to dramatic upsurge of neutrophil infiltration into the liver with concomitant increase of macrophages and Th17 cell accumulation and collagen deposition in the liver. In contrast, inhibition or deletion of neutrophil elastase (NE) significantly reduced lipid deposition, metabolic stress, and inflammation in the liver in mice fed obesogenic diets. Inhibition of NE dramatically reduced the expression of chemokines, accumulation of neutrophils, macrophages, and Th17 cells, and progress of fibrosis in the liver.

Conclusion: Together, our data suggest that NE contributes to NASH progression through regulating metabolic signaling and inflammatory damage in the liver.

119 COMPARATIVE ANALYSIS OF CEREBROSPINAL FLUID MARKERS AND MULTIMODAL IMAGING IN PREDICTING ALZHEIMER'S DISEASE PROGRESSION

Akshara Balachandra, Michael Romano, Xiao Zhou, Michalina Jadick, Shangran Qiu, Diya Nijhawan, Sang Chin, Rhoda Au, Vijaya Kolachalama.

Station # 6

Objectives: Cerebrospinal fluid (CSF) levels of p-tau, t-tau, and A β -42 are widely accepted biomarkers for Alzheimer's Disease (AD). However, lumbar punctures (LP) are limited by medical risks, and lack spatial specificity and standardization. We sought to identify imaging-based biomarkers that can reliably predict 2-year risk of mild cognitive impairment (MCI) to AD progression to reduce LP-related morbidity and AD misdiagnosis.

Methods: We trained deep learning models composed of a fully convolutional network (FCN)

linked with a multi-layer perceptron (MLP) to predict the 2-year risk of AD progression in subjects with MCI using T1w MRI, fluorodeoxyglucose (FDG) PET, and florbetapir (amyloid) PET images from Alzheimer's Disease Neuroimaging Initiative (n=328). A fusion model incorporating all three imaging modalities was evaluated to utilize the additive benefits of each imaging modality. An MLP using only the above three CSF biomarkers was trained for comparison.

Results: Among the unimodal models, the FDG model provided the highest accuracy of all 3 modalities, while the amyloid model was the most sensitive but least specific. The CSF biomarker-based model was the most specific overall. The fusion model was the most accurate overall, comparably sensitive as the amyloid model, and as specific as the CSF model. It also had a higher F1 score than all other models.

Conclusion: Our fusion model is more accurate and sensitive than, and as specific as a CSF-based model in predicting AD progression risk. The FCN-MLP framework can be extended to incorporate easy-to-obtain non-invasive features to develop more accurate risk models and explore distinct AD phenotypic signatures.

44 **GSTP1 AS A MEDIATOR OF IMMUNE RESPONSE IN BRONCHIAL PREMALIGNANT LESIONS**

Julia Camassola Breda, Carter Merenstein, Christopher Stevenson, Mary Reid, Avrum Spira, Marc Lenburg, Sarah Mazzilli, Jennifer Beane, Eric Burks.

Station # 7

Objectives: Bronchial premalignant lesions (PMLs) precede the development of lung squamous cell carcinoma (LUSC) and understanding the epithelial and immune changes associated with PML progression are crucial for early diagnosis of LUSC. Previous work has identified transcriptional subtypes of bronchial PMLs highlighting immune alterations associated with lesions progression. Glutathione S-transferase P (GSTP1) has been identified as a possible modulator of STAT3 & NF-KB pathways in progressive PMLs, and here we try to validate the relationship between increased GSTP1 expression and immunoregulatory pathways.

Methods: Using immortalized bronchial epithelial and LUSC cell lines we validated the expression of GSTP1 and target genes (NF-KB, pSTAT3, CSF1, TNF-alpha) identified in transcriptomic signatures in PMLs via qPCR. We stimulated an immune response in LUSC cells +/- GSTP1 with interleukins 13 and 8, LPS, H₂O₂ and cigarette smoke condensate and performed qRT-PCR on the target genes. We also stained LUSC tumor samples (n=101) arrayed in a tissue microarray for GSTP1 and immune markers (CD3, CD163, MPO, IL17, IL23) and quantified protein expression using QuPath software.

Results: We have found significant upregulation of our target genes upon GSTP1 knockdown plus LPS and H₂O₂ treatments at 48 hours. We also observed an upregulation of GSTP1 in LUSC TMAs, within the tumor, correlated with downregulation of other inflammatory proteins and immune markers.

Conclusion: The anti-correlation observed between GSTP1 and immune cell markers and pathways in vitro and in vivo suggests that GSTP1 may represent a targetable chemoprevention candidate.

88 **SINGLE-NUCLEUS RNA-SEQ REVEALS CELLULAR HETEROGENEITY IN RARE LUNG CANCER HISTOLOGIES**

Darren Chiu, Morgan Thompson, Elizabeth Duffy, Eric Burks, Joshua Campbell, Sarah Mazzilli, Jennifer Beane.

Station # 8

Objectives: Molecular characterization of cancer cells and the tumor microenvironment using single-cell RNA-sequencing (scRNA-seq) provides clinical insight into disease progression, prognosis, and treatment response. However, scRNA-seq relies on freshly dissociated tumor tissues, which limits its ability to profile frozen tissues. In this study, we developed a method to profile frozen lung tumor tissues using single-nucleus RNA-sequencing (snRNA-seq).

Methods: The nuclei were isolated from frozen OCT-embedded lung sections from BMC surgical resection using the TST-based single nuclei isolation protocol and profiled by the 10X Genomics Chromium. We analyzed 2,389 and 8,288 nuclei from one lung adenocarcinoma (LASC) and one lung large cell neuroendocrine carcinoma (LCNEC), respectively.

Results: Tumor cells were separated from the normal epithelial cells by inferring the copy number variations (CNV), where intratumor heterogeneous CNV patterns were detected in both samples. Trajectory inference of the LASC sample suggested alveolar cells and adenocarcinoma-like cancer cells were transcriptomically more similar than squamous-like cancer cells with three distinct CNV patterns. The tumor microenvironment of both tumor samples reflected heterogeneous cell populations and functional states, including cancer-associated fibroblasts, CD4+ T (naïve, regulatory), and CD8+ T(exhaustive, effector) cells.
Conclusion: This study demonstrates the feasibility of generating single-cell data from frozen lung tumor tissues.

105 BATCH EFFECT CORRECTION OF METAGENOMIC DATA USING COMBAT-SEQ

Howard Fan, William Johnson, Jessica Petrick, Julie Palmer.
Station # 9

Objectives: In this study, we examined the use of ComBat-Seq, a batch effect adjustment tool for RNA-seq count data, to correct for batch effect present in metagenomic data representing the human oral microbiome while preserving variations due to desired biological factors.

Methods: We applied ComBat-Seq to correct for batch effect in our post-filtered oral microbiome dataset. We included several biological variables to preserve in the adjusted data, including outcome, region, smoking status, and BMI category. To determine the effectiveness of ComBat-Seq, we performed and compared two separate analyses for investigating differentially abundant microbes associated with smoking: a stratified analysis using the unadjusted data in which each batch group was analyzed individually and a single analysis using the adjusted data.

Results: 21 genera were identified to be differentially abundant across smoking status. Of the 13 genera identified from the stratified analysis, 7 were also identified from the batch-corrected analysis. In addition, the batch-corrected analysis identified 8 new genera for which the batch groups had conflicting results. Overall, for differentially abundant genera, the batch-corrected analysis resulted in increased statistical significance overall compared to results from the stratified analysis due to the increased sample size.

Conclusion: Our findings indicate that ComBat-Seq was effective in removing batch effect found in metagenomic data while preserving variances due to desired biological factors such as smoking status. Batch effect correction in microbiome data improved the detection of differentially abundant genera associated with factors of interest.

122 BAYESIAN STRUCTURE LEARNING FOR HIERARCHICAL REGULATORY NETWORKS

Anthony Federico.
Station # 10

Objectives: Network analysis offers a powerful technique to model the relationships between genes within biological regulatory networks. Inference of biological network structures is often performed on high-dimensional data, yet is hindered by the limited sample size of high throughput ‘omics’ data typically available. Comparing networks across multiple phenotypic groups further dilutes already limited sample sizes, presenting an even greater challenge for network inference.

Methods: To overcome these challenges, we present an efficient structure learning framework that exploits known organizing principles of biological networks to incorporate elements of constraint-based and shared learning within a Bayesian inference paradigm. Using this dual-approach we can efficiently learn multiple networks with large-scale data on high performance computing environments in a highly parallel fashion.

Results: We show that our method greatly improves the accuracy and stability of learned networks on simulated data, and recaptures previously validated interactions on real datasets. We reconstructed Pan-Cancer networks with RNA-seq data from The Cancer Genome Atlas (TCGA) to evaluate the method and demonstrate its scalability and found our networks largely recapitulated previous literature findings.

Conclusion: We present a method for building data driven constraints based on fundamental biological principles.

17 MULTI-MODAL MODELS FOR MUTATIONAL SIGNATURES

Kelly Geyer, Masanao Yajima, Jonathan Huggins, Joshua Campbell.

Station # 11

Objectives: Various biological processes can contribute to the overall mutational load observed in human cancers. Each mutational process (or signature) produces a unique fingerprint in the tumor genome by producing different types of mutations. For example, a mutational signature consisting of C>A transversions is most readily observed in lung cancers from smokers while a signature of C>T mutations can be observed in skin cancers caused by UV exposure. Each tumor may have different combinations of each signature. Therefore, methods such as Non-negative Matrix Factorization (NMF) are needed to simultaneously deconvolve each signature and estimate the level of each signature within each tumor. In addition to causing single base substitutions (SBS) in the genome, these mutational processes may also cause other types of alterations such as double-base substitutions (DBS) and insertions and deletions (INDELS).

Methods: NMF and other deconvolution algorithms do not have the capability to deconvolve signatures across multiple data modalities. We address this shortcoming by developing a Poisson Bayesian model that better characterizes mutational signatures using multiple data modalities, called Multi-Modal NMF (MM-NMF).

Results: MM-NMF had promising recovery results in simulated datasets and could recover previously characterized correlations between a C>A SBS signature and CC>AA DBS signature in lung tumors.

Conclusion: The impact of adding additional information into the deconvolution process will also allow for a more complete characterization of the mutational activity within each tumor, which is important for clinical diagnosis and translational medicine.

75 CONAN: DIFFERENTIAL NETWORK CONNECTIVITY ANALYSIS

Lina Kroehling, Oluwatosin Olayinka, Samantha Clayton, Anthony Federico, Eric Reed, Gary Benson, Stefano Monti.

Station # 12

Objectives: Gene expression and other 'omics' data are frequently used to identify biological differences between samples (for example, those from disease and normal groups). Typically, changes are analyzed at the individual gene level, thus missing aggregate changes. We present ConAn (Differential Network Connectivity Analysis), a tool and associated R package, for analyzing changes in gene co-expression modules, or sets of associated genes that are frequently functionally related.

Methods: Gene co-expression modules are sets of genes that display correlated expression levels across samples. They can be represented in a network graph where nodes are genes, edge weights are correlation coefficients, modules are connected components (based on an edge weight cutoff), and module connectivity is the average of the edge weights. ConAn identifies changes in the connectivity of a module between conditions, and uses statistically rigorous resampling-based methods for calculating significance.

Results: Extensive simulations show the high sensitivity and specificity of ConAn. We applied ConAn to a published Breast Cancer dataset and found one differentially connected module upregulated in the luminal A subtype when compared to basal subtypes. The module's hub gene PLN1 is associated with mortality only in the luminal A subtype, and not basal subtype.

Conclusion: ConAn provides an important new methodology for elucidating biologically significant variation through detection of correlated changes. Using this tool, we were able to provide in-silico support for a previously observed pattern of prognosis in BRCA molecular subtypes.

167 HEMATOPOIETIC MOSAIC CHROMOSOMAL ALTERATIONS IN THE NEW ENGLAND CENTENARIAN STUDY.

Anastasia Leshchik.

Station # 13

Objectives: Mosaic chromosomal alterations (mCAs) are structural alterations that include deletions, duplications, or copy-neutral loss of heterozygosity. mCAs are reported to be associated with survival, age, cancer, and cardiovascular disease. Previous studies of mCAs in large population-based cohorts (UK Biobank, MGBB, BioBank Japan, and FinnGen) have

demonstrated a steady increase of mCAs as people age. The distribution of mCAs in centenarians and their offspring is not well characterized.

Methods: We applied MOosaic CHromosomal Alteration (MoChA) caller on 2298 genome-wide genotype samples of 1582 centenarians, 443 centenarians' offspring, and 273 unrelated controls from the New England Centenarian Study (NECS). Integrating Log R ratio and B-allele frequency (BAF) intensities with genotype phase information, MoChA employs a Hidden Markov Model to detect mCA-induced deviations in allelic balance at heterozygous sites consistent with genotype phase in the DNA microarray data. We analyzed mCAs spanning over 100 k base pairs, with an estimated cell fraction less than 50%, within samples with genome-wide BAF phase concordance across phased heterozygous sites less than 0.51, and with LOD score of more than 10 for the model based on BAF and genotype phase.

Results: We used Poisson regression to show that centenarians and their offspring tend to accumulate fewer mCAs (RR = 0.63, p=0.045) compared to the controls.

Conclusion: Our analysis showed that somatic mCAs increase with older age up to approximately 102 years, but the prevalence of the subjects with mCAs tend to decrease after that age, thus suggesting that accumulation of mCAs is less prevalent in long-lived individuals.

103 DIFFERENTIAL REGULATION ANALYSIS QUANTIFIES MIRNA REGULATORY ROLES AND MOLECULAR SUBTYPE-SPECIFIC TARGETS

Boting Ning, Jennifer Beane, Marc Lenburg.

Station # 14

Objectives: Rewiring of transcriptional regulatory networks has been implicated in many biological and pathological processes. However, most current methods for detecting rewiring events (differential network connectivity) are not optimized for miRNA-mediated gene regulation and fail to systematically examine predicted target genes in study designs with multiple groups.

Methods: We developed a novel method to address the current. The method first estimates miRNA-gene expression correlations with Spatial Quantile Normalization to remove the mean-correlation relationship. Then, for each miRNA, genes are ranked by their correlation strength per group. Enrichment patterns of predicted target genes are compared using the Anderson-Darling test and significance levels are estimated via permutation. Finally, graph embedding or difference in enrichment score maximization is performed to prioritize group-specific target genes.

Results: In miR-155 KO RNA-seq data from four mice immune cell types, our method successfully identified miRNA with known regulatory differences and prioritized targets were involved in functional pathways with cell-type specificity. Moreover, the subtype-specific targets identified from the TCGA BRCA data were uniquely altered by miRNA KO in the cell line of the same subtype.

Conclusion: Our work provides a new approach to characterize miRNA-mediated gene regulatory network rewiring across multiple groups from transcriptomic profiles. The method may offer novel insights into cell-type and cancer subtype specific miRNA regulatory roles.

84 ANALYSIS OF LONGITUDINAL NASOPHARYNGEAL MICROBIOME PATTERNS IN MATERNALLY HIV-EXPOSED AND UNEXPOSED INFANTS IN ZAMBIA

Aubrey Odom.

Station # 15

Objectives: Over 1 million HIV-exposed (HIV-E) infants are born to HIV-infected women worldwide every year. We hypothesize that while most of these children will not become infected with HIV, their nasopharyngeal (NP) microbiomes may quantifiably differ from infants that are not HIV-E due to their maternal exposure in the womb.

Methods: Infants were profiled at 2-3 week intervals over 3.5 months with maternal NP swabs also collected on the first and last dates. HIV-E (n=10) and healthy control (n=10) infants were matched for statistical analysis based on the month of study entry and mother's age and education. Swabs were processed using 16S ribosomal sequencing. We used Hotelling T-squared test statistics to test whether microbiome profiles in paired infants were notably varied among the 7 timepoints, and if HIV-E mothers and infants had similar profiles at the first and last timepoints. Linear mixed models with fixed effects of timepoint and HIV status and

random subject intercepts enabled prediction of relative taxon abundances for infants.

Results: We found that paired infants only presented significantly different microbiome profiles at the second of 7 timepoints ($p=0.0225$). HIV-E mothers-infant pairs had significantly different profiles at the first timepoint, although control mother-infant pairs did not ($p=0.3337$). Linear mixed models showed that of 14 species tested, 12 exhibited substantial instability across timepoints, and 7 were highly associated with HIV exposure in infants.

Conclusion: From our preliminary findings, we find key insights that allow us greater understanding into the ways in which HIV-E infant microbiomes are influenced by their mother's vaginal microbiome.

Session 1 – Floor 2 Thursday 10/7 9:30 am - 10:30 am

97 IL-23 SIGNALING IN EARLY STAGE LUNG CANCERS

Roxana Pfefferkorn, Emily Green, Eric Burks, Jennifer Beane, Sarah Mazzilli.

Station # 1

Objectives: Interleukin-1B (IL-1B) is a well-known mediator of inflammation and immune modulation. IL-1B promotes tumor invasiveness and induces pro-inflammatory cytokine IL-23, which increases cell proliferation through interaction with the immune microenvironment. Inhibition of IL-1B was found to reduce both the incidence and mortality of non-small cell lung cancer; however, the role of IL-23 in the context of lung cancer progression is still unclear.

Methods: We address this through a comparative study of tumor microarrays (TMA) of early-stage lung adenocarcinomas (LUAD, $n=180$) and lung squamous cell carcinoma (LUSC, $n=100$) to explore the IL-23 dependent tumor microenvironment. TMA cores were stained for proteins involved in IL-23 signaling (IL-23, IL-17, pStat3) and immune cell markers (CD3, CD163, MPO, CD56) QuPath was used for quantification of staining intensity through tissue identification, cell segmentation, and tissue classification of the TMA cores.

Results: We found a significant ($p<0.001$) correlation between pStat3 and IL-17 expression in immune infiltrates of LUAD but not LUSC samples. IL-17 expression was significantly ($p<0.001$) correlated with neutrophil recruitment and invasion into the tumor in both LUSC and LUAD.

Conclusion: We are also investigating these markers in whole lung tumor sections to investigate peripheral changes in IL-23 signaling and associate these findings with serum levels of these markers from the same patients to uncover the role of IL-23 in lung tumor progression for development of targeted immunotherapies and earlier detection.

Session 1 – Floor 2 Thursday 10/7 9:30 am - 10:30 am

132 IMMUNE CHARACTERIZATION IN BRONCHIAL PREMALIGNANT LESIONS USING SCRNASSEQ

Conor Shea, Ipsita Dey-Guha, Avrum Spira, Mary Reid, Marc Lenburg, Sam Janes, Jennifer Beane, Sarah Mazzilli, Joshua Campbell.

Station # 2

Objectives: Immune escape mechanisms and a depletion of immune cells have been associated with histologic progression of bronchial premalignant lesions and progression to invasive lung squamous carcinoma. Single-cell RNA sequencing (scRNAseq) of these lesions may further elucidate the cross-talk between epithelial and immune populations in progressive versus regression lesions.

Methods: Seventeen lesions were biopsied via bronchoscopy. Cells were sorted by CD45+/- FACS gating for Cel-Seq2 sequencing. Celda was used to bi-cluster genes into modules and cells into clusters. Cell types were labeled by marker gene expression. Bulk RNA sequencing of matched samples was used to study the expression of inflammation-related genes, which may go undetected in scRNAseq data.

Results: After QC, we analyzed 1,234 leukocytes (median $n_{UMI} = 2215$; median $n_{Gene} = 962$). Subpopulations identified include macrophages, CD4/8+ T, B, and natural killer cells. Samples with high grade histology (dysplasia, carcinoma *in situ*) were enriched in CD4+ Tregs and myeloid cells compared to low grade histology samples (hyperplasia, metaplasia), which were enriched in Natural Killer and cytotoxic CD8+ T cells ($\chi^2 = 298.95$, $p = 0.001$). The anti-

inflammatory gene TGF β was upregulated in high grade compared to low grade lesions (linear model, $p = 0.002$).

Conclusion: Our results suggest a change in immune composition and inflammatory responses across lesion histology that suggest a shared role for the immune system in premalignancy and malignancy. The immune signatures we derive can suggest potential targets for immune-mediated chemoprevention, some of which may be druggable.

127 USING DEEP LEARNING TO CHARACTERIZE PATHOLOGY IMAGES OF BRONCHIAL PREMALIGNANT LESIONS

Divya Venkatraman, Rushin Gindra, Emily Green, Sarah Mazzilli, Eric Burks, Vijaya Kolachalama, Jennifer Beane.

Station # 3

Objectives: Lung squamous cell carcinoma arises in the epithelial layer of the bronchial airways and is preceded by the development of bronchial premalignant lesions (PMLs). Pathological assessments of PMLs have significant intra- and inter-observer variability, so we sought to use deep learning to identify features in the H&E stains whole slide images (WSIs) associated with PML histology.

Methods: Two thoracic pathologists independently assigned histology grades to the epithelium in human endobronchial biopsies whole slide images (WSIs) ($n=93$). Using the expert annotations, we developed two deep learning approaches, a supervised segmentation network and an unsupervised sparse autoencoder framework, to quantify detailed tissue-level characteristics of PMLs on the WSIs.

Results: The inter-annotator agreement on the WSIs was 0.2970, and our supervised network based on the pathologist annotations achieved a mean Dice score of 0.4198, indicating moderate performance. The unsupervised framework, however, encoded the nuclei in individual patches and clustered them into 8 different groups, thus capturing nuclei-level features. The clusters were qualitatively associated with pathologist PML histology.

Conclusion: Overall, we show that deep learning may be used to guide pathologists in PML grading and may improve biomarkers of PML progression.

134 INTERACTIVE ANALYSIS OF SINGLE-CELL RNA-SEQUENCING DATA WITH SINGLE-CELL TOOLKIT (SCTK)

Yichen Wang.

Station # 4

Objectives: Single-cell RNA sequencing (scRNAseq) allows researchers to profile transcriptional activity in individual cells.

Methods: We developed the Single Cell Toolkit (SCTK), an scRNAseq analysis package that enables users to perform scRNAseq analysis interactively with a graphic user interface (GUI).

Results: With SCTK, users without programming experience can perform quality control, normalization, dimension reduction, clustering, differential expression, pathway projection, and cell type annotation using popular packages such as Seurat.

Conclusion: Compared to other analysis packages, SCTK brings together more options that allows for deeper customization, exploration, and visualization of their data. For more information, visit setk.camplab.net.

with dementia from those with normal cognition. For the task related to classification of demented participants from non-demented ones, the LSTM model achieved a mean AUC of 0.659 ± 0.043 , and the CNN model achieved a mean AUC of 0.730 ± 0.039 .

Conclusion: This proof-of-concept study demonstrates the potential that raw audio recordings of neuropsychological testing performed on individuals recruited within a community cohort setting can provide clues to assessing dementia status.

69 AN INDUCED PLURIPOTENT STEM CELL BASED MODEL TO STUDY LUNG MESENCHYME DEVELOPMENT AND DISEASE

Andrea Alber, Liang Ma, Hector Marquez, Carlos Villacorta-Martin, Jonathan Lindstrom-Vautrin, Laertis Ikonou, Darrell Kotton.

Station # 7

Objectives: In this project we aim to establish an induced pluripotent stem (iPS) cell-based model to study lung mesenchyme development, epithelial-mesenchymal interactions and to model respiratory diseases affecting the lung mesenchyme.

Methods: We have generated an iPS cell line from a published Tbx4 lung enhancer reporter (Tbx4-LER) mouse, which specifically labels lung mesenchymal progenitors by GFP expression, and have established a protocol for the *in vitro* differentiation of these iPSCs towards the lung mesenchymal lineage. We have also developed a system for co-culture of lung mesenchymal and lung epithelial progenitors.

Results: Our differentiation protocol yields an average of 25% of GFP+ lung mesenchymal progenitors. RT-qPCR and single cell RNAseq show that GFP+ cells express various lung mesenchyme markers at similar levels as primary embryonic mouse lung mesenchyme. Furthermore, GFP+ cells are competent to differentiate towards more mature mesenchymal lineages such as smooth muscle and lipofibroblasts. Recombinant cultures of GFP+ lung mesenchymal and Nkx2-1+ lung epithelial progenitors form 3D organoids composed of juxtaposed derivatives of epithelium and mesenchyme, and retain more Nkx2-1 expression than Nkx2-1+ cells cultured alone. Finally GFP+ cells can induce lung epithelial fate when co-cultured with non-lung epithelial progenitors.

Conclusion: We have generated and purified an iPSC-derived population expressing key features of the functional and molecular phenotype of developing lung mesenchymal progenitors, providing a new tool to study lung development, a model of mesenchymal-epithelial interactions, and a platform to study lung mesenchymal diseases.

140 PATIENT-SPECIFIC IPSCS CARRYING AN *SFTPC* MUTATION REVEAL THE INTRINSIC ALVEOLAR EPITHELIAL DYSFUNCTION AT THE INCEPTION OF INTERSTITIAL LUNG DISEASE

Konstantinos Alysandratos, Scott Russo, Anton Petcherski, Evan Taddeo, Rebeca Acín-Pérez, Carlos Villacorta-Martin, J. C. Jean, Surafel Mulugeta, Luis Rodriguez, Benjamin Blum, Ryan Hekman, Olivia Hix, Kasey Minakin, Marall Vedaie, Seunghyi Kook, Andrew Tilston-Lunel, Xaralabos Varelas, Jennifer Wambach, F. Cole, Aaron Hamvas, Lisa Young, Marc Liesa, Andrew Emili, Susan Guttentag, Orian Shirihai, Michael Beers, Darrell Kotton.

Station # 8

Objectives: Alveolar epithelial type 2 cell (AEC2) dysfunction is implicated in the pathogenesis of adult and pediatric interstitial lung disease (ILD), including idiopathic pulmonary fibrosis (IPF), however, identification of disease-initiating mechanisms has been impeded by inability to access primary AEC2s early on.

Methods: Here we present a human *in vitro* model permitting investigation of epithelial-intrinsic events culminating in AEC2 dysfunction, using patient-specific induced pluripotent stem cells (iPSCs) carrying an AEC2-exclusive disease-associated variant (*SFTPC*^{L73T}).

Results: Comparing syngeneic mutant vs gene-corrected iPSCs after differentiation into AEC2s (iAEC2s) we find that mutant iAEC2s accumulate large amounts of misprocessed and mistrafficked pro-SFTPC protein, similar to *in vivo* changes, resulting in diminished AEC2 progenitor capacity, perturbed proteostasis, altered bioenergetic programs, time-dependent metabolic reprogramming, and NF- κ B pathway activation. Treatment of *SFTPC*^{L73T}-expressing iAEC2s with hydroxychloroquine, a medication used in pediatric ILD, aggravates the observed perturbations.

Conclusion: Thus, iAEC2s provide a patient-specific preclinical platform for modeling the epithelial-intrinsic dysfunction at ILD inception.

89 A MULTIMODAL iPSC PLATFORM FOR CYSTIC FIBROSIS DRUG TESTING

Andrew Berical.

Station # 9

Objectives: CFTR modulators are approved in a subset of individuals with CF, however hundreds of disease-causing mutations have been described and many patients continue to struggle without targeted therapy. Less common CFTR mutations such as the class 1 premature stop codons have been difficult to study using existing pre-clinical models. iPSCs are now routinely generated from anyone and can be differentiated into CFTR-expressing airway epithelial cells. This platform has great potential for CFTR functional testing and development of future therapeutic options.

Methods: We differentiated patient-derived iPSCs into airway epithelial cells using published protocols. We then adapted two known assays of CFTR function - 3D forskolin induced swelling and electrophysiologic testing - to our iPSC-derived cells, in the presence and absence of approved as well as experimental CFTR modulators.

Results: Using non-CF donors as well as CF donors (3 separate CFTR genotypes), we found that iPSC-derived airway epithelial cell spheroids swell in response to forskolin via a CFTR dependent mechanism, with improvement after CFTR modulator treatment. Similarly, we generated iPSC-derived ALI cultures and tested electrophysiologic response to CFTR modulators. Phe508del cultures demonstrate significant modulator rescue of both forskolin generated as well as CFTR-specific current in 3/3 cell lines.

Conclusion: In conclusion, we have adapted two separate assays which demonstrate baseline and rescued function of the CFTR channel. This platform may hold significant potential for the development of novel therapeutics for less common CFTR mutations, such as the class 1 non-sense mutations.

39 GENERATION OF HUMAN ALVEOLAR EPITHELIAL TYPE I CELLS FROM PLURIPOTENT STEM CELLS

Claire Burgess, Carlos Villacorta-Martin, Xaralabos Varelas, Darrell Kotton.

Station # 10

Objectives: In the distal lung, alveolar epithelial type I cells (AT1s) are uniquely flattened to allow for the diffusion of oxygen into the capillaries. This structure has made them challenging to study and isolate. As a result, there are no established models for the study of human AT1 biology, and little is known about the mechanisms regulating their differentiation. We sought to engineer a human *in vitro* model of AT1s through the directed differentiation of induced pluripotent stem cells (iPSCs). The Hippo signaling pathway has been implicated in mouse AT1 development, so we tested the effect of the Hippo pathway effector YAP in self-renewing mature iPSC-derived iAT2s.

Methods: Cells were transduced with a lentivirus encoding constitutively active nuclear YAP (YAP-5SA) or a control WT-YAP lentivirus. We performed bulk RT-qPCR and observed loss of SFTPC and upregulation of multiple AT1 markers. To study this transition in more detail, including cell population heterogeneity, we performed single cell RNA sequencing on the lentiviral-transduced cells.

Results: We observed that those expressing YAP-5SA appear to cluster separately from control iAT2s by UMAP projection and have downregulated AT2 genes while upregulating AT1-specific genes, including AGER, CAV1, and PDPN. Additionally, we developed a reporter iPSC line containing a knock-in AGER^{tdTomato} that is detectable post YAP-5SA transduction, allowing for the tracking and isolation of AT1-marker expressing cells.

Conclusion: Our results suggest a role for the Hippo effector protein YAP in the differentiation of human AT1s and establishes an iPSC reporter line able to serve as a potential human AT1 *in vitro* model system.

101 MULTI-MODAL CHARACTERIZATION OF THE PERIPHERAL BLOOD OF CENTENARIANS AT SINGLE CELL RESOLUTION REVEALS A DISTINCT IMMUNE CELL TYPE COMPOSITION AND TRANSCRIPTIONAL SIGNATURE OF EXTREME LONGEVITY

Todd Dowrey, Tanya Karagiannis, Carlos Villacorta Martin, Paola Sebastiani, Stefano Monti, Thomas Perls, George Murphy.

Station # 11

Objectives: Humans have the innate ability to live longer, healthier lives. One example of this is the exceptional lifespan and healthspan displayed by centenarians or those who live in excess of 100 years of age. Interestingly, the immune system of these individuals may be more effective at combatting insult and disease that occurs throughout a typical lifetime. We set out to profile the immune system of centenarians at unprecedented resolution to identify a signature of exceptional longevity that supports resilience to aging-related disease.

Methods: Whole blood samples were collected from 7 centenarians and 2 younger aged controls and used to isolate peripheral blood mononuclear cells. These PBMCs were then analyzed using the combination of single cell transcriptional and antibody-derived tag (ADT) protein-level multimodal profiling.

Results: The centenarian immune systems displayed a higher cell type distribution score when compared to younger aged controls, which indicates a more diverse and potentially more effective immune system that persists to extreme age. Centenarians also show a unique transcriptional signature independent of typical aging which was enriched for pathways that relate to immune activation and metabolic processes.

Conclusion: We identified distinct differences in the immune systems of centenarians which may contribute to enhanced resiliency and the ability to evade aging-related disease. Induced pluripotent stem cell lines have been generated from these centenarians which can be used as an in vitro model system to investigate and validate proposed resiliency mechanisms and treatments aimed at combatting aging-related disease.

52 HORMONE THERAPY TO ACCELERATE REGENERATION FROM SEXUALLY DIMORPHIC ACETAMINOPHEN-INDUCED LIVER INJURY

Elissa Everton, Carlos Villacorta-Martin, Jonathan Lindstrom-Vautrin, Fatima Rizvi, Valerie Gouon-Evans.

Station # 12

Objectives: Acetaminophen (APAP) is the most commonly used pain reliever in the United States, yet overdose is the leading cause of acute liver failure in the world. The only available treatments are N-acetyl cysteine (NAC), which only has a short window of effectiveness, or liver transplant.

Methods: Sex hormones drive sexual dimorphism in many liver processes, and more constant growth hormone (GH) secretion in females contributes to higher metabolic activity compared to male livers. This project deciphers the mechanism of sexual dimorphism in APAP-induced liver injury and repair, and leverages it by utilizing GH therapy to accelerate liver recovery in both sexes.

Results: Consistent with literature, our data show higher resistance of female mice to APAP, shown by reduced liver necrosis, cell death, and detection of serum injury markers compared to males. After injury, our scRNA-seq analyses reveal that female hepatocytes express significantly greater levels of GH receptor and GH pathway activation, and that female endothelial cells express greater levels of the receptor for the GH mediator IGF-1 than their male counterparts. We also found that one injection of recombinant hGH significantly and rapidly repairs the liver tissues of both males and females following sex-specific sub-lethal doses of APAP and promotes survival compared to NAC-treated controls.

Conclusion: These data suggest a regenerative advantage in female livers, which can be recapitulated with GH treatment to accelerate recovery in both sexes. Understanding the biological mechanisms behind these processes will provide the biological foundation to establish a GH therapy to treat APAP overdose, a currently unmet clinical need.

151 PSC-DERIVED ORGANOID BASED MODEL OF INTESTINAL FILOVIRUS INFECTION

Elizabeth Yvonne Flores, Elke Mühlberger, Gustavo Mostoslavsky.

Station # 13

Objectives: Affected Ebola virus (EBOV) disease patients lose copious amounts of fluids in a matter of days, rapidly deteriorating into hypovolemic shock and death. Similar intestinal manifestations were also reported for Marburg (MARV) disease, another filovirus. At present, no animal models available, including non-human primates, can recapitulate the gastrointestinal symptoms of EVD patients. Our objective is to establish a human intestinal infection platform to model the effects of filovirus infection on intestinal epithelial integrity.

Methods: We generated a recombinant EBOV expressing ZsGreen as a reporter gene and used this virus to infect day 30 colonic HIOs. Robust EBOV-ZsGreen infection was observed at 1 day post-infection (dpi) followed by virus spread by 3 dpi. Day 30 colonic HIOs were infected with EBOV or MARV at an MOI of 10 or left uninfected. Cellular RNA was harvested at 1 and 3 dpi and used for Illumina bulk RNA-sequencing of triplicate samples.

Results: Successful robust EBOV and MARV infections of iPSC-derived HIOs, affecting mostly epithelial CDX2⁺ enterocytes was achieved. The infected cells showed signs of cell damage, and transcriptomics analysis indicated the modulation of cell junction pathways and a set of ion transporters known to play a role in the induction of diarrhea.

Conclusion: Taken together, these data suggest EBOV and MARV compromise barrier integrity of the intestinal epithelium and cause abnormal ion flux as the basis for gastrointestinal dysfunction and diarrhea.

135 HIPSC-DERIVED NEURONS FROM CJD INDIVIDUALS WITH THE E200K MUTATION RECAPITULATE PATHOLOGICAL HALLMARKERS OF THE DISEASE

Aldana Gojanovich, Nhat Le, Robert Mercer, David Harris, Gustavo Mostoslavsky.

Station # 14

Objectives: Genetic Creutzfeldt-Jakob disease (gCJD) caused by the E200K mutation on the PRNP gene encoding the prion protein is the most common subtype of genetic prion disease worldwide. We report the establishment of the largest CJD E200K-specific hiPSC library and their differentiation towards cortical neurons to characterize the mutant PrP.

Methods: Samples for reprogramming were obtained from 22 individuals of a large family including carriers and non-carriers of the E200K mutation. Some of these hiPSC lines were selected for differentiation into pyramidal cortical neurons, a brain region highly affected by this mutation.

Results: A systematic comparison of hiPSC-derived neurons expressing E200K PrP to those expressing only the normal form revealed the presence of disease-relevant phenotypes. By analyzing the biochemical properties of PrP and Tau protein, a microtubule-associated protein involved in neurodegenerative diseases known as tauopathies, we found that the E200K hiPSC-derived neurons accumulate pathological forms of PrP which co-localize with paired helical filaments of tau protein. Neurofibrillary tangle-like aggregates of tau and neurofilament were also observed. At the postsynaptic site, N-Methyl-D-aspartic acid receptors and postsynaptic density 95 colocalization is disrupted in neurons expressing E200K PrP.

Conclusion: Our study shows, for the first time, that hiPSC-derived neurons expressing endogenous levels of mutant PrP can model certain aspects of human prion disease, offering a powerful platform for investigating subtype pathologies and testing putative therapeutics.

141 NOTCH ACTIVATION DURING MESODERM INDUCTION MODULATES EMERGENCE OF THE T/NK CELL LINEAGE FROM HUMAN IPSC.

Dar Heinze, Seonmi Park, Andrew McCracken, Mona Haratianfar, Jonathan Lindstrom-Vautrin, Carlos Villacorta-Martin, Aditya Mithal, George Murphy, Gustavo Mostoslavsky.

Station # 15

Objectives: Develop a robust method of producing mature T cells from iPSCs to study T cell biology and for CAR-T therapy. Notch 1 is known to be required for the production of definitive hematopoietic stem cells *in vivo*, leading us to hypothesize that activation of the Notch pathway would drive access to the T/NK cell lineage.

Methods: A Tet-On construct driving the expression of the Notch 1 intracellular domain was inserted into multiple iPSC lines. These were used in an optimized hematopoietic progenitor differentiation protocol followed by co-culture with OP9:hDLL4 feeder cells or an FC-DLL4 coating to drive T/NK cell specification.

Results: We found Notch activation from day 0-2 of differentiation yielded a robust increase in T/NK lineage cells. Probing this result further, we showed that only the putative hemogenic endothelial population normally turns on the notch pathway, and that exogenous Notch activation does not alter cell cycle phase or appear to delay or accelerate differentiation time-lines. In the co-culture environment, hematopoietic progenitor density was a key determinant of T vs NK lineage fate. We confirmed T cell identity with surface markers, the upregulation of T cell genes, scRNA seq, and robust proliferation of stimulated cultures. Finally, a feeder-free T cell maturation protocol produced a very consistent T cell population by day 40, however stimulation yielded a marked shift toward gamma-delta T cells.

Conclusion: Early Notch activation augments normal Notch upregulation during hematopoietic differentiation to yield progenitors with improved T/NK cell potential. These cells mature into CD8+ T cells, however additional work is needed to improve TCR-AB output.

Session 1 – Floor 3 Thursday 10/7 9:30 am - 10:30 am

70 TRANSPLANTATION OF MURINE PLURIPOTENT STEM CELL DERIVED DISTAL TIP-LIKE CELLS INTO IMMUNOCOMPETENT MICE

Michael Herges, Carlos Villacorta-Martin, Darrell Kotton.

Station # 1

Objectives: Recent work suggests that mouse Sox9+ embryonic lung epithelial tip cells cultured *in vitro* can engraft and differentiate in injured immunocompromised mouse lungs, providing a potential method for cell-based therapy of lung injury. However, the use of primary embryonic donor cells and immunocompromised recipients severely limits the clinical applicability of this approach. Directed differentiation of mouse pluripotent stem cells (mPSCs) may provide an alternative source of donor cells, but current protocols do not produce Sox9+ progenitor cells comparable to those generated by primary culture.

Methods: Here we describe an optimized protocol for the directed differentiation of mPSCs into distal tip-like cells.

Results: The resulting cells express high levels of distal tip markers, maintain low levels of mature alveolar markers, and can be expanded in culture, similar to cultured primary embryonic tip cells. These mPSC-derived tip-like cells can then be transplanted into syngeneic and immunocompetent injured mouse lungs, where they gave rise to AT1-like and AT2-like cells, as characterized by immunohistochemistry and single cell sequencing.

Conclusion: Together this work provides the first evidence of successful transplantation of PSC-derived cells into immunocompetent mice. Further characterization of this model system will provide important information for the development of PSC-derived cell therapy of human pulmonary diseases.

60 MECHANISMS OF SELF-RENEWAL OF iPSC-DERIVED ALVEOLAR EPITHELIAL TYPE 2 CELLS

Jessie Huang, Carlos Villacorta-Martin, Darrell Kotton.

Station # 2

Objectives: Alveolar epithelial type 2 cells (AEC2s) are facultative progenitors that are normally quiescent, but can proliferate upon lung injury. We previously developed an *in vitro* human iPSC-derived AEC2 (iAEC2) model in which putative AEC2-like cells can self-renew in 3D sphere cultures, but the signals that drive this extensive self-renewal remain to be thoroughly defined. Thus, the objective is to determine pathways that may have roles in iAEC2 self-renewal.

Methods: Directed differentiation of iAEC2s was performed on the “SPC2” iPSC line carrying an SFTPC^{tdTomato} reporter. iAEC2s were passaged using single-cell dissociation every 10-14 days. Proliferation kinetics of iAEC2s was assessed via EdU uptake, and 6 time points during one 14-day passaging cycle were chosen for scRNA-seq. Changes in gene expression were validated by RT-qPCR. Small molecule inhibitors were added to iAEC2s in culture, and cells

imaged with fluorescence microscopy and processed for RT-qPCR.

Results: iAEC2s proliferate robustly at the beginning of each passage, with reduced proliferative capacity as they become confluent in culture, followed by resumed proliferative state after passaging. AEC2 markers peak at 7 days after each passage. Expression of transcriptomic signatures of AEC2 maturation were inversely correlated with cytokinesis markers, indicating a cyclic pattern of self-renewal and gene expression alterations over time in culture.

Conclusion: We applied an unbiased analysis of temporal changes in signaling pathways during iAEC2 self-renewal, and future analyses of this dataset may provide critical insight into how AEC2s contribute to alveolar repair and lung regeneration.

157 CHARACTERIZING AATD ASSOCIATED METABOLIC DYSREGULATION IN SYNGENEIC PATIENT iPSCS

Joseph Kaserman, Feiya Wang, Jonathan Lindstrom-Vautrin, Carlos Villacorta-Martin, Andrew Wilson.

Station # 3

Objectives: Alpha-1 antitrypsin deficiency (AATD) is an inherited cause of chronic liver disease driven by accumulation of misfolded protein aggregates and ER stress. We have previously shown that iPSC-derived hepatic cells (iHeps) that express the Z mutation have evidence of transcriptomic alterations across multiple metabolic pathways, and we hypothesize that ZZ and MZ iHeps will have metabolic dysregulation resulting from proteotoxic driven ER stress and mitochondrial dysfunction.

Methods: We selected iPSCs from ZZ AATD patients and that have undergone CRISPR-based correction generating syngeneic MZ and MM iPSCs. Syngeneic iPSCs were differentiated to the hepatic stage and the global metabolome was profiled using liquid chromatography-mass spectrometry with extraction methods to enrich for both the lipid and amide metabolites.

Results: Principle component analysis from both the amide and lipid metabolome demonstrated three clusters separated by AAT genotype. When ZZ and MZ were compared to MM iHeps there were 128 and 132 differential metabolites. Applying pathway mapping we found that ZZ and MZ iHeps were significantly enriched in branched chain amino acid biosynthesis and aminoacyl-t RNA biosynthesis while MM iHeps were enriched in synthetic pathways including the urea cycle. Concordant with these findings analysis of our transcriptomic data showed that there was downregulation of key urea cycle enzymes in ZZ and MZ iHeps.

Conclusion: Metabolomic profiling of ZZ and MZ iHeps demonstrated dysregulation of multiple metabolic pathways associated with the ER and mitochondria including ureagenesis.

115 UTILIZING THE IPSC DIRECTED DIFFERENTIATION PLATFORM TO IDENTIFY DOSE AND STAGE DEPENDENT ROLES OF BMP, TGF-B AND RETINOIC ACID SIGNALING IN LUNG PROGENITOR SPECIFICATION

Jake Le Suer.

Station # 4

Objectives: The directed differentiation of human induced pluripotent stem cells (hiPSCs) to alveolar and airway lineages first requires specification of lung progenitors, identified by expression of transcription factor NKX2.1. However, due to an incomplete knowledge and imprecise implementation of key signaling pathways in foregut patterning and lung specification, the efficacy of NKX2.1+ lung progenitor specification in the directed differentiation protocol is variable and low. Given their well-documented role in lung development we hypothesized that BMP, TGF-B and Retinoic Acid signaling pathways could be more precisely modulated in our directed differentiation platform to increase the proportion of cells specified towards an NKX2.1+ lung epithelial fate.

Methods: BMP, TGF-B and Retinoic Acid were activated, inhibited or omitted during foregut patterning and lung specification.

Results: Increased cell density, reduced concentration of BMP and TGF-B inhibitors during anteriorization and removal of Retinoic Acid during lung specification, together resulted in over a 4 fold increase in the percentage NKX2-1GFP+ cells. Additionally, we identified a relationship between the density of iPSCs prior to differentiation and concentration of BMP

and TGF-B inhibitors during anteriorization required to drive robust NKX2.1 induction.

Conclusion: In summary, the data underscores dose and timing dependent roles for BMP, TGF-B, Retinoic Acid signaling during foregut patterning and lung specification using this in vitro model of human lung development.

45 REGENERATION OF MOUSE TRACHEAL EPITHELIUM VIA SYNGENEIC TRANSPLANTATION OF PLURIPOTENT STEM CELL-DERIVED BASAL-LIKE CELLS

Liang Ma, Bibek Thapa, Michael Herriges, Jonathan Lindstrom-Vautrin, Carlos Villacorta-Martin, Darrell Kotton.

Station # 5

Objectives: Our goal is to reconstitute injured or diseased airway epithelium via transplantation of airway stem cells generated from pluripotent stem cells (PSC) as a pre-clinical step towards cell-based therapy for airway diseases such as cystic fibrosis.

Methods: Mouse PSCs were differentiated into airway basal-like cells (iBCs) via directed differentiation, whereby the milestones of lung development are recapitulated in vitro. iBC cultures were analyzed with FACS, qPCR, and scRNA-Seq. iBCs were then labeled with a GFP-expressing lentivirus and transplanted into syngeneic immunocompetent WT mouse tracheas post-airway epithelial injury. Recipient tracheas were analyzed by FACS, and IF microscopy and scRNA-Seq. A second round of injury with EdU labeling were used to study whether transplanted cells can participate in post-injury repair.

Results: iBC cultures were mainly composed of *Ngfr*⁺ basal-like cells with a minor population of secretory-like cells. 2 months post-transplantation, GFP⁺ iBC comprised up to ~50% of recipient tracheal epithelium while maintaining airway epithelial fate (*Nkx2.1*⁺, *Sox2*⁺), contributing to basal (*Krt5*⁺, *Trp63*⁺), secretory (*Scgb1a1*⁺, *Cftr*⁺), and ciliated (*Foxj1*⁺, *Dnah5*⁺) cell populations. While GFP⁺ cells assumed quiescence after epithelial reconstitution, 1 week after a second round of injury, EdU⁺/GFP⁺ cells were observed, indicating GFP⁺ cells can re-enter cycle in response to injury.

Conclusion: In vitro directed differentiation of mPSCs results in airway basal-like cells that can be transplanted into syngeneic immunocompetent mouse trachea epithelium, contribute to major airway epithelial lineages, and participate in airway regeneration.

146 DEFINING NKX2-1-DEPENDENT TRANSCRIPTOMIC SIGNATURES IN LUNG DEVELOPMENT

Taylor Matte, Mary Lou Beermann, JC Jean, Jonathan Lindstrom-Vautrin, Jonathan Lindstrom-Vautrin, Carlos Villacorta Martin, Jake LeSuer, Andrew Berical, Darrell Kotton, Finn Hawkins.

Station # 6

Objectives: NK2 Homeobox 1 (NKX2-1) is a critically important transcription factor in lung development, with all lung epithelia being derived from an NKX2-1+ progenitor pool. *Nkx2-1* knockout mice have hypoplastic lungs, and humans with *NKX2-1* mutations suffer from respiratory insufficiency, hypothyroidism, and neurological problems, a disease known broadly as brain-lung-thyroid syndrome. Despite its known importance, NKX2-1's developmental role is not fully defined.

Methods: To study this role, we harnessed iPSCs generated from a patient with a frameshift mutation in exon 3 of *NKX2-1*, with expected haploinsufficiency. This cell line was CRISPR corrected while also inserting a GFP reporter, producing two isogenic lines that differ only at the *NKX2-1* locus. Directed differentiations to an alveolar fate were performed in both lines, with NKX-GFP+ cells being sorted and RNA sequenced at three developmental timepoints.

Results: RNA-seq analysis revealed a transcriptomic signature that increasingly diverged between mutant, corrected cells over time. Among these transcriptomic differences, we observed downregulation of surfactant proteins in mutant alveolospheres, consistent with previous data. There was also upregulation of airway markers in mutant cells at the most mature timepoint, pointing to NKX2-1's role in proximal-distal patterning during development.

Conclusion: In summary, these experiments provide insight into the developmental consequences of aberrant NKX2-1 activity.

117 DERIVATION OF THYROID PROGENITORS FROM HUMAN INDUCED PLURIPOTENT STEM CELLS

Alberto Posabella, Hendrik Undeutsch, Andrea Alber, Anita Kurmann, Anthony Hollenberg, Darrell Kotton.

Station # 7

Objectives: Hypothyroidism resulting from congenital lack of functional thyrocytes, surgical tissue removal, or gland ablation, represents a particularly attractive endocrine disease target that may be conceivably cured by transplantation of long-lived functional thyroid progenitors or mature follicular epithelial cells.

Methods: To generate thyroid follicular progenitors from human induced pluripotent stem cells (hiPSCs), we sought to develop a directed differentiation approach by activating or inhibiting endogenous developmental signaling pathways. Thus, we engineered an hiPSC-line carrying a tdTomato reporter targeted to the PAX8 locus and a GFP reporter targeted to the NKX2-1 locus.

Results: We profiled all cells (regardless of fluorochrome expression) captured on days 12 and 29 of in vitro differentiation. By day 12, tdTomato/GFP co-expression was observed in 17% of all cells and these cells appeared to be early thyroid follicular progenitors as they uniquely co-expressed the thyroid lineage selective transcription factors, NKX2-1, PAX8, FOXE1, and HHX. By day 29 tdTomato+/GFP+ cells represented 72.1% of all cells and had upregulated TG, TSHR, NIS and TPO expression in addition to the previously described four thyroid lineage markers, suggesting time-dependent differentiation and maturation of thyroid follicular epithelial cells

Conclusion: Thus, we have employed a novel hiPSC line to optimize a protocol able to generate human thyroid progenitors and mature follicular epithelial cells, representing a purifiable source of human thyroid lineage cells whose functional and thyroid reconstituting potential can be tested in vivo in animal models of hypothyroidism.

59 VEGFA INDUCES CHOLANGIOCYTE DRIVEN LIVER REGENERATION IN MOUSE MODELS OF LIVER INJURY

Fatima Rizvi, Elissa Everton, Valerie Gouon Evans.

Station # 8

Objectives: The remarkable proliferative capacity of hepatocytes becomes severely compromised in case of massive acute liver injury or chronic disease. Growing evidence supports the notion that biliary epithelial cells (BEC) can undergo hepatocyte conversion when hepatocyte proliferation is exhausted. This raises an exciting possibility to exploit the regenerative potential of BECs by forcing their cell conversion into hepatocytes to treat liver diseases. We hypothesize that liver injury in mice induces in a subset of BECs expression of KDR (VEGFR2) that could potentially be activated by VEGFA to induce BEC-to-hepatocyte conversion.

Methods: viral vector was administered to impair hepatocyte proliferation. Following injury, injections of nucleoside modified mRNA encoding VEGFA complexed to lipid nanoparticles were administered intravenously. Experiments were conducted in *Krt19-Cre-ERT2; R26-STOP^{FL/FL}*-tdTomato mice to fate trace BECs and *Kdr-2A-Cre^{ERT2}-2A-eYFP,R26^{LSL}*-tdTomato to trace KDR-expressing cells.

Results: Both acute and chronic liver injuries induced KDR expression on a subset of BECs. The BEC lineage tracing as well as tracing of KDR-expressing cells indicated that transient VEGFA expression in the liver robustly increased the numbers of tdTomato-positive hepatocytes, as well as fully reverted steatosis and fibrosis in chronically injured livers.

Conclusion: Altogether, this study reveals a novel therapeutic benefit of VEGFA to harness BEC-driven liver regeneration to treat chronic and acute liver diseases.

148 MODELING COLORECTAL CANCER INITIATION USING HUMAN iPSC-DERIVED INTESTINAL ORGANOIDS

Victor Schingo, Andrew McCracken, Dar Heinze, Aditya Mithal, Gustavo Mostoslavsky.

Station # 9

Objectives: Our objective is to model pre-cancerous events in human colorectal cancer (CRC) formation using iPSC-derived intestinal organoids with inducible expression of three oncogenes. Mutations in KRAS, EGFR, and CTNNB1 are commonly associated with the

development of CRC. We have used a CDX2-GFP+ human induced pluripotent stem cell (iPSC) line to generate lines containing an inducible form of all three oncogenes and the reporter BFP knocked-in into the AAVS1 safe harbor locus.

Methods: We confirmed the appropriate integration of all three oncogenes KRAS (G12D), EGFR (L858R), and CTNNB1 (S33C) via PCR, gel electrophoresis, and Sanger sequencing. Oncogene expression was verified by increased concentrations of doxycycline induction in our undifferentiated iPSC, analyzed by flow cytometry and qRT-PCR.

Results: We found that in the KRAS and EGFR iPSC lines, integration of the mutant constructs occurred in both alleles, while CTNNB1 was monoallelic. Induction of oncogene expression using doxycycline in undifferentiated iPSC caused a change in morphology and a corresponding increased expression of BFP in each line. Using qRT-PCR, we confirmed the expression of KRAS and EGFR but unconvincing results from CTNNB1 post doxycycline induction.

Conclusion: Further differentiation of these novel inducible lines into 3D intestinal organoids will allow us to study the early events associated with oncogene activation in the context of human CRC.

47 **MULTIMODULAR APPROACH TO IMPROVE HEPATOCYTE TRANSPLANTATION TO TREAT ALPHA-1 ANTITRYPSIN DEFICIENCY ASSOCIATED LIVER DISEASE**

Anna Smith, Hua Liu, Valerie Gouon-Evans.
Station # 10

Objectives: The genetic disease alpha-1 antitrypsin deficiency (AATD) causes AAT protein to misfold, leading to polymerization in hepatocytes, cell death, and fibrosis. Curing AATD requires replacing diseased hepatocytes with wild type, but donor organs for whole liver transplantation and primary human hepatocytes (PHH) for cell therapy are scarce. Instead, gene edited AATD patient specific induced pluripotent stem cells could provide an unlimited supply of AAT producing autologous hepatocyte like cells (HLC) for transplantation. Mechanisms that limit HLC engraftment in mouse models of liver diseases are not fully understood, but include poor survival, proliferation, and maturation of transplanted cells. We hypothesize that stimulating key regenerative pathways in transplanted hepatocytes using hepatocyte growth factor (HGF) and epidermal growth factor (EGF) will improve survival, proliferation, and thus engraftment of PHHs and HLCs in NSG-PiZ mice, an immune deficient mouse model of human AATD liver disease.

Methods: We established a safe way to transiently express HGF and EGF in the liver using non-integrative nucleoside-modified mRNA encapsulated in lipid nanoparticles (mRNA-LNP).

Results: Importantly, we find that transplanted HLC survival in NSG-PiZ mice is transiently improved with HGF/EGF mRNA-LNP treatment.

Conclusion: Ongoing studies aim to evaluate the benefit of expression of HGF and EGF using mRNA-LNP to improve engraftment of PHHs and HLCs engineered to express physiological levels of receptors for HGF and EGF to mitigate AATD associated liver disease.

43 **UNDERSTANDING CELL STATE CHANGES IN MURINE ADULT LUNG FOLLOWING PNEUMONECTOMY INJURY**

Bibek Thapa, Jason Rock, Darrell Kotton.
Station # 11

Objectives: Alveolar epithelial type 2 cells (AT2s) of adult mouse lungs are facultative progenitors capable of proliferating and transdifferentiating into alveolar epithelial type 1 cells (AT1s) during homeostasis or in response to injury. A growing literature has employed lineage tracing of AT2s and various mouse lung injury models to study this process; however, the signaling mechanisms that regulate alveolar epithelial responses to lung injury remain poorly understood.

Methods: To profile these responses, we employed AT2 lineage tracing in a post-pneumonectomy regrowth mouse model. We performed single-cell RNA sequencing of mouse lung cells at four days following left lung pneumonectomy vs. control sham surgery.

Results: Data analyses revealed proliferating AT2s unique to the post-pneumonectomy lung, without evidence of transdifferentiating cells. The proliferating AT2s expressed lower mature AT2s markers, such as Slpi and Sftpa1, compared to non-proliferating AT2s in the same lung.

Interestingly, at this early time point, we did not detect any transcriptional signature differences in endothelial or mesenchymal cells.

Conclusion: These results suggest AEC2s as early responding cells post-pneumonectomy, re-entering cell cycle soon after pneumonectomy followed later by transdifferentiation into AEC1s. Future work will investigate possible niche interactions between AEC2s and other cell types of the lung and how these interactions might regulate AEC2 transdifferentiation into AEC1s during compensatory lung regrowth following pneumonectomy.

99 MULTI-MODAL PROFILING OF HUMAN FETAL LIVER HEMATOPOIETIC STEM CELLS REVEALS THE MOLECULAR SIGNATURE OF ENGRAFTMENT

Kim Vanuytsel, Carlos Villacorta-Martin, Jonathan Lindstrom-Vautrin, Zhe Wang, Wilfredo Garcia-Beltran, Vladimir Vbranac, Dylan Parsons, Evan Lam, Taylor Matte, Todd Dowrey, Sara Kumar, Mengze Li, Gustavo Mostoslavsky, Ruben Dries, Joshua Campbell, Anna Belkina, Alejandro Balazs, George Murphy.

Station # 12

Objectives: Insights into the remarkable engraftment potential of fetal liver (FL) hematopoietic stem cells (HSCs) could be harnessed to improve *ex vivo* HSC expansion, increase engraftment efficiency, and enable *in vitro* HSC generation.

Methods: Using CITE-seq, a technique that combines single cell RNA sequencing with oligo-tagged antibodies, we profiled 26,407 FL cells at both the transcriptional and protein level. In these studies, we have analyzed CD34⁻ cells, CD34⁺ cells and >7,000 CD34⁺ cells further enriched by expression of GPI-80, a marker tightly linked to engraftment potential, to explicitly characterize HSCs.

Results: Superior engraftment potential of the GPI-80⁺ fraction confirmed enrichment for bona fide HSCs. Dissection of the associated transcriptional signature revealed prominent expression of factors linked to aging and the concomitant decline of HSC functionality such as LMNA. Moreover, factors involved in guarding the balance between quiescence and self-renewal such as ID1, ID3 and NFE2L2 defined a transcriptional cluster that was preferentially enriched upon GPI-80 selection and thus best represents engraftable HSCs. Integration of transcriptomic and antibody-derived tag data suggested that CD201 (*EPCR*) could further enrich for cells corresponding to this refined engraftment signature, which was validated in transplantation studies.

Conclusion: In summary, we have achieved unprecedented resolution of the engraftable HSC compartment in the human FL. This comprehensive characterization of engraftment potential using multi-modal profiling to define an essential biological function at a key developmental timepoint serves as a useful resource for the field.

79 APPLYING CRISPRi IN IPSC-DERIVED ALVEOLAR EPITHELIAL CELLS TO INTERROGATE COPD GWAS

Rhiannon Werder, Michael Cho, Xiaobo Zhou, Darrell Kotton, Andrew Wilson.

Station # 13

Objectives: Low lung function in adulthood precedes chronic obstructive pulmonary disease (COPD) diagnosis and genome-wide association studies (GWAS) demonstrate overlapping risk variants with both COPD and low lung function. However, how gene variants contribute mechanistically to COPD pathogenesis and lung function is poorly understood. In this study, we aimed to determine the role of lung function genes in type 2 alveolar epithelial cells (AT2s).

Methods: We utilized established lung directed differentiation protocols to produce human iPSC-derived type 2 alveolar epithelial cells (iAT2s) and used a CRISPR interference (CRISPRi) approach to temporally knock-down genes of interest.

Results: By screening genes of interest we determined that the absence of certain genes (e.g. *HHIP*, *DSP*, *TGFB2* or *FAM13A*) altered proliferation and/or increased surfactant gene expression (*SFTPC*, *SFTPA1* and *SFTPA2*) expression in iAT2 cells. Further exploration of *DSP* knock-down revealed a loss of desmosomes, alterations to tight junctions and increased mitochondrial activity, likely related to heightened proliferation in the absence of *DSP*.

Conclusion: In conclusion, we have developed a CRISPRi platform to knock-down genes of interest identified from COPD and lung function GWAS. We found that the majority of genes

we assessed affected at least one aspect of AT2 function, and used this platform to thoroughly interrogate the function of *DSP* in AT2 cells. Future studies will further explore molecular mechanisms for genes of interest in AT2 cells, and this platform could be broadly applied to other disease areas or cell types of interest.

109 DE NOVO HEMATOPOIESIS FROM THE FETAL LUNG

Anthony Yeung, Carlos Villacorta-Martin, Jonathan Lindstrom-Vautrin, Anna Belkina, Kim Vanuytsel, Vladimir Vrbanac, Alejandro Balazs, George Murphy.

Station # 14

Objectives: Hemogenic endothelial cells (HECs) are specialized cells that undergo endothelial to hematopoietic transition (EHT) to give rise to the earliest precursors of hematopoietic stem cells (HSCs). Although HECs are thought to be primarily limited to the aorta gonad mesonephros (AGM), EHT has been described in various other hematopoietic organs and embryonic vessels. The lung has been shown to be a reservoir for hematopoietic stem and progenitor cells (HSPCs), but lung HECs have never been described. Here we demonstrate that the fetal lung is also a source of HECs that have the functional capacity to undergo EHT to produce HSPCs.

Methods: We adapted an explant model of HEC cultures using both murine and human fetal lungs. The EHT process observed in these cultures were assayed using single cell RNA sequencing, flow cytometry and immunofluorescent histology.

Results: Explant cultures of murine and human fetal lungs showed adherent endothelial cells transitioning into floating hematopoietic cells accompanied with the gradual loss of an endothelial signature. scRNA-Seq combined with functional assays demonstrated that fetal lung HECs rely on canonical signaling pathways to undergo EHT, including SMAD, Notch and YAP. Lastly, fetal lung derived HSPCs expressing the endothelial marker VE-cadherin were capable of engraftment into irradiated recipient mice.

Conclusion: Collectively these data suggests that the fetal lung may be another extramedullary site of de-novo hematopoiesis.

142 IDENTIFYING BIOMARKERS FOR INFLAMMATORY BOWEL DISEASE USING EXTRACELLULAR VESICLES

Kanchana Ayyar, Ria Shah, Alan Moss.

Station # 15

Objectives: There is an unmet need for novel markers of mucosal inflammation in patients with Inflammatory Bowel Disease (IBD). Extracellular vesicles (EV) are tiny packets of protein and nucleic acids that are secreted by mucosal cells into the intestinal lumen. We sought to isolate these cellular signals for RNA analysis.

Methods: Intestinal luminal fluid (ILF) was collected from healthy individuals and IBD patients during colonoscopy. EVs were isolated by ultracentrifugation, RNA was extracted and converted to cDNA. A Taqman array plate containing 96 different genes was used to quantify gene expression.

Results: The mean and mode size of particles isolated from the ILF was 173.3nm and 119.4nm respectively (n=81). The average concentration of EVs isolated from ILF was 2.49×10^{12} particles/ml (n=81). 23 genes were differentially expressed between healthy and IBD group. Most of the differentially expressed genes are involved in the Th17 pathway and play a role in inflammation.

Conclusion: ILF contains abundant EVs, with RNA cargo. Gene expression studies illustrate differences in RNA profile between controls and patients with IBD.

Session 1 – Floor 4 Thursday 10/7 9:30 am - 10:30 am

50 THE CROSS-SECTIONAL ASSOCIATION BETWEEN HEPATIC STEATOSIS AND SARCOPENIA: THE FRAMINGHAM HEART STUDY

Max Rosenthaler, Sarah Altajar, Na Wang, Joanne Murabito, Michelle Long.

Station # 1

Objectives: Sarcopenia, defined as a loss of skeletal muscle mass and function, is associated with nonalcoholic fatty liver disease (NAFLD); however, it is not known if the association is fully explained by shared risk factors. We investigated the association between liver fat and

sarcopenia in the Framingham Heart Study Offspring cohort.

Methods: Liver fat was measured on computed tomography between 2008-2011. We excluded heavy alcohol use and missing covariates, such as cardiometabolic risk factors and body mass index (BMI). Muscle mass in a subset (n=485), was measured by 24-hour urinary creatinine. Physical function was defined by hand grip strength and walking speed. Sarcopenia was defined as the presence of low muscle mass and/or low physical function < sample median. Multivariable-adjusted linear and logistic regression models evaluated cross-sectional associations between liver fat and low muscle mass, grip strength, and walking speed after adjusting for covariates.

Results: The prevalence of hepatic steatosis in our study sample was 30% (n=1073). We observed a significant positive association between liver fat and muscle mass in multivariable-adjusted linear regression models; however, the association was no longer significant after adjusting for BMI. The odds of sarcopenia, defined by low muscle mass and/or slow walking speed, increased by 28% for each standard deviation increase in liver fat (OR 1.28; 95% CI 1.02, 1.60) and persisted after accounting for in multivariable-adjusted models (OR 1.30, 95% CI 1.02, 1.67).

Conclusion: In our community-based cohort study, we observed a significant association between liver fat and sarcopenia.

197 PURIFICATION OF EXOSOMES FROM INTRALUMINAL FLUIDS FOR THE STUDY OF IBD

Sarah Watanabe, Alan Moss, Carla Mazzeo.

Station # 2

Objectives: A method of purification based on size exclusion chromatography to isolate exosomes from colonic luminal fluids aspirates and fecal samples of patients with Inflammatory Bowel Disease (IBD). First stage for the study of exosomes as non-invasive and novel monitoring/prognosis biomarker for Crohn Disease (CD) and the elucidation of exosomes' mechanism in the development of IBD.

Methods: A series of centrifugation was made on Intraluminal fluid (ILF) samples from patient with active IBD and Healthy. 2ml of the resulting supernatant were loaded in a SEC column. Fractions of 2ml were collected and identified as positive for exosome by dot blot developed with Anti-Syntenin antibody (as a exosome biogenesis's marker) All fractions containing exosomes were pooled and concentrated to 500ul by AMICON columns. After concentration exosomes's samples were quantified in a NTA for the characterization of exosomes from ILF samples and for the comparison of the number of exosomes in active IBD and Healthy patients.

Results: Based on one of the best methods for exosomes's purification, we have obtained and isolate exosomes successfully from ILF samples. The exosomes from active IBD patients and healthy were characterized (DOT BLOT and NTA) and quantified (NTA).

Conclusion: We developed a novel system to collect and purified exosomes from ILF, without the necessity to precipitate them or ultracentrifuge them. Those techniques have the aggravation of modify the functionality of exosomes. Through this novel technique we able to obtain functional exosomes for the study of their mechanism on IBD and analyze their cargo in the search of potential biomarkers for non-invasive diagnose of IBD.

191 ASSOCIATION BETWEEN HEAVY ALCOHOL CONSUMPTION AND TRIMETHYLAMINE N-OXIDE

Samuel Mensah, Debbie Cheng, Matthew Freiberg, Vladimir Palatkin, Gregory Patts, Sally Bendiks, Elena Blokhina, Natalia Gnatienco, Hilary Tindle, Sonam Tandon, Dmitry Lioznov, Jeffrey Samet, Kaku So-Armah.

Station # 3

Objectives: We studied the link between heavy alcohol consumption and trimethylamine n-oxide (TMAO), an intestinal microbiome-dependent metabolite and a cardiovascular disease risk factor.

Methods: Participants were from the St PETER HIV clinical trial aimed at reducing smoking and alcohol intake among people living with HIV (PLWH) in Russia. Participants included had at least 5 days where heavy drinking occurred in the past 30 days before baseline assessment. Heavy drinking days (HDD), the exposure, was categorized into quartiles. The outcome was

plasma TMAO levels. Multiple linear regression adjusted for age, gender, body mass index, kidney function, recent antibiotic use, HIV-1 RNA, and recent seafood ingestion.

Results: Participants (N=218) had a mean age of 38 (± 6), and were 33% female. The quartiles of HDD had these boundaries: 1st (lowest) quartile 0 to 6HDD, 2nd quartile 7 to 8HDD, 3rd quartile 9 to 12HDD, and 4th (highest) quartile 13 to 30HDD. In the multivariable regression analysis, we did not detect an association between an increasing number of heavy drinking days and plasma TMAO (ratio of means: 4th vs. 1st quartile of heavy drinking days 1.18 (95% CI: 0.84, 1.67); 3rd vs. 1st quartile 1.14 (95% CI: 0.80, 1.62); 2nd vs. 1st quartile =1.37 (95% CI: 0.98, 1.93).

Conclusion: We did not detect an association between heavy drinking days and TMAO levels in this sample of PLWH with heavy alcohol use. Future work should include a wider range of alcohol consumption including non-consumption.

184 REDUCED ALCOHOL CONSUMPTION AND CHANGE IN RELATIVE ABUNDANCE OF *BUTYRATE KINASE (BUK)* GENE IN GUT MICROBIOME OF PEOPLE WITH HIV (PWH)

Sonam Tandon, Richa Singhal, Shirish Barve, Gregory Patts, Samuel Mensah, Matthew Freiberg, Jeffrey Samet, Kaku So-Armah.

Station # 4

Objectives: The objective of this study is to explore changes in *buk* gene abundance in the gut microbiome among PWH who reduce their alcohol consumption. *Buk* gene is critical in the synthesis of butyrate which benefits intestinal barrier function and mucosal immunity.

Methods: We selected 17 people with reductions in alcohol use over 3 months from the St. PETER HIV clinical trial to reduce alcohol and smoking among PWH in Russia. Alcohol was self-reported by 30-day Timeline Followback. We conducted whole metagenomic sequencing on fecal samples at baseline and 3 months. We described participant characteristics among those with decreased (Tertile 1), mixed (Tertile 2) and increased (Tertile 3) *buk* gene abundance over 3 months.

Results: Table 1

Conclusion: Higher *buk* gene abundance corresponded with lowest quantity and frequency of alcohol use at baseline (Table 1). Future work should include additional participants to enable adjusted regression analyses.

Table 1. Descriptive statistics of the cohort divided into Tertile 1 with decreased *buk* gene abundance at T2, Tertile 2 with mixed increase or decrease in *buk* gene abundance at T2 (N=17) and Tertile 3 with increased *buk* gene abundance over 3 months.

VARIABLES	BASELINE			3 MONTHS		
	Tertile 1 (n=6)	Tertile 2 (n=5)	Tertile 3 (n=6)	Tertile 1 (n=6)	Tertile 2 (n=5)	Tertile 3 (n=6)
Age, years	40 (38, 42)	35 (32, 37)	39 (34, 41)			
Sex, Female; n (%)	1 (17)	1 (20)	1 (17)			
Years since HIV Diagnosis	9 (6, 9)	14 (8, 16)	15 (8, 19)			
Total Grams of Alcohol*	1598 (1429, 2352)	1882 (1490, 2352)	1302 (1150, 1357)	229 (0, 263)	59 (48, 95)	10 (0, 63)
Number of Drinking Days*	22 (17, 30)	20 (20, 20)	12 (10, 15)	6 (0, 8)	1 (1, 2)	0.5 (0, 1)
Heavy Drinking Days*	21 (15, 27)	20 (14, 20)	10 (10, 10)	1 (0, 2)	1 (0, 1)	0 (0, 1)
Drinks per Week*	27 (24, 39)	31 (25, 39)	22 (19, 23)	4 (0, 4.4)	1 (0.8, 1.6)	0.2 (0.3, 0.4)
Number of Cigarettes*	28 (15, 30)	29 (27, 30)	21 (10, 40)	2 (0, 8)	0.3 (0, 3)	0.4 (0, 7)
Copies of HIV-1 RNA	5 (5, 5)	10 (9, 11)	6 (5, 9)	5 (5, 5) ^d	13 (9, 16) ^d	6 (5, 7) ^d
CD4 Count	576 (500, 631)	201 (82, 264)	383 (265, 407)	505 (453, 705)	109 (74, 334)	330 (290, 458)

All continuous variables are presented as p50(p25, p75); *per 30 days, b: n=3, d: n=2

166 ASSEMBLING 2D SLICES INTO 3D SPATIAL TRANSCRIPTOMICS DATASETS

George Chen, Liam Murray, Ruben Dries.

Station # 5

Objectives: Spatial transcriptomics is a new and rapidly developing field of technology that allows transcription within tissues to be examined with spatial context and without the need for single-cell dissociation. Our lab has recently established an experimental pipeline to create such data, and while it's becoming feasible to produce 2D spatial datasets, creating a 3D dataset from your favorite cell niche remains extremely challenging. One promising approach would be to stack multiple 2D slices into a 3D dataset, but this requires an additional alignment step due to differences in how tissue is manually placed in the read/capture areas. Since spatial expression data itself offers few clues on slice alignment, we depend on the accompanying images taken of each slice.

Methods: Here, we implemented an easy-to-use image processing pipeline in our spatial

toolbox Giotto, which takes H&E images of each slice and aligns them using the “register virtual stack slices” plugin in Fiji.

Results: The result is a set of aligned images and a list of accompanying transformations. These transforms can then also be applied to the spatial coordinates of each slice to produce a coherent 3D spatial dataset. To validate our results, we compared the neighbors of each cell and found an enrichment of the same cell types after alignment.

Conclusion: The increase in enrichment indicates more homogenous cellular transitions between different stacks as expected in a 3D model. Spatial coordinate alignment using image registration greatly improves the 3D dataset and downstream spatial network-based analyses.

169 ENDOTHELIAL SCAVENGER RECEPTORS IN THE HEMATOPOIETIC NICHE

Khalilun Enkhbayar, Justine Wagaman, Dana Ragoonanan, Helen Wang, Emily Henault, Elliott Hagedorn.

Station # 6

Objectives: The hematopoietic stem and progenitor cell (HSPC) niche is a supportive microenvironment comprised of distinct cell types, including specialized vascular endothelial cells that promote HSPC function. We previously identified several molecules with endocytosis-related functions, including the stabilin scavenger receptors stab1/2, which are expressed selectively by niche endothelial cells in zebrafish. Our objective was to investigate the role of these receptors in vascular endocytosis and HSPC niche regulation.

Methods: To evaluate endocytic activity we intravenously injected a fluorescent endocytosis sensor into zebrafish embryos at 48-72 hours post fertilization then performed high-resolution live cell imaging. In parallel experiments we co-injected a scavenger receptor inhibitor and examined HSPC migration, in addition to vascular endocytosis, within the niche.

Results: The endocytosis sensor revealed robust uptake specifically within niche endothelial cells. The inhibitor blocked this uptake and led to an accumulation of HSPCs in the niche. Injection of the same endocytosis sensor into stab2 mutant zebrafish showed reduced niche endothelial uptake, suggesting stab2 could be driving this activity.

Conclusion: Collectively, our results demonstrate that niche endothelial cells are extremely endocytic and implicate a role for stab2 in HSPC migration within the niche. These studies could guide new strategies for targeting vascular endocytosis to modulate stem cell function or deliver nanoparticle-based therapeutics to the blood stem cell niche.

173 PATHWAY ANALYSIS OF IMMUNE CHECKPOINT GENE REGULATION AS ALTERED IN TYPE 2 DIABETES: IMPLICATIONS FOR BREAST CANCER PATIENTS TREATED WITH CHECKPOINT INHIBITORS

christina ennis, pablo LLevenes, Manohar Kolla, Naser Jafari, Anna Belkina, Gerald Denis.

Station # 7

Objectives: Type II diabetes mellitus (T2D) both increases breast cancer incidence and decreases survival. Exosomes are crucial components of intercellular communication and are associated with increased breast cancer aggressiveness. Given this function, we hypothesized that T2D adipocyte-derived exosomes drive T cell exhaustion. Here, we characterize expression patterns and regulatory networks driving T2D immune phenotypes.

Methods: Exosomes were isolated from culture media from either insulin-resistant (IR) or -sensitive (IS) ex vivo TNFa-treated human primary breast tissue mature adipocytes. Human PBMCs from nondiabetic (ND) and T2D donors were stimulated ex vivo for 48 hours, and treated with exosomes, plus modulators of the BET protein family and AMPK pathway. Exhaustion markers on immune subsets were then analyzed via multicolor flow cytometry. Cytokines were collected from conditioned media and analyzed via Th17 cytokine staining panel.

Results: We observed that IR-derived exosomes increase exhaustion in immune subsets. Additionally, we define signal transduction pathways among BET proteins, AMPK signaling, and immune checkpoint expression. Lastly, we identify changes in cytokine profile between IS and IR treated groups.

Conclusion: Metabolic health does not inform the current standard of care in breast medical oncology. Our findings suggest a network of immune regulation imparted by exosomes and

offer a deeper understanding of immune checkpoint regulation in T2D, suggesting new insights into treatment of diabetic breast cancer patients.

100 PHOTOACOUSTIC STIMULATION OF PRIMARY EMBRYONIC NEURONS IN *XENOPUS LAEVIS*

Gavin Rosen, Mackenzie Hulme, Linli Shi, Chen Yang, Laura Lowery.

Station # 8

Objectives: Axon guidance during embryonic development is crucial for the formation of proper neural connectivity. Stimulating neurons and subcellular structures in a non-invasive and spatially precise manner poses many advantages to neuromodulation and guiding axons to create novel connectivity across barriers or in disease conditions. Our aim is to test the effects of photoacoustic stimulation on embryonic neurons in vitro by utilizing a tapered fiber optoacoustic emitter (TFOE) on an established model system of visualizing growth cone dynamics.

Methods: *Xenopus laevis* was used as a model system for in vitro visualization of growth cone dynamics. Primary embryonic neurons were cultured from stage 20 *X. laevis* embryos. The TFOE converted laser pulse trains of 3ms bursts to generate an ultrasound field by which the growth cones of extending axons could be stimulated in a non-invasive manner.

Results: A coordinate system was established to quantify the intrinsic behavior of growing axons in terms of growth speed and angle. Stimulation conditions were applied to identified healthy growth cones, and varied changes to both growth direction and speed were demonstrated relative to initial trajectories.

Conclusion: Stimulation conditions will be optimized in order to determine a more consistent pattern in growth cone behavioral changes. Additionally, we plan to utilize calcium imaging to assess the degree to which photoacoustic stimulation is affecting axon electrophysiology.

58 INVESTIGATING THE ROLE OF THE COREST REPRESSOR COMPLEX IN MELANOMA METASTASIS IN VIVO

Ainsley Hutchison, Mackenzie Hulme, Bengisu Gur, Joe Ebbert, Rhoda Alani, Laura Lowery.

Station # 9

Objectives: Skin cancer is the most common cancer in the United States. While melanoma accounts for only 1% of skin cancers, it is responsible for the majority of skin cancer deaths, due to its ability to metastasize. Thus, blocking metastasis would be a great breakthrough in treatment strategies. Although numerous genetic mutations have been characterized in melanoma, a frustrating challenge in treating this disease is that there are no clear differences in the genetic mutations in primary tumors versus those that metastasize. However, several studies of melanoma patient samples have identified that there are common epigenetic modifications that correlate with metastatic state. The drug that our collaborators have developed (called corin) specifically targets the CoREST complex, which affects epigenetic modifications that occur during cancer metastasis.

Methods: While they have previously shown that corin can block melanoma tumor growth, it is hypothesized that it might also be effective at blocking melanoma metastasis. Our aim is to demonstrate the efficacy of corin in reducing metastasis of melanocytes in a *Xenopus laevis* model, using the drug ivermectin to induce a metastatic-like state in the melanocytes of *Xenopus* embryos.

Results: The addition of corin in these treatments showed that corin could reduce the metastatic behaviors. Western blot data from lysates of *Xenopus* embryos treated with corin showed expected epigenetic changes.

Conclusion: Future studies will continue to elucidate the mechanisms by which corin may block melanoma metastasis.

171 ADIPOCYTE-ORIGIN EXOSOMES REGULATE BREAST CANCER AGGRESSIVENESS IN OBESITY AND METABOLIC DISEASE

Naser Jafari, Manohar Kolla, Tova Meshulam, Jordan Shafran, Yuhan Qiu, Allison Casey, Gerald Denis.

Station # 10

Objectives: Obesity and metabolic diseases, such as insulin resistance and Type 2 diabetes (T2D), associate with breast cancer progression in post-menopausal women. The critical cellular and molecular factors remain poorly defined.

Methods: Exosomes were purified from mouse or human adipocyte conditioned media and added to mouse or human breast cancer cell lines. We measured induction of epithelial-to-mesenchymal transition (EMT) and cancer stem-like genes linked to breast cancer progression; cell migration and invasiveness.

Results: Signatures of cancer aggressiveness are elevated if exosomes are derived from insulin-resistant adipocytes or adipose tissue of T2D patients, vs insulin-sensitive. TSP5, a thrombospondin family protein previously associated with cancer, is differentially abundant in exosomes from T2D or insulin-resistant adipocytes and drives EMT.

Conclusion: Exosome crosstalk between abnormal adipocytes and breast cancer cells drives tumor aggressiveness in T2D.

78 ESTABLISHING A SINGLE-CELL RNA-SEQ PIPELINE FOR TREATMENT NAIVE TRIPLE NEGATIVE BREAST CANCER BIOPSIES

Emma Kelley, George Chen, Yibing Wei, Christina Ennis, Ruben Dries.

Station # 11

Objectives: Triple negative breast cancer (TNBC) is the most fatal form of breast cancer; and despite recent advances, treatments remain limited. Single-cell RNA-sequencing allows us to unravel the heterogeneity of the tumor microenvironment (TME). However, obtaining high quality data from the treatment naive TME has historically been experimentally challenging. The main barriers are access to tissue, which is limited to small core biopsies, and the supposed necessity to work directly with fresh samples. Here we set out to establish a protocol to create high quality single-cell data from a single preserved fresh frozen biopsy.

Methods: We systematically optimized the cryopreservation step, identified the ideal cocktail of enzymes for dissociation, and miniaturized each step to further reduce cell loss and increase cell viability.

Results: Altogether we were able to establish a protocol that can be used on a single frozen biopsy, while maintaining a cell viability of more than 90%. After experimental and computational steps of quality control our first datasets contained more than 6,000 cells with more than 20,000 detected genes and covered all abundant cell types in the TME.

Conclusion: This breakthrough will allow us to multiplex multiple biopsies in the future to create a large-scale single-cell TNBC map while simultaneously minimizing batch effects. Finally, although this pipeline was designed to increase our understanding of the treatment naive TNBC TME at single cell resolution, we expect that it will be applicable to many studies that would benefit from a single cell perspective, but are limited to small (biopsy) samples.

160 EXOSOMES PRODUCED BY ADIPOCYTES INDUCE EMT, IMMUNE EXHAUSTION & TUMOR METASTASIS, IN BOTH *IN VIVO* & *IN VITRO* MODELS OF TNBC

Yuhan Qiu, Conor Ross, Naser Jafari, Manohar Kolla, Isabella Pompa, Pablo Llevenes, Carla Mazzeo, Kiana Mahdaviyani, Naomi Ko, Gerald Denis.

Station # 12

Objectives: Patients with triple negative breast cancer (TNBC) and comorbid T2D have higher risk of metastasis and shorter survival. However, mechanisms that couple T2D to TNBC outcomes are unknown. Here we hypothesize that exosomes secreted by tumor microenvironment breast adipocytes, drive epithelial-to-mesenchymal transition (EMT) in TNBC, immune exhaustion and metastasis via Ampk-Akt signaling.

Methods: Exosomes were purified from conditioned media of 3T3-L1 mature adipocytes that were insulin sensitive (IS) or insulin resistant (IR), then characterized and quantified by NanoSight. Murine 4T1 cells, a TNBC model, were treated with exosomes *in vitro*. In *in vivo* models, mice were injected with 4T1 cells treated with IS vs IR exosomes. mRNA was extracted from tumor for RNAseq. Metastatic sites in lung and liver were visualized by H&E staining and clonogenic assay. Immune exhaustion of lymphocytes and neutrophils were measured by flow cytometry.

Results: In 4T1 cells treated with IR exosomes, EMT was upregulated and PD-L1 expression increased. Tumor-bearing mice exhibited earlier tumor onset and metastasis in IR groups.

Immune exhaustion markers showed modified expression in TILs from IS vs IR groups. RNA-seq analysis revealed differences among IS vs IR groups that suggest dysregulated Ampk-Akt pathways.

Conclusion: Exosomes from adipocytes modify the tumor microenvironment, immune cell population, and promote metastasis to distant organs through Ampk-Akt. Metabolic diseases such as T2D reshape the TNBC microenvironment, promoting metastasis and decreasing survival. TNBC patients with T2D should be closely monitored for metastasis with metabolic medications considered.

19 THE FETAL HEMATOPOIETIC NICHE IS DISPENSABLE UNDER STEADY STATE CONDITIONS

Dana Ragoonanan, Helen Wang, Khaliun Enkhbayar, Emily Henault, Serine Avagyan, Rebecca Freeman, Elliott Hagedorn.
Station # 13

Objectives: The blood stem cell niche is a specialized microenvironment that supports the function of hematopoietic stem and progenitor cells (HSPCs). In both zebrafish and mammals, HSPCs are born in the dorsal aorta and then migrate to a transient fetal niche - the fetal liver in mammals and the caudal hematopoietic tissue (CHT) in zebrafish. After expanding over the course of several days, HSPCs then migrate to the adult niche (the bone marrow in mammals and kidney marrow in fish). The objective of our study was to evaluate the functional requirement of the fetal niche in zebrafish.

Methods: To block CHT formation we surgically removed the zebrafish tail at 24 hours post fertilization then used imaging and in situ hybridization to analyze HSPC localization.

Results: In the absence of a CHT, we observed delayed thymus colonization and early HSPC migration to the kidney. With a custom-made feeding system, we grew tailless fish to adulthood. Flow cytometric analysis of the adult kidney marrow showed a slight increase in the progenitor population and a corresponding decrease in the myeloid compartment.

Conclusion: Our results suggest the fetal HSPC niche shapes progenitor-to-myeloid development and thymocyte maturation but is largely dispensable for HSPC function and animal survival under normal laboratory conditions. These studies provide novel insight into the functional requirement of the fetal blood stem cell niche, which could guide new therapeutic strategies to improve blood stem cell transplantation or inform new methodology to grow and expand human HSPCs in vitro.

87 CELLULAR CHARACTERIZATION OF PROSTATE CANCER CELLS WITH FUNCTIONAL LOSS OF *ATRX* OR *DAXX*

Marija Stojanova, Elizabeth Nelson, Mindy Graham, Alan Meeker, Christopher Heaphy.
Station # 14

Objectives: Some cancer cells utilize a telomerase independent mechanism for essential telomere maintenance, termed Alternative Lengthening of Telomeres (ALT). ALT occurs exclusively in cancer cells, making it an ideal target for therapeutic intervention.

Methods: Mutations in the chromatin remodeling genes *ATRX* and *DAXX* are strongly associated with ALT; thus, we knocked out (KO) these genes via CRISPR-Cas9 in the ALT-negative prostate cancer cell lines, CWR22Rv1 and LAPC4. In CWR22Rv1, *ATRX*^{KO} and *DAXX*^{KO} clones were created. In LAPC4, *ATRX*^{KO} and *ATRX*^{KO} *TERC*^{mut} clones were created. The matched parental and KO clones were characterized for cell proliferation (MTS assay), clonogenic survival (colony formation assay), and invasion (matrigel invasion assay) to assess how these key mutations would alter cellular properties consistent with metastasis.

Results: Compared to parental CWR22Rv1, most of the *DAXX*^{KO} clones showed increased proliferation, colony formation, and invasion; whereas, the *ATRX*^{KO} clones showed decreased proliferation and colony formation, but no change in invasion. Compared to parental LAPC4, there were no consistent changes in proliferation, colony formation, and invasion among the *ATRX*^{KO} and *ATRX*^{KO} *TERC*^{mut} clones.

Conclusion: Overall, these data suggest that *ATRX* or *DAXX* KO alters cancer-relevant cellular properties. Thus, better characterizing cells with functional loss of *ATRX* or *DAXX* may lead to new insights about therapeutically targeting ALT-positive cancers.

164 DEVELOPMENT OF AN *IN VITRO* 3D CO-CULTURE MULTIPLEXING STRATEGY FOR A SYSTEMATIC RECAPITULATION OF THE HETEROGENOUS AND DYNAMIC BREAST TUMOR MICROENVIRONMENT

Yibing Wei, Rose Zhao, Emma Kelley, Jijai Chen, Kylor Lachut, Clare Melley, Ruben Dries, Ph.D.

Station # 15

Objectives: Triple-negative breast cancer (TNBC) is notable for high levels of intra and inter-patient heterogeneity within the tumor microenvironment (TME) and with infiltration of macrophages of different subtypes. Deciphering the intricate crosstalk grammar between macrophages and cancer cells in the drug-treated TME calls for unbiased models compatible with high-throughput approaches that can capture the tumor structure complexity as a whole.

Methods: Here, we designed an *in vitro* high-throughput workflow which supports the growth of 7,584 TNBC spheroids of identical size co-cultured with macrophages on a plate, while simultaneously tracking their movement. This platform will allow us to apply a combined experimental-computational multiplexing strategy to deconvolve TNBC subtypes (SNPs), macrophage population subtypes (barcoding) and drug treatment (hashtags) at the single-cell level.

Results: With this strategy we can cost-effectively simulate 96 unique experimental conditions at once with minimal batch-effects.

Conclusion: Altogether, this will reveal the dynamic TNBC-macrophage interactions in response to anti-tumor therapeutic intervention in a systematic manner.

Session 2 – Floor 5 Thursday 10/7 10:30 am - 11:30 am

159 DOMAIN-SPECIFIC COGNITIVE FUNCTIONS PREDICT NEUROPATHOLOGICAL TRAITS IN FRAMINGHAM HEART STUDY

Donghe Li.

Station # 1

Objectives: To investigate the relationships between antemortem NP tests and post-mortem neuropathological traits from the same participants.

Methods: 23 NP and 21 neuropathological traits were measured in 159 brain donors from the Framingham Heart Study. The NP tests were divided into memory, language, executive, and visuospatial domains. NP tests and neuropathological traits were normalized and performed association analysis by adjusting sex, age, and interval age. The model of predicting AD status and neuropathological traits, including terms for domain-specific NP tests, age at death, sex, and APOE ϵ 4 status, were also evaluated.

Results: AD was significantly associated ($P < 0.05$) with memory, language, and executive function. Braak stages, plaque scores, and AT8 showed a strong association with the cognitive domain ($P < 0.02$). Significant associations were observed between pTau396 and the visuospatial ($P = 0.03$), pTau181 ($P = 0.02$), pTau202 ($P = 0.0089$), pTau231 ($P = 0.008$), PSD95 ($P = 0.04$) and ratio of AB_{42}/AB_{40} ($P = 0.03$) were associated with memory. For complement component proteins, the C4A level was nominally significant with language ($P = 0.03$) and the C4B level with executive function ($P = 0.02$). pTau396 was predicted as AUC is 0.806 (0.46-0.85), and AB_{42}/AB_{40} is 0.739 (0.44-0.89), where the visuospatial was the top-ranked predictors in both traits.

Conclusion: This study demonstrated for the first-time associations of antemortem language and executive function with post-mortem complement component protein levels. Among pTau related traits, pTau396 was only associated with visuospatial and was primarily predicted by visuospatial domain accompanied with AB_{42}/AB_{40} .

107 CHRONIC ACTIVATION OF THE ARYL HYDROCARBON RECEPTOR LEADS TO IMMUNE SUPPRESSION AND TUMOR FORMATION IN BOTH ORAL AND LUNG CANCERS

Megan Snyder, Brian Lara, Jessica Kenison-White, Zhongyan Wang, Kangkang Yang, David Sherr.

Station # 2

Objectives: There is unmet medical need to understand the regulation of immune suppression in tumors in order to develop more robust immunotherapies. We have shown that the aryl

hydrocarbon receptor (AhR) is a central player in regulating immune checkpoints in oral squamous cell carcinoma (OSCC) and may also play a similar role in lung cancer. Determining AhR's role in immune suppression will open the door for improved immunotherapies.

Methods: C57Bl/6 wildtype mice were injected subcutaneously with CMT167^{WT} or CMT167^{AhR-KO} lung carcinoma cells. Tumor growth and survival were tracked. Tumor digests and tumor draining-lymph nodes were phenotyped. Malignant cell PD-L1 expression in the absence or presence of exogenous AhR agonists was also determined *in vitro* in both cell lines via flow cytometry and qPCR.

Results: AhR deletion in both oral and lung cancer cells leads to decreased tumor growth and increased tumor immunity. AhR^{KO} partially (~80%, lung) or completely (oral) prevents tumor formation in our models. AhR^{KO} tumors have greater numbers of tumor infiltrating CD4⁺ and CD8⁺ T cells per tumor volume by 5 weeks post challenge. Malignant cells cultured with AhR agonists showed increased PD-L1 protein and RNA expression in the WT but not the KO cell line, indicating AhR's involvement in regulating PD-L1 and providing an explanation for the increased tumor immunity after transplant of AhR^{KO} cells.

Conclusion: AhR drives PD-L1 expression in malignant cells. AhR^{KO} enables tumor immunity, leading to reduction or total elimination of tumor growth. Immunological benefits correlated with AhR^{KO} cells in lung and OSCC models suggests the AhR's potential as a viable immunotherapeutic target in at least two cancers

55 PULMONARY TUBERCULOSIS IS ASSOCIATED WITH THE DEVELOPMENT OF BROAD AND POTENT NEUTRALIZING ANTIBODIES IN CHRONIC HIV-1

Bukola Adeoye, Alex Olson, Yvetane Moreau, Manish Sagar.

Station # 3

Objectives: Mycobacterium tuberculosis (TB) has been shown to enhance antibody responses against diverse viruses. Thus, we hypothesized that active TB co-infection enhances the development of HIV-1 specific neutralizing antibodies (nAbs).

Methods: We compared humoral responses among plasma samples from 15 HIV-1 participants with TB (HIV-1/TB) and 16 HIV-1 participants without TB. Neutralization and antibody-dependent cellular cytotoxicity (ADCC) against 12 and 10 HIV-1 isolates were used to estimate breadth and potency scores. Single genome amplification was used to compare HIV-1 envelope diversity. Plasma cytokines and antibody levels were measured using the flow and Luminex-based assay respectively.

Results: HIV-1/TB and HIV-1 infected participants had similar baseline plasma virus levels ($p = 0.33$) and CD4 counts ($p = 0.40$). Anti-HIV-1 neutralization ($p = 0.02$), but not ADCC ($p = 0.7$) was broader and more potent among HIV-1/TB than HIV-1 group. Plasma IgG titer, CD4 count, viral load, and envelope diversity did not associate with plasma neutralizing and ADCC capacity. However, high plasma levels of CXCL13, RANTES, and APRIL observed in the HIV-1/TB group are associated with neutralization breadth and potency.

Conclusion: These results suggest that low viral envelope diversity in the setting of enhanced plasma markers of germinal center efficiency is associated with the emergence of broad and potent nAbs. Dissecting mechanisms that account for the enhanced HIV-1 neutralization in HIV-1 individuals with active TB could be leveraged in the generation of a more effective humoral response in HIV-1 vaccination and treatment.

83 EPIDEMIOLOGICAL FACTORS AND HUMORAL IMMUNE RESPONSES ASSOCIATED WITH SARS-COV-2 RE-INFECTION OR PROLONGED SHEDDING

David Bean, Janet Monroe, Manish Sagar.

Station # 4

Objectives: The factors associated with SARS-CoV-2 re-infection or persistent viral shedding are not well understood.

Methods: To identify the characteristics associated with a SARS-CoV-2 re-infection or prolonged viral shedding, Boston Medical Center patients were identified with a confirmed primary SARS-CoV-2 infection that either tested positive (Repeat Infection or Prolonged Shedding (RIPS), $n = 106$) or only negative (Primary Infection with Repeat Negative (PIRN), $n = 1,921$) for SARS-CoV-2 via RT-PCR at least sixty days after their primary infection.

Demographics were compared between the two groups and humoral immune responses were analyzed using SARS-CoV-2 specific ELISA and pseudovirus neutralization assays.

Results: The odds of not having stable housing, being pregnant, and being on immunosuppressive medication were higher in the RIPS group as compared to the PIRN group. SARS-CoV-2 spike and nucleocapsid IgG levels and pseudovirus neutralization were not statistically different after the primary infection between 16 matched individuals from the PIRN and RIPS groups. Neutralization potency was lower after the second positive SARS-CoV-2 test result compared to the antibody response after the primary infection in the majority of individuals tested in the RIPS group.

Conclusion: These results suggest repeat infection or persistent viral shedding may occur due to inadequate immune responses and repeated exposure to the virus.

110 INTEGRASE STRAND TRANSFER INHIBITORS ALTER ADIPOKINE PROFILES AND METABOLIC ACTIVITY OF ADIPOCYTES IN-VITRO

R. Taylor Pickering, Kaitlin Soden, Archana Asundi, Nina Lin.

Station # 5

Objectives: Integrase strand transfer inhibitors (INSTIs), a newer class of antiretroviral therapy (ART), have been shown to promote excess weight gain in people living with HIV through poorly understood mechanisms. Thus, we sought to examine the effects of modern ART on adipocyte biology related to weight gain.

Methods: Paired cultures of omental and abdominal subcutaneous human preadipocytes and newly differentiated adipocytes from HIV uninfected individuals were treated with an integrase inhibitor; Dolutegravir (DTG) or protease inhibitor; Darunavir (DRV) then switched between ART. Triglyceride content, lactate production and lipolysis were assessed by enzymatic assay and normalized to DNA content. Adipokine secretion was determined with ELISA and oxygen consumption rates were determined using Seahorse.

Results: Exposure to DTG and DRV did not affect cell viability or triglyceride accumulation. Exposure to DTG significantly increased expression of PPAR γ , a late adipogenic marker, in both depots (1.6, 1.3-fold, $p < 0.05$). DTG suppressed both leptin and adiponectin (ADCN) secretion (0.7 pg vs. 1.4 pg leptin/ngDNA; 35.1 pg vs. 15.5 pg ADCN/ngDNA, $p < 0.05$), and this was partially rescued when switched to DRV (1.1 pg leptin; 41.7 pg ADCN, $p < 0.05$). DTG significantly increased lactate production 2-fold in both preadipocytes and adipocytes ($p < 0.05$), and suppressed oxygen consumption rates.

Conclusion: Exposure to INSTIs altered key aspects of adipose biology in-vitro. The decrease in leptin, a major satiety hormone, may help explain the increased weight gain seen in individuals taking INSTIs. Further, increases in lactate and decreased oxygen consumption may indicate impaired mitochondria.

71 SMALL MOLECULES THAT CORRECT ABERRANT TNF RESPONSE INCREASE INNATE RESISTANCE TO TUBERCULOSIS

Shivraj Yabaji, Sujoy Chatterjee, Igor Kramnik.

Station # 6

Objectives: TNF plays crucial roles in host resistance to tuberculosis (TB) and TB granulomas. We have found that necrosis of TB granulomas and TB susceptibility in a mouse model are mediated by an aberrant macrophage response to TNF leading to unresolving oxidative and proteotoxic stress and type I interferon pathway hyperactivity. This response is mediated by the *sst1* locus encoding interferon-inducible nuclear proteins Sp110 and Sp140.

Methods: We identified transcriptional signatures associated with the susceptible phenotype and searched for small molecules that correct the aberrant TNF response.

Results: Two compounds, ISRIB and Rocaglamide A (RocA), significantly decreased the aberrant TNF response. After infection of susceptible macrophages with virulent M. tuberculosis, Roc A improved control of the bacterial replication, induced autophagy, and promoted M1-like macrophage polarization, while ISRIB improved the macrophage survival. The Roc A and ISRIB combination produced the synergistic effect. In vivo, ISRIB reduced pulmonary granulomas in Mtb-infected susceptible mice.

Conclusion: Our studies provide a model and methodology for the discovery and testing of novel host-directed therapies for TB. These immune-modulating therapies are becoming increasingly important, considering the global threat of drug-resistant bacteria.

46 A NOVEL RODENT MODEL OF CENTRAL VENOUS STENOSIS

Nagla EL ZINAD, Saran Lotfollahzadeh, CONNOR KIM, Meng wei Zhang, JOSEPHINE Orrick, Murad Elsadawi, Vipul C Chitalia.

Station # 7

Objectives: Central venous stenosis (CVS) is a dreaded complication observed in patients with, end-stage kidney disease (ESKD) patients. Dialysis catheters in one of the central veins such IJV, SCV, INV or SVC result in stenosis, which is termed as CVS. This complication has devastating on the prospect of dialysis access. The main purpose of this project research is to develop an animal model that recapitulates the development of CVS.

Methods: CKD was developed in Sprague Dawley rats using adenine-induced model (N= 20). Rats on normal diet served as controls. All the animals underwent guide wire injuries to their right IJV to resemble the type of injury caused by dialysis catheters. Rats were then euthanized and harvested on days 0, 5 and 14 . Injured IJV and contralateral uninjured IJV tissue samples were collected

Results: Compared to the injured IJV, injured vein demonstrated thrombosis followed by neo-intimal hyperplasia (NIH) on days 5 and 14 . Cell-type specific markers (CD31) and smooth muscle actin (SMA) showed disruption of endothelial cells from the site of injury.

Conclusion: This is the first report demonstrating successful generation of CVS in a rodent model. This study will facilitate the development for further research into the pathogenesis and mediators of effect CVS in patients with ESKD.

54 QUANTIFICATION OF CELLULAR COMPONENTS OF AVF EXPLANTS

Connor Kim, John Le, Yichi Zhang, Wenqing Yin, Mostafa Belghasem, Mengwei Zhang, Saran Lotfollahzadeh, Josephine Orrick, Nagla Elzinad, Vijaya Kolachalama, Vipul Chitalia.

Station # 8

Objectives: Dialysis Access is the lifeline of patients on Hemodialysis. The Arteriovenous Fistula (AVF) is used as the primary dialysis modality in patients with End Stage Kidney Disease (ESKD). This process is characterized by dilation of the vein, and remodeling of the venous wall consisting of vascular smooth muscle cell (VSMC) proliferation, extracellular matrix (ECM) deposition, etc. The cellular components driving the vascular remodeling are poorly understood. We set out to examine explanted AVF from 22 ESKD patients.

Methods: H&E, Pentachrome, and Sirius Red staining were used to analyze the components from explanted AVF. Annotations were completed in a bioimaging software (QuPath). Image quantification was performed using a “Random Forest” learning classifier to identify the amount of cellular and non cellular components.

Results: Several pathologies were noted including calcification, bleeding, needle tracks, proteoglycan accumulation, and VSMC proliferation. Our analysis involved segmenting the tissue into three main regions: dominantly VSMCs; dominantly proteoglycans; and a mix of VSMCs, proteoglycans, and collagen. A machine learning approach was able to quantify the three regions of interest into percentages of the entire tissue.

Conclusion: This is the first study examining the remodeling of AVF obtained from human patients. Color analysis performed on the whole slide image revealed that while saturation and value of yellow and blue colors vary, their hues are localized on a small range; this is the key to separating each region of interest. These results will pave the foundation to understanding the molecular modulators of venous remodeling during fistula maturation.

68 ZEB2 CONTROLS KIDNEY STROMAL PROGENITOR DIFFERENTIATION AND INHIBITS ABNORMAL MYOFIBROBLAST EXPANSION AND KIDNEY FIBROSIS

Sudhir Kumar, Xueping Fan, Hila Milo Rasouly, Richa Sharma, David J. Salant, Weining Lu.

Station # 9

Objectives: FOXD1⁺ derived stromal cells support the kidney vasculature and nephron development. However, FOXD1⁺ stromal progenitors also serve as myofibroblast precursors in kidney fibrosis. The signals that regulate the FOXD1⁺ stromal progenitor’s differentiation are not well understood. We examined the role of ZEB2 in kidney stromal cell differentiation.

Methods: We generated *Zeb2* stromal-specific conditional knockout mice (cKO) by crossing

Zeb2 flox mice with *Foxd1Cre* mice and analyzed the phenotype of *Zeb2* cKO mice and control mice. Kidney histology, renal function, and lifespan were studied. Protein expression analyses were performed by immunostaining and Western blotting.

Results: Deletion of *Zeb2* in FOXD1⁺ stromal progenitors produced dysplastic and hypovascular kidneys. The *Zeb2* deficient FOXD1⁺ stromal progenitors in these kidneys took on a myofibroblast cell fate that led to kidney fibrosis and kidney failure. Cell marker studies confirmed that these myofibroblasts expressed pericyte and resident fibroblast markers including PDGFR β , CSPG4, Desmin, GLI1, and NT5E. Notably, elevated interstitial collagen deposition was accompanied by increased expression of activated SMAD1/5/8, SMAD2/3, and SMAD4.

Conclusion: ZEB2 maintains the cell fate of FOXD1⁺ stromal progenitors and loss of ZEB2 leads to differentiation of FOXD1⁺ stromal progenitors into myofibroblasts and kidney fibrosis.

102 ROLE OF PIP COMPLEX IN PODOCYTES INDICATED BY PODOCYTE-SPECIFIC KNOCKOUT OF INTEGRIN-LINKED KINASE (ILK)

Aksel Laudon, Sudhir Kumar, Weining Lu.

Station # 10

Objectives: Podocytes adhere to the glomerular basement membrane (GBM) through integrin adhesion complexes that link the foot process actin cytoskeleton with the GBM extracellular matrix. Parvin, ILK, and PINCH form a ternary complex (PIP) at integrin adhesions. It has been reported that podocyte-specific ILK knockout mice exhibit progressive glomerular morphological changes including podocyte foot process effacement and loss. However, the role of the PIP complex in podocyte adhesion is not well understood.

Methods: *ILK^{flox/flox}PodCre⁺* (ILK cKO) mice were generated for podocyte-specific knockout of ILK. Immunofluorescence staining with co-labeling of α -parvin and PINCH-2 with established podocyte marker nephrin was performed in ILK cKO and wild type kidney sections at four and sixteen weeks of age. Kidney glomerular protein expressions were analyzed by confocal microscopy.

Results: We found that α -parvin and PINCH-2 colocalize significantly with nephrin in wild type samples. However, in ILK cKO samples at both four- and sixteen-week time points, α -parvin and PINCH-2 exhibit redistribution and a complete loss of colocalization with nephrin.

Conclusion: Loss of ILK disturbs the PIP complex and alters α -parvin and PINCH-2 expression and localization in podocytes. This finding indicates that α -parvin and PINCH-2 function in podocytes is ILK-dependent. Our results also suggest that the PIP complex is required for normal podocyte adhesion.

35 PHARMACOLOGICAL MANIPULATION OF LSF SUPPRESSES WNT SIGNALING IN COLON CANCER CELLS AND INHIBITS COLON TUMOR GROWTH IN MICE

Saran Lotfollahzadeh, Dominic Lo, Meng Wei Zhang, Nagla Elzinad, Josephine Orrick, Kim Connor, Scott Schaus, Ulla Hansen, Vipul Chitalia.

Station # 11

Objectives: Hyper-activated Wnt signaling driven by nuclear β -catenin in the colonic epithelium represents the seminal event in colorectal cancer (CRC) tumorigenesis. The clinical translation of Wnt inhibitors is unsuccessful. Late SV40 Factor (LSF) is a transcription factor and a potent oncogene. We evaluated the role of LSF in CRC and Wnt signaling.

Methods: We used two allogeneic and syngeneic xenograft mice models, using HT-29 and MC-38 cells. The mice were randomly separated into two groups. Once the tumor volume reached 100 mm³, 5 mg/kg Factor Quinolinone Inhibitor (FQI2-34), a specific inhibitor of LSF DNA binding, was injected intraperitoneally. Immunoprecipitation and Wnt signaling assays were performed.

Results: We showed that LSF and β -catenin interacted in CRC cell lines, and this interaction was disrupted by the FQI2-34 treatment. FQI2-34 suppressed Wnt activity in CRC cell lines in a dose-dependent manner. Leveraging both CRC xenograft models, we noted that FQI2-34 suppressed CRC tumor growth, significantly reduced nuclear β -catenin, downregulated Wnt targets; AXIN-2, SOX-9, augmented apoptosis, and suppressed the proliferation of xenograft cells. Adenocarcinomas from a series of stage 4 CRC patients showed a positive correlation between the LSF expression and Wnt targets.

Conclusion: The study uncovers the Wnt inhibitory and CRC growth-suppressive effects of FQI compounds in CRC cells, as a novel target in CRC therapeutics.

40 SUBCELLULAR LOCALIZATION OF ORF9B, A MYSTERIOUS SARS-COV-2 PROTEIN IN ENDOTHELIAL CELLS

Josephine Orrick, Marc Napoleon, Winnie Zhang, Connor Kim, Nagla Elzinad, Saran Lotfollahzadeh, Jena Goodman, Michael Kirber, Ali Munawar, Vipul Chitalia.

Station # 12

Objectives: SARS-CoV-2 is a 29,903 nucleotide positive-sense RNA genome. Within the SARS-CoV-2 genome, there are 14 known open reading frames (ORF) encoding 27 proteins such as spike (S), envelope (E), membrane (M), and nucleocapsid (N). The N protein is an RNA-binding protein critical for viral genome packaging. Within the N gene, the accessory protein ORF9b is encoded, whose role in SARS-CoV-2 remains enigmatic. ORF9b has nuclear export signal motif and a central hydrophobic cavity proposed to be involved with lipid binding to organelle membranes, consistent with a role in virion assembly. We set out to examine the subcellular localization of ORF9b in endothelial cells to understand its functional relevance.

Methods: We generated a full length and two truncated mutants of ORF9b lacking the lipid-binding domain. These plasmids were expressed in endothelial cells with a flag tag. Super resolution (STED) microscopy was performed using organelle markers.

Results: Our STED images showed the colocalization of full length and one truncated ORF9b within the mitochondria (R=0.7, 0.75) and in the endoplasmic reticulum (R=0.7, 0.7). There was no localization observed in the Golgi apparatus.

Conclusion: ORF9b is predominantly localized in mitochondria and endoplasmic reticulum. Which may indicate a role in fatty acid oxidation and lipid synthesis. This study will provide the framework for functional studies to examine the biological relevance of ORF9b in SARS-CoV-2 patients.

32 OXIDATIVE STRESS AND HYPOXIA DOWNREGULATE TMIGD1 IN CALPAIN 2-DEPENDENT MANNER TO MODULATE RENAL TUBULE CELL SURVIVAL

Mengwei Zhang, Wenqing Yin, John Le, Josephine Orrick, Connor Kim, Nagla Elzinad, Saran Lotfollahzadeh, Nader Rahimi, Vipul Chitalia.

Station # 13

Objectives: Tubular damage due to hypoxia and oxidative stress is a fundamental contributor to acute kidney injury (AKI). We previously identified tubule-specific transmembrane and immunoglobulin domain-containing 1 (TMIGD1) protein that is critical for the renal tubular cell survival. TMIGD1 is downregulated by hypoxia and oxidative stress observed commonly in AKI. Calpain 2 is a calcium dependent protease.

Methods: To explore the effects of oxidative stress and hypoxia on TMIGD1 protein expression, HEK293T and MDCK cells were treated with hydrogen peroxide, cobalt (II) chloride hexahydrate, and hypoxia chamber. HK-2 cells were transfected with calpain 1, calpain 2, or control silencing oligos to examine targets. Calpain inhibitor 1 was injected into ischemia reperfusion rodent model to examine renal tubular damage.

Results: Hypoxia and oxidative stress downregulated TMIGD1 protein, which was abrogated by calpain inhibitor 1 (inhibits both calpain 1 and calpain 2). Silencing experiments show that TMIGD1 was critically regulated by calpain 2 only. Treatment of calpain inhibitor 1 abrogated the renal tubular damage in ischemia reperfusion rodent model.

Conclusion: Our studies demonstrate that calpain inhibitor 1 has a protective function in modulating TMIGD1 during oxidative stress and hypoxia to prevent renal tubular injury. These results uncover the role of calpain 2 on TMIGD1 which can be further pursued as a target for AKI.

106 LYSYL OXIDASE LIKE-2 IN CHONDROPROGENITOR FUNCTION AND OSTEOARTHRITIS

Faiza Ali, Manish Bais.

Station # 14

Objectives: While the progressive joint disease osteoarthritis(OA) affects a significant portion of the aging US population. Identifying agents that promote cartilage regeneration and protect against cartilage damage could provide breakthroughs for OA prevention and treatment. However, there is no chondroprotective agent that is approved for clinical application. LOXL2 is elevated in the regenerative response during fracture healing in mice and has a critical role in chondrogenic differentiation. The goal of the present study is to evaluate the role of LOXL2 in post traumatic OA.

Methods: To evaluate the cartilage-specific loss of LOXL2, we generated tamoxifen TM-inducible, cartilage-specific LOXL2 knockout mice. Immunostaining and Safranin-O-staining was performed. In another group of animals, treadmill exhaustion test, allodynia test and Gait analysis is done as functional tests.

Results: Reduced LOXL2 and aggrecan levels in LOXL2-KO compared to LOXL2-WT mice. The comparison of sham between LOXL2-WT and LOXL2-Ko showed similar changes, whereas DMM knee has severe changes. The data shows that DMM surgery in LOXL2-cKO knee cartilage reduced proteoglycan, aggrecan, LOXL2, lubricin whereas elevated MMP13, and IL-1 β compared to LOXL2-WT. In another study to evaluate the role of adenovirus delivered LOXL2 in knee joint, the treadmill exhaustion test showed that treadmill running for time and distance are impaired in the group with Adv-RFP-EMPTY injected group and rescued in Adv-RFP-LOXL2.

Conclusion: LOXL2 appears to protect mice from DMM-OA induced impaired functional changes. Loxl2 attenuates accessibility to chromatin of specific epigenetic regulators in chondrocytes using ATACseq.

14 NOVEL COCRYSTALLIZATION OF APOLIPOPROTEIN A-I WITH BUTYRIC ACID

Grace Ferri.
Station # 15

Objectives: High-density lipoprotein, or HDL, is known as the anti-atherogenic “good cholesterol” in the process of reverse cholesterol transport. HDL is composed of free cholesterol scavenged from the body and a protein known as apolipoprotein A-I (apoA-I). In order to facilitate cholesterol excretion from the body, apoA-I must first bind cholesterol and form HDL. The enzyme lecithin-cholesterol acyltransferase then acts on the cholesterol bound to apoA-I within the HDL, which prevents the cholesterol from reentering the cells of the body. However, the mechanism by which apoA-I presents cholesterol to LCAT remains unknown. The objective of this project was to cocrystallize apoA-I with lipid substrate to elucidate this mechanism.

Methods: In order to understand the molecular details of the mechanism by which apoA-I activates LCAT and thereby initiates cholesterol esterification with fatty acid, apoA-I was cocrystallized with butyric acid. Butyric acid is a small, soluble fatty acid modeling the product of the first step of LCAT action and representing the substrate upon which LCAT would act to esterify cholesterol.

Results: Crystals were grown from a truncated apoA-I construct designed with and without butyric acid. The three-dimensional crystal structure of the mutant apoA-I protein construct was solved in the absence of butyric acid.

Conclusion: When the lipid-bound crystal structure is solved, the residues of the truncated apoA-I construct binding to butyric acid will illustrate how the conformation of apoA-I changes in the presence of lipid. If the hypothesized binding mechanism is supported, the binding residues may prove to be targetable by anti-atherogenic drugs.

Session 2 – Floor 6 Thursday 10/7 10:30 am - 11:30 am

172 PULMONARY LYMPHATIC VESSEL REMODELING IN RESPONSE TO INFLUENZA INFECTION

Senegal Carty, Erin Crosssey, MD, PhD, Fengzhi Shao, Alexandra Ysasi, Michelle Zeng, Jin Yuan, MD, PhD, Jhonatan Henao-Vasquez, Anne Hinds, Alan Fine, MD, Matthew Jones, PhD.

Station # 1

Objectives: Pulmonary inflammation requires delicate regulation to limit tissue damage while promoting pathogen clearance. The pulmonary lymphatic system is critical to this, as it removes excess fluid, is a pathway for immune cell trafficking and can directly affect immune cell phenotype via lymphatic endothelial cell (LEC) signaling. Influenza infection is a common cause of severe disease, but the pulmonary lymphatic system's response to it is understudied. We hypothesize that lymphatics are remodeled to facilitate flu clearance and regulate immune cell activity.

Methods: To test our hypothesis, we performed immunohistochemistry (IHC) to detect PROX1, the master regulator of LEC fate, in flu-infected and control murine lungs. This allowed us to enumerate LECs to determine whether lymphangiogenesis, in contrast to lymphatic dilation, was occurring. To investigate whether new LECs arose through proliferation or progenitor recruitment, we quantified the proportion that incorporated EdU. We also measured the expression of soluble VEGFR2 (sVEGFR2), an inhibitor of lymphangiogenesis, via qRT-PCR and Western blot.

Results: Our studies reveal that the LEC population triples by 21 days post infection (dpi) in flu-infected lungs, and that about 20% of LECs incorporate EdU by 7 dpi. We also found that sVEGFR2 expression is markedly decreased in infected lungs.

Conclusion: These results show that flu infection induces pulmonary lymphangiogenesis, and strongly suggest that this is mediated largely by LEC proliferation. We postulate that sVEGFR2 downregulation promotes this growth. Future work will further probe this potential connection, as well as LEC phenotypical changes in response to the flu.

143 ERG DEFICIENCY CONTRIBUTES TO PULMONARY FIBROSIS VIA AFFECTING TISSUE LYMPHANGIOGENESIS

Adri Chakraborty, Grace Marden, Vrinda DAMBAL, Ashna Panchmatia, Yashasvi Tharani, Maria Trojanowska.

Station # 2

Objectives: Pulmonary Fibrosis (PF) is characterized by extensive tissue remodeling, tissue scarring, and incomplete resolution of inflammation. Lymphatic network contribute to both promoting and mitigating lung fibrosis. Reduced expression of ERG transcription factor has been linked with vascular injury and perivascular inflammation in PF. We aim to determine if ERG deficiency affects the etiology of lymphangiogenesis and pathogenic fibrosis in lungs.

Methods: *Prox1CreERT2/Erg^{fl/fl}* mice lung samples were processed for flow cytometry, IHC, western blot and qPCR for lymphangiogenic and inflammation genes. siERG treated Human pulmonary lymphatic endothelial cells (HPVLECs) gene expression changes were validated. Human IPAH lung biopsies were immune-stained for LYVE-1, PROX-1 and VWF.

Results: We demonstrated that lymphatic endothelial (LEC) specific deletion of ERG in *Prox1CreERT2/Erg^{fl/fl}* mice resulted in significant up-regulation of Type-1 collagen, *Tgf-β* expressing iBALTs and activated macrophages supporting spontaneous lung fibrosis. An increase in Ly6C (+/-) monocytes, alveolar macrophages, eosinophils, and CD103+ dendritic cells suggested an inflammatory milieu in the lungs. Down-regulation key lymphangiogenic genes was also observed (*Flt4, Vegf-C*). An increase in lymphatic structure remodeling in diseased IPAH lungs was concurrent with fibrotic progression. Key lymphangiogenic genes (*FLT4, LYVE-1, PROX-1*) were reduced and leukocyte recruitment genes (*TLR-4, CXCR-4*) were increased upon siERG treatment of HPVLECs.

Conclusion: Loss of ERG contributes to lymphatic dysfunction and lung fibrosis, through the induction of tissue inflammation.

112 A ROLE FOR DISTINCT LYMPHATIC ENDOTHELIAL CELL SUBSETS IN PULMONARY LYMPHANGIOGENESIS

Erin Crosse, Senegal Carty, Matt Jones, Alan Fine.

Station # 3

Objectives: The lymphatic system consists of a network of vessels lined by specialized lymphatic endothelial cells (LECs) that are responsible for tissue fluid homeostasis and immune cell trafficking, but the mechanisms for LEC response to environmental cues are poorly understood.

Methods: We have found marked induction of lymphangiogenesis after influenza A virus (IAV) infection in the adult mouse lung, making this a useful model to study the dynamics of

the lymphatic system.

Results: The number of LECs increases more than 3-fold at 7 and 21 days post-IAV infection (dpi). Using EdU labeling, we found that 15-25% of pulmonary LECs are proliferating at 7 dpi as compared to 1% of LECs in homeostatic conditions, suggesting a subset of LECs have proliferative potential. Increase in LEC number is preceded by increasing lymphatic vessel diameter, thus mechanically sensitive signals such as Hippo pathway may be particularly important in LECs. We found that nuclear localization of YAP, one of the primary transcription factor effectors of the Hippo pathway, is significantly reduced in LECs during IAV infection.

Conclusion: Our preliminary data suggest that distinct functional LEC subtypes may exist during lymphangiogenesis. To further investigate this we have adapted a novel mouse model for GFP-tagging LEC nuclei to facilitate single nuclei RNA sequencing. We have also harnessed a mouse model for conditional deletion of YAP/TAZ in LECs, and plan to assess whether perturbation of the Hippo pathway affects lymphangiogenesis in the context of IAV infection. We also plan to use lineage reporter strategies to determine whether proliferative potential of LEC subsets in adulthood is determined by cell lineage.

178 LUNG B CELL DYNAMICS DURING RESPIRATORY INFECTION

Neelou Etesami, Kimberly Barker, Anukul Shenoy, Carolina Lyon De Ana, Wesley Goltry, Anna Belkina, Joseph Mizgerd.

Station # 4

Objectives: Using a murine model of anti-pneumococcal immunity, we showed that protective lung resident memory B (BRM) cells seed the lung in response to *Streptococcus pneumoniae* (Sp) exposures and are maintained independently of induced bronchus-associated lymphoid tissue (iBALT). We used the Sp model to elucidate the dynamics of B cell establishment in an iBALT-independent context.

Methods: C57BL/6 mice were repeatedly exposed to a self-limiting Sp serotype intratracheally and analyzed with flow cytometric and enzyme-linked assays.

Results: Lung B cells required 2 exposures to Sp to seed the lung and develop the BRM pool. This followed a large increase of B cells entering the lung days after the 2nd exposure, correlating with lung increases of the follicular chemokine CXCL13. B cell establishment was abrogated by administration of an S1PIR inhibitor during the 2nd exposure to Sp, preventing recruitment from the periphery. Depletion of CD4+ cells during the 2nd exposure contracted extravascular B2 B and B1 B cells and decreased BRM cell proportions. Airspace Sp-reactive IgG and IgA, but not IgM or plasma Sp-reactive antibodies, were decreased in anti-CD4 treated mice.

Conclusion: Our data suggest that lung B cell expansion is dependent on recruitment from peripheral lymphoid organs, and show a dependence on CD4+ T cells for the development of BRM cells derived from lineages responding to T-independent and T-dependent antigens.

30 INDUCED PLURIPOTENT STEM CELL MODELING OF COMMON VARIABLE IMMUNE DEFICIENCY-ASSOCIATED *NFKB1* MUTATIONS

Kevin Hayes, Aditya Mithal, Gustavo Mostoslavsky, PJ Maglione.

Station # 5

Objectives: Patients with Common Variable Immune Deficiency (CVID) experience recurrent infections due to profound antibody deficiency. Through poorly defined etiologies, they are also at a higher risk for developing comorbidities like lung disease and gastritis. From previous experiments on sample plasma, our lab has shown that patients with these complications express high levels of NF- κ B regulated cytokines. In this pathway, the gene *NFKB1* encodes a key transcriptional regulator of cytokine production, and is one of the most commonly mutated genes in CVID. Mutations in this gene can alter pathway activity, but previous studies have failed to capture how a given variant can impact disease phenotypes. Therefore, our work focuses on understanding the relationship between NF- κ B dysregulation and the onset of complicated CVID. We hypothesize that *NFKB1* variants alter cytokine production in CVID patients leading to a dysregulated immune response capable of supporting comorbid phenotypes.

Methods: To test this, our lab is the first to generate a line of induced pluripotent stem cells (iPSCs) from a CVID patient that presented with complications and an *NFKB1* frameshift

mutation.

Results: By differentiating these cells into macrophages, we have measured significant differences in their cytokine response to lipopolysaccharide when compared to wild type cells.

Conclusion: Future experiments will use gene editing to see how the correction of NFKB1 impacts these differences.

61 AIRWAY MULTICILIATED CELL HETEROGENEITY IN RESPONSE TO INFLUENZA INFECTION

Jhonatan Henao Vasquez, Jin Yuan, Senegal Carty, Erin Crossey, Fengzhi Shao, Lee Quinton, Katrina Traber, Joseph Mizgerd, Alan Fine, Matthew Jones.

Station # 6

Objectives: Once thought to be a homologous population, we found evidence of heterogeneity among airway multiciliated cells. These populations can be distinguished by the expression of MIWI2. Preliminary data suggested that MIWI2 deficient mice exhibited an enhanced clearance of Influenza A virus (IAV), leading to the hypothesis that MIWI2 multiciliated cells exacerbates IAV infection. To address this hypothesis, we are generating *in vitro* and *in vivo* models involving air-liquid interface (ALI) epithelial cell cultures, a recombinant reporter IAV (mNeon), and a genetically modified mice (MIWI2^{+/Tom} reporter).

Methods: ALIs were generated from tracheal basal cells isolated from wildtype and MIWI2^{+/Tom} mice both haploinsufficient and deficient in MIWI2. These ALI cultures will be infected with IAV and outcomes of interest will be viral load and cellular heterogeneity in the context of genotype and infection. mNeon-IAV will also be used to infect wildtype and MIWI2^{+/Tom} mice followed by flow cytometric analysis to determine epithelial cell heterogeneity and reporter expression over a time course of IAV infection.

Results: ALIs DAB staining show an increase in MIWI2 when exposed to notch inhibitor, DAPT. Flow data show MIWI2 cells are not initially infected 3 days post-infection.

Conclusion: In summary, we anticipate that these studies will help address a major knowledge gap regarding the host response of airway multiciliated cell subsets during infection.

12 A MOUSE SINGLE-CELL LUNG ATLAS OF COMPLEMENT GENE EXPRESSION

Archana Jayaraman, Neha Chaudhary, Joseph Mizgerd, Joshua Campbell, Markus Bosmann.

Station # 7

Objectives: In this study, we aimed to profile the cellular distribution of complement gene expression in the lung.

Methods: Open-access single cell RNA-seq data from young (3 months) and old C57BL/6 mice (24 months; GEO: GSE124872) were analyzed using the Seurat package.

Results: Across 30 distinct cell types, mesothelial cells, lipofibroblasts and interstitial fibroblasts expressed the largest number of complement genes, including proteases (eg., *C1ra*), complement components (*C3*), receptors (*Calr*), and regulators (*Serp1g1*; Fig. 1). *C5* was expressed mainly in AT2 cells.

Conclusion: We present a novel perspective on the local production of specific complement genes in healthy lungs, highlighting their role in tissue-specific immunity and homeostasis.

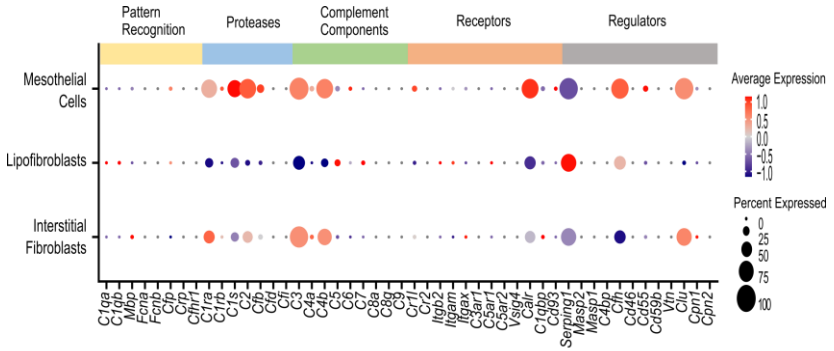


Figure 1. Dotplot depicting distribution and expression of complement genes in mesothelial cells, lipofibroblasts and interstitial fibroblasts in lungs from young mice (3 months old, n=8). Size of dots represents the percentage of cells expressing a gene and color intensity represents the average expression level.

72 HETEROGENEITY OF CD4⁺T CELLS IN PNEUMOCOCCAL PNEUMONIA

Carolina Lyon De Ana, Anukul Shenoy, Kimberly Barker, Emad Arafa, Neelou Etesami, Ian Martin, Anna Belkina, Brian Tilton, Wesley Goltry, Matthew Jones, Lee Quinton, Joseph Mizgerd.

Station # 8

Objectives: Non-lethal exposures to *Streptococcus pneumoniae* (Spn) provide protection against subsequent heterotypic pneumonia. Part of this protection is driven by CD4⁺ resident memory T cells (T_{RM}s). We aim to evaluate CD4⁺ T_{RM}s, their functions and their potential contribution to lung immunity.

Methods: C57BL/6 mice received Spn serotype 19F (Sp19F) intratracheally twice, one week apart. Lungs were collected and processed for spectral cytometry. FTY720 was administered intraperitoneally for 12 days.

Results: Infection with Spn enriched CD4⁺ T cells in the lungs during infection and then for prolonged periods after. To characterize T cell subsets, we evaluated spectral cytometry data using unbiased T-stochastic neighbor embedding (t-SNE) plots, which showed CD4⁺ T cells clustered into subgroups defined as CD11a⁺, CD11a⁺CD69⁺GL7⁺, CD11a⁺CD69⁺GL7⁺ and CD11a⁺CD69⁻GL7⁻. All CD11a⁺ subsets were CD62L^{low}CD44^{high} memory cells. FTY720 treatment resulted in reduction only of CD11a⁺ subsets. Flow cytometry showed GL7⁺ subsets were not CXCR5⁺PD1⁺BCL6⁺ follicular T cells. Compared to GL7⁻ subsets (mostly RORγT⁺), GL7⁺ cells expressed more Gata-3. Ex-vivo cytokine staining revealed GL7⁺ subsets secreted more T helper (Th) 2-like cytokines.

Conclusion: CD11a⁺CD69⁺GL7⁺ T cells represent a novel subset of lung CD4⁺ T_{RM}s with a surface marker profile previously unreported in memory T cells. Unlike the characteristic Th17-specific phenotype of GL7⁻ T_{RM}s after Spn infections, the GL7⁺ subset may be functionally different with unique roles in the lung. Their contributions to heterotypic immunity and lung protection are the focus of ongoing studies.

136 ASSOCIATIONS OF PLASMA BAFF AND SOLUBLE BAFF WITH AUTOIMMUNE AND LYMPHOPROLIFERATIVE COMPLICATIONS IN CVID

Erik Matson, Paul Maglione.

Station # 9

Objectives: The objective of this study was to measure and correlate levels of soluble BAFF receptors with their ligands in subsets of CVID patients related to complicative status and *Tnfrsf13b* genetic variants.

Methods: Plasma samples from healthy controls and patients diagnosed with CVID or X-linked agammaglobulinemia were assayed via ELISA to detect levels of soluble BAFF, BAFF-R, TACI, and BCMA. CVID patients were stratified into complicated status based on their history of diagnosis with autoimmune or lymphoproliferative disease.

Results: BAFF was significantly elevated in complicated CVID compared to uncomplicated CVID and healthy controls. There were elevations of sBAFF-R and sTACI with reduced sBCMA in uncomplicated and complicated CVID compared to healthy controls. Ratios of

sTACI to BAFF and sBCMA to BAFF were significantly reduced in complicated vs. uncomplicated COVID, and there was no difference in these ratios between uncomplicated COVID and healthy controls. Ratios of sBAFF-R to BAFF was significantly elevated only in uncomplicated COVID relative to healthy controls.

Conclusion: In healthy control plasma, sBCMA is the predominant soluble BAFF receptor that is able to bind BAFF. Elevations of sBAFF-R and sTACI in COVID plasma may be reflective of the lower maturational status of B cells in COVID and/or compensatory mechanisms to mitigate the lack of sBCMA. Rationalizing levels of sTACI to BAFF suggests that complicated COVID B cells have reduced ability to upregulate processing of sTACI in response to BAFF compared to uncomplicated COVID. Furthermore, the data suggest that uncomplicated COVID patients are capable of upregulating sBAFF-R to a greater extent than complicated COVID patients.

67 LIF-MEDIATED TISSUE INJURY AND APOPTOSIS DURING PNEUMONIA

Elim Na, Filiz Korkmaz, Christine Odom, Lillia Baird, Matthew Jones, Joseph Mizgerd, Katrina Traber, Xaralabos Varelas, Lee Quinton.

Station # 10

Objectives: Pneumonia is a worldwide public health concern representing a leading burden of disease. Leukemia inhibitory factor (LIF), an IL-6 family cytokine, is crucial for tissue protection during pneumonia. However, cellular targets and signaling networks required for LIF-mediated protection are unknown.

Methods: Microarray analysis was conducted on sorted epithelial cells from C57BL/6 mice that received *E. coli* co-instilled with control IgG or LIF-neutralizing IgG for 6 or 24 hours. TUNEL staining and flow cytometry were used to identify and quantify apoptotic cells. Wildtype and EpiLIFR^{ΔΔ} mice (lacking LIFR on lung epithelium) were infected with *E. coli* for 24 hours, and pneumonic outcomes were measured. Single-cell RNA-sequencing (scRNAseq) was conducted on lung cells from C57BL/6 mice treated with IgG saline, IgG *E. coli*, or anti-LIF *E. coli* for 24 hours.

Results: GSEA revealed that apoptosis-related pathways were upregulated in anti-LIF compared to IgG. TUNEL staining and flow cytometry confirmed that there were more apoptotic cells in anti-LIF compared to IgG. Results from the EpiLIFR^{ΔΔ} mice indicated a significant increase in lung injury following LIFR deletion. ScRNAseq revealed that ATII, endothelial, and mesenchymal cells express *Lifr*. Unsupervised clustering showed significant changes in ATII cells during pneumonia, with additional differences following LIF neutralization.

Conclusion: While epithelial LIFR contributes to lung protection during pneumonia, future studies will focus on the mechanisms underlying LIF-mediated protection in other cell types, possibly revealing novel targets for clinical intervention in patients with or at risk for lung infections.

124 LIVER ACTIVITY MODULATES THE LUNG DURING ENDOTOXEMIA AND PNEUMONIA

Christine Odom, Yuri Kim, Filiz Korkmaz, Elim Na, Lillia Baird, Matthew Jones, Joseph Mizgerd, Katrina Traber, Lee Quinton.

Station # 11

Objectives: Patients with sepsis and other forms of systemic distress are highly susceptible to nosocomial pneumonia, demanding understanding of host immune pathways involved. The hepatic acute phase response (APR) is initiated following infection and injury, and we have shown that this liver response is necessary to limit pneumonia susceptibility following a systemic challenge with endotoxemia. We hypothesized that liver-dependent lung protection following endotoxemia remodels the lung transcriptome and proteome to fortify pulmonary defense.

Methods: WT mice and APR-deficient littermates lacking hepatocyte STAT3 (hepSTAT3^{-/-}) were challenged with endotoxemia to elicit systemic inflammation, followed by induction of pneumonia. Lungs and bronchoalveolar lavage fluid (BALF) were collected at multiple timepoints. RNAseq, BALF proteomics, and supporting experiments were performed to comprehensively investigate the influence of STAT3-mediated liver activity on lung remodeling.

Results: Endotoxemia elicited robust transcriptional changes in the lung, with nearly 2,000

differentially expressed genes due to liver STAT3 deficiency, suggesting an altered baseline in mutant mice prior to infection. Proteomics revealed genotype-dependent differences in the airspaces following lung infection, implicating a network of dispatched liver-derived mediators such as fibrinogen.

Conclusion: Results indicate liver activation substantially modifies biological pathways in the following systemic inflammation, causing reduced immune responsiveness to subsequent pathogens. Further studies are needed to confirm whether such lung changes directly influence pneumonia susceptibility.

42 PLATFORM TO INVESTIGATE NEUTROPHIL HETEROGENEITY AND DIFFERENTIATION IN MURINE LUNG

Riley Pihl, Nia Shaw, Katrina Traber.

Station # 12

Objectives: Understanding immune dysfunction in pneumonia has emerged as a crucial avenue for developing novel therapeutic strategies. Our recent work has shown pneumonic neutrophils are transcriptionally dynamic, yet the role of these changes requires further investigation. The goal of this work is to develop a platform to characterize neutrophil differentiation and function after migration across the lung epithelium.

Methods: We have developed an *ex vivo* culture system to model trans-epithelial neutrophil migration. Murine lung epithelial cells were grown at air-liquid interface (ALI). ER-Hox-B8 cells, a genetically modified neutrophil progenitor line which reliably differentiates into neutrophils, migrated across the ALI toward the chemokine CXCL1. Neutrophils crossing the lung epithelial layer were harvested and transcription of target genes was measured.

Results: We have successfully generated ALI cultures, and differentiated ER-Hox-B8 into neutrophil-like cells. These neutrophils can be stimulated to migrate across an ALI toward the neutrophil chemokines CXCL1 and RNA can be isolated from these cells to measure transcriptional changes related to migration.

Conclusion: Our *ex vivo* migration platform is a reliable system to compare differences in neutrophil phenotype under different test conditions, such as differing migratory stimulus, health of ALI, and neutrophil activation. Work to use this platform to characterize the differential phenotypes of neutrophils by a variety of methods in the context of pneumonia is currently ongoing.

76 MOUSE MODEL OF LATE-ONSET NEUTROPHILIC ASTHMA REVEALS NOVEL CELLULAR AND MOLECULAR CIRCUITS UNDERLYING DESTRUCTIVE AIRWAY NEUTROPHILIA.

Anukul Shenoy, Filiz Korkmaz, Carolina Lyon De Ana, Christine Odom, Kimberly Barker, Wesley Goltry, Ian Martin, Feng-Zhi Shao, Matthew Jones, Lee Quinton, Felicia Chen, Anna Belkina, Joseph Mizgerd.

Station # 13

Objectives: Late-onset neutrophilic asthma (NA) presents as severe, steroid-refractory, airway inflammation with unclear etiologies and poor outcomes. Here, we aim to develop a mouse model to study this adult-onset disease.

Methods: Flow-cytometry, spectral-cytometry, histology and mRNA-analyses were used to describe cellular components of NA in mice.

Results: Transient and recurrent aeroexposure to ovalbumin over extended durations induced hallmark features of NA including rapid peribronchial neutrophilic inflammation and severe lung damage. Development of NA extensively remodeled the lung myeloid and lymphocytic landscape suggesting a new state of homeostasis. Indeed, mice with NA harbored diverse clusters of lung-resident CD4⁺ memory T_{RM} cells including a RORγt-negative but IL17A⁺ T_{H17} subset. These novel T_{H17} cells on antigenic reencounter rapidly secrete IL17A which then signals lung epithelial (predominantly airway secretory cell) and stromal cells to express CXCL5 and instigate neutrophil recruitment and destructive airway inflammation. Finally, we discovered that lung epithelial antigen presentation regulates disease severity by virtue of its ability to instruct CD4⁺ T_{RM} phenotypes in NA. Specifically, genetic ablation of lung epithelial MHCII limits T_{H1} T_{RM}⁻ and resultant IFNγ⁻ responses; the latter cytokine being a potent suppressor of IL17A-induced CXCL5 and neutrophilia.

Conclusion: Our results suggest that transient and frequent exposure to aeroallergens, as

would occur in humans progressing into adulthood, may reprogram cellular and molecular circuits within lungs to trigger neutrophilic asthma. Ongoing studies are testing sensitivity of NA to IFN γ therapy.

139 LUNG MESENCHYMAL CELL RESPONSES TO PNEUMONIA

Alicia Soucy, Joshua Campbell, Tianmu Hu, Filiz Korkmaz, Anukul Shenoy, Wesley Goltry, Ian Martin, Katrina Traber, Matthew Jones, Lee Quinton, Joseph Mizgerd.
Station # 14

Objectives: Fibroblasts are in regular contact with the endothelium, epithelium, and neutrophils transmigrating into the infected alveolar space, however whether fibroblasts or other mesenchymal cells respond during or after pneumonia is unknown.

Methods: To test this, we compared cells from uninfected mice to those with 24 hours of pneumococcal pneumonia. ICAM1 and TNFR1 increased on fibroblasts in pneumonic mice. To further study how mesenchymal cells respond to pneumonia, chromium 10X genomics single-cell RNA sequencing was used to compare CD45⁺ CD31⁻ CD326⁻ cells from naive, pneumonic, or resolved lungs. Utilizing SPRING-generated nearest neighbor graphs, continuous gene expression topologies were visualized while high dimensional relationships between complex cell populations were preserved.

Results: Five mesenchymal cell types were identified: matrix fibroblasts, myofibroblasts, pericytes, smooth muscle cells, and mesothelial cells. Transcriptome changes revealed distinct immune responses across all cell-types. Mesenchymal cells modulated their expression of proteoglycans in response to pneumonia, suggesting they alter the extracellular matrix through which leukocytes crawl. Cells also expressed diverse inflammatory mediators in a cell-specific fashion, some of which have been confirmed at the protein level. The distribution and transcriptomes of cell clusters from the naive and resolved groups of mice were not different.

Conclusion: These results suggest that the lung mesenchymal cell responses to pneumonia are transient, with a return to the original mesenchymal cell landscape and activities in lungs with immune protection after resolution of pneumonia.

138 DOUBLE DELETION OF C5A1 AND C5A2 DURING STREPTOCOCCAL PNEUMONIA

Sarah Walachowski, Markus Dudek, Leonid Eshkind, Vanessa Tansi, Joseph Mizgerd, Markus Bosmann.
Station # 15

Objectives: The complement system is essential for the clearance of encapsulated bacteria such as *Streptococcus pneumoniae* (*Spn*), recognized as a major pathogen of pneumonia. Yet, it is not entirely clear whether C5 and its activation product C5a have beneficial or detrimental effects on the outcome of *Spn* infection. C5a binds to its two homologous C5a receptors, C5aR1 and C5aR2. The extent of functional overlap and role distribution between C5aR1 and C5aR2 remains enigmatic. A critical barrier to allow studies on the role distributions of C5aRs has been the absence of a mouse strain with dual deletion of both receptors, which are encoded as adjacent linked genes on mouse chromosome 7.

Methods: CRISPR/Cas9 guided gene editing was combined with zygote/pronucleus microinjections in C57BL/6J mice to generate a C5aR1/C5aR2 double-KO strain.

Results: PCR-based screening and Sanger sequencing confirmed a 12.6 kB deletion of the coding regions of C5aR1 and C5aR2 of the new mouse strain. Phenotyping of C5aR1/2^{-/-} mice was followed by functional studies including intratracheal injections of recombinant mouse C5a or intranasal injections of *Spn TIGR4*. The airway influx of neutrophils by C5a was abrogated in C5aR1/2^{-/-} mice. Surprisingly, the dual genetic absence of C5a receptors was associated with a higher build-up of neutrophil numbers in alveolar spaces after *Spn TIGR4* infection. In a transcriptome-wide screen, FACS-sorted myeloid cells from infected lungs of double and single knockout mice were subjected to RNA sequencing.

Conclusion: Identifying novel differentially expressed genes in the C5aR1/2^{-/-} mice during *Spn* infection will help to uncover potential synergisms and redundancies of C5aR1 and C5aR2.

16 AIRWAY MULTICILIATED CELL MIWI2 AND INFLUENZA PATHOGENESIS

JIN YUAN, Carty Senegal, Erin Crossey, Jhonatan Henao Vasquez, Fengzhi Shao, Joseph Mizgerd, Matthew Jones, Alan Fine.

Station # 1

Objectives: We identified a unique subset of airway multiciliated cells expressing MIWI2 protein. Given the role that MIWI2 plays in gene silencing and defending germline against endogenous viruses, we hypothesized that multiciliated cell MIWI2 regulates the expression of exogenous viruses, such as influenza A virus (IAV) in the lung.

Methods: 100 plaque forming units of influenza strain A/Puerto Rico/8/1934 (PR8) or normal saline was directly instilled into the left lung lobes of *Miwi2^{+/HA}* mice. MIWI2+ airway epithelial cells were detected by using anti-HA antibody with quantification of HA+ cells performed at 3 days, and 2 and 4 weeks post-infection. To examine the impact of MIWI2 deficiency on viral infection, *Miwi2^{wt/dTomato}* and *Miwi2^{tdTomato/dTomato}* (MIWI2-deficient) mice were subjected to PR8 infection. At 7 days post-infection, plaque assays were performed and RT-qPCR was utilized to measure expression of IAV nucleoprotein (NP) mRNA. Two-tailed Student's *t*-tests were used for statistical analysis.

Results: The number of MIWI2+ airway epithelial cells did not change significantly over the course of IAV infection (vs normal saline). Most notably, however, MIWI2-deficient mice exhibited a significantly lower number of infectious viral particles in plaque assays on day 7 (vs *Miwi2^{wt/dTomato}*, $p < 0.005$). At the same time point, a statistically significant lower expression of NP mRNA was observed, as compared to saline controls ($p < 0.05$).

Conclusion: Our results show that lungs deficient in MIWI2 contain lower levels of infectious viral particles and NP mRNA after IAV infection. These data are the first to demonstrate a role for MIWI2 in the pathogenesis of respiratory viral infections.

156 DYSFUNCTIONAL ERG SIGNALING DRIVES PULMONARY VASCULAR AGING AND PROGRESSIVE FIBROSIS

Jisu Lee, Nunzia Caporarello, Tho Pham, Dakota Jones, Jiazhen Guan, Jefferey Meridew, Grace Marden, Takashi Yamashita, Daniel Tschumperlin, Maria Trojanowska, Giovanni Ligresti.

Station # 2

Objectives: Idiopathic Pulmonary Fibrosis (IPF) is an age-related disease. The impact of lung vasculature on IPF progression remains largely unexplored. Since aging-associated epigenetic alterations contribute to vascular dysfunction, we hypothesize that investigating the impact of aging on endothelial chromatin remodeling and transcription would provide novel insights into IPF progression.

Methods: We carried out multi-omics analysis using RNA-seq and ATAC-Seq on freshly isolated endothelial cells (ECs) from young and aged mouse lungs following bleomycin-induced lung fibrosis. Loss of function experiments, scRNA-seq, and FACS analysis were employed to investigate EC alterations in fibrotic mouse and human lungs.

Results: Multi-omics revealed widespread reduction of chromatin accessibility in lung ECs with aging. We identified ERG as a transcription factor implicated in pulmonary vascular repair and inflammation whose function was altered in aged lung ECs. Loss of endothelial ERG in young mice led to increased lung inflammation, vascular rarefaction, and persistent lung fibrosis following injury mirroring fibrotic aged lungs. Whole lung scRNA-seq and FACS analysis revealed reduced number of lung progenitor ECs, known as general capillary ECs, in ERG deficient mice and this alteration was also observed in IPF lungs.

Conclusion: Aging leads to a reduction of chromatin accessibility in lung ECs. Impaired endothelial ERG functions in aged lungs contributes to vascular dysfunction and persistent lung fibrosis following injury. Aging-associated epigenetic remodeling may affect ERG-mediated transcription leading to lung vascular disrepair, inflammation, and persistent fibrosis.

81 COMPARATIVE TRANSCRIPTIONAL ANALYSIS OF LUNG FIBROBLASTS FROM YOUNG AND AGED MICE IDENTIFIES PIM1/NFATC1 AXIS AS A DRIVER OF PERSISTENT FIBROSIS

Tho Pham, Jisu Lee, Jaizhen Guan, Nunzia Caporarello, Dakota Jones, Jeffrey Meridew, Qi Tan, Steven Huang, Daniel Tschumperlin, Giovanni Ligresti.

Station # 3

Objectives: Despite strong association between aging and idiopathic pulmonary fibrosis (IPF), few studies have provided transcriptional mechanisms linking aging to the persistent nature of IPF. Unveiling transcriptional programs driving persistent fibrosis in aging can lead to the identification of novel therapeutic strategies aimed at slowing disease progression.

Methods: RNA-seq analysis on freshly isolated young and aged lung fibroblasts following bleomycin-induced lung fibrosis was employed. Immunohistochemistry was used to validate target genes in IPF lung tissues. Gain and loss of function experiments, and pharmacological approaches using human lung fibroblasts and IPF lung explants were performed to evaluate functional roles of identified gene pathways.

Results: We found that in response to bleomycin-induced lung injury, aged lung fibroblasts exhibited a sustained profibrotic state characterized by elevated expression of genes implicated in inflammation, extracellular matrix (ECM) remodeling, and survival. We identified the kinase proviral integration site of Moloney virus 1 (PIM1) and its target Nuclear Factor of Activated T Cells 1 (NFATc1) as putative drivers of sustained profibrotic gene signatures. PIM1 overexpression in human lung fibroblasts potentiated fibrogenic activation which was dependent on NFATc1. Pharmacological inhibition of PIM1 in IPF-derived lung fibroblasts *in vitro* and IPF lung explants *ex vivo* attenuated activation and reduced expression of ECM remodeling genes and collagen secretion.

Conclusion: PIM1/NFATc1 axis perpetuates profibrotic transcriptional programs in aged lung fibroblasts and contributed to persistent fibrosis in IPF lungs.

196 REDOX REGULATION OF SIRT1 IN AORTIC ANEURYSM IN MARFAN'S SYNDROME

Enkhjargal Budbazar, Sandra Sulser Ponce de Leon, Jena Brooke Goodman, Yu Wang, Yuko Tsukahara, Jingyan Han, Francesca Seta.

Station # 4

Objectives: Aortic aneurysm (AA) is the major deadly sequelae of Marfan's syndrome (MFS), a connective tissue genetic disorder caused by mutation in the *fibrillin1* gene. We previously showed that vascular smooth muscle (VSM) sirtuin-1 (SirT1) protects mice against aortic dissection and that SirT1 activity regulates by reversible oxidative post-translational modifications (ReOx). We hypothesize that increased oxidative stress and ReOx on SirT1 contribute to AA in MFS by activating matrix metalloproteinases (MMPs), extracellular matrix-degrading enzymes associated with AA.

Methods: Dihydroethidium (DHE) staining, MMP activity and biotin switch assays performed.

Results: Mortality (47%) and incidence of AA (98%) were significantly higher in *fibrillin1* mutant mice (Fbn1^{mgR/mgR}), a mouse model of MFS (n=49) compared to WT (0%, n=25). Reactive oxygen species (1184.0 ± 119.3 vs. 780.2 ± 73.3 fluorescence/area, p=0.020) and MMP activity, measured *in situ* on aortic sections (653.7 ± 73.9 vs. 422.8 ± 58.1 fluorescence/area, p=0.035) were significantly higher in Fbn1^{mgR/mgR} (n=12) compared with WT (n=8) mice. ReOx SirT1 was higher in VSM cells from Fbn1^{mgR/mgR} than WT mice (1.7 ± 0.3 vs. 1.0 ± 0.2 AU, n=7, p=0.051). Interestingly, TGF-β1 (20 ng/mL), a pro-fibrotic cytokine, known to be increased in MFS aortas, significantly induced ReOx on SirT1 in VSM cells (1.4 ± 0.2 vs. 1.0 ± 0.0 AU, n=7, p=0.037).

Conclusion: These results suggest that TGF-β1 may inactivate SirT1 by increasing oxidant stress and ReOx modifications in VSM cells, leading to MMP activation in aortas of MFS individuals. Preventing SirT1 reversible oxidation may represent a potential therapeutic strategy against AA in MFS individuals.

73 A NOVEL OXALATE-CURCUMIN-BASED IMAGING PROBE: ENABLING TO VISUALIZE REACTIVE OXYGEN SPECIES IN ATHEROSCLEROSIS

Fangzhou Cheng.

Station # 5

Objectives: Sustained overproduction of reactive oxygen species (ROS) in the vasculature is a unified mechanism linking various risk factors with atherosclerosis. Due to the high reactivity and short lifespan, ROS detection, particularly *in vivo*, has long been a significant technical challenge. Herein, we investigate whether a near-infrared fluorescence imaging probe (CRANAD-61)—via its oxalate moiety, reacts with ROS and shifts the wavelength from 675Ex/760Em to 640Ex/720Em—can be employed to detect lesional ROS.

Methods: We injected CRANAD-61 intravenously in Western-diet-fed ApoE-deficient mice and waited for 30 minutes to detect the ROS signals. Also, we compared the ROS levels in the same lesion recognized by CRANAD-61 and Dihydroethidium (DHE, a widely used ROS probe).

Results: Our results showed that ROS mainly accumulated in macrophages in aortic lesions as reflected by the fluorescence signals at 640Ex/720Em (green channel) in Mac2 positive cells. Similar results were observed in aortic lesions incubated with CRANAD-61 *in vitro*. Lastly, we found that DHE-oxidation derived signals were mainly located in nuclei and were highly dependent on DHE concentration, whereas ROS signals detected by CRANAD-61 were in cytosol and remained constant regardless of CRANAD-61 concentration.

Conclusion: We conclude that CRANAD-61 can achieve high accuracy in ROS detection *in vivo* and thus may be used as a new method for detecting ROS in the cardiovascular system and atherosclerosis.

183 ELUCIDATING THE ROLE OF BCL11B IN AORTIC ANEURYSM DEVELOPMENT

Jena Goodman, Jeff Valisno, Lisia Vargas, Steven Tabor, Michael Kirber, Francesca Seta.

Station # 6

Objectives: Aortic aneurysms (AA) form as a result of complex pathological remodeling, including both the extracellular matrix and vascular smooth muscle cells, however the molecular mechanism is not well understood. We recently discovered transcription factor BCL11B regulates vascular tone by altering calcium-dependent cytoskeletal actin polymerization and contractile signaling pathways in vascular smooth muscle cells (VSMC). Interestingly, mice with VSMC specific Bcl11b deletion develop aortic aneurysm in response to hypertensive stimuli. Our aim is to test the hypothesis that BCL11b mediates VSMC interaction with the extracellular matrix (ECM) by altering focal adhesion activity.

Methods: Using VSMCs isolated from WT or BCL11b KO mice, we performed live-cell calcium imaging to identify potential alterations in ER calcium stores and store operated calcium entry. We also performed Western blots and super resolution microscopy to identify the composition, prevalence, and activity of focal adhesions.

Results: We have preliminary data showing a difference between WT and Bcl11b KO mice ER calcium store content $2.1 \pm .31$ vs $1.16 \pm .34$ (FURA ratio, n=2) and calcium re-uptake after stimulation 108 ± 16 vs 51 ± 31 (seconds, n=2). Preliminary data also suggests there is a difference in focal adhesion number and size (n=1).

Conclusion: Bcl11b may be a causal gene implicated in the development of aortic aneurysm by regulating calcium dependent crosstalk between cytoskeletal arrangement and the extracellular matrix through focal adhesions.

180 UTILIZING THE COMPARATIVE TOXICOGENOMIC DATABASE TO DISCOVER NOVEL PATHWAYS CONNECTING CHRONIC BINGE DRINKING TO ATHEROSCLEROSIS

Rebecca Johnson.

Station # 7

Objectives: The impacts of chronic binge drinking on the cardiovascular system is relatively unexplored within current research. Using bioinformatics resources, potential cellular signaling pathways involved in this relationship will be identified.

Methods: Utilizing the Comparative Toxicogenomics Database (CTD), a bioinformatic system

that establishes toxicological relationships between chemicals, genes, phenotypes, and diseases, an unbiased approach was taken to predict and connect the pathways disturbed in binge drinking with those altered in atherosclerosis.

Results: Two significant pathways were identified through use of methodology. The first involves eNOS, which was listed on the CTD in a 139 gene pathway as an inflammatory in a pro-atherogenesis system. The second pathway involves Cytochrome P450 2E1 (CYP2E1), an alcohol metabolizing enzyme, which was shown to be a key interactor with ethanol, having a total of 236 known connections on the CTD. CYP2E1 has a documented relationship with reactive oxygen species (ROS) in literature, which have been shown to have an impact on the development of atherosclerosis.

Conclusion: We demonstrated the potential critical pathways involved in the development of atherosclerosis induced by binge drinking patterns. These identified pathways can be targeted in future laboratory analysis to discover treatments that could remedy these disturbed pathways.

137 THE EFFECTS OF POD-BASED E-LIQUIDS ON VASCULAR ENDOTHELIAL CELL FUNCTION

Sana Majid, Robert Weisbrod, Jessica Fetterman, Naomi Hamburg.

Station # 8

Objectives: Pod-based e-cigarettes including JUUL represent the most popular product type that more efficiently deliver nicotine; however, their cardiovascular effects are poorly understood. Here, we evaluated the effects of the JUUL e-liquid and its individual components on vascular endothelial function.

Methods: We assessed endothelial function (cell viability by TUNEL and nitric oxide bioavailability using DAF-2DA) in human aortic endothelial cells (HAECs) exposed for 90 minutes to one of four JUUL pod flavors (Menthol, Mint, Mango and Virginia Tobacco) or constituents propylene glycol (PG)/vegetable glycerol (VG) at 30:70 ratio with and without nicotine salt, as well as their heated particle fractions separated with a mini-MOUDI impactor. In healthy young adults, we assessed endothelial cell function via endothelial nitric oxide synthase (eNOS) activation use in nonusers of tobacco products (n=4), pod users (n=4) and combustible cigarette users (n=3).

Results: We observed significant increases in cell death with JUUL e-liquid flavors across 0.0001-1% dilutions. PG/VG vehicle alone and with nicotine salt induced cell death to similar levels as the JUUL e-liquids. All JUUL e-liquids at 0.0001% dilution impaired A23187-stimulated nitric oxide production. Exposure to particle fractions of JUUL e-liquids at 0.001% dilution also decreased A23187-stimulated nitric oxide production. Endothelial cells from pod users showed reduced eNOS activation compared with nonusers (P=0.023), with levels of reduction similar to combustible cigarette users (P=0.281).

Conclusion: Our data suggest endothelial toxicity of pod-based e-liquids and their constituents, including in young adult users.

121 ALCOHOL BINGE DRINKING SELECTIVELY STIMULATES PROTEIN S-GLUTATHIONYLATION IN AORTA AND LIVER OF *APOE*^{-/-} MICE

Kerstin Seidel, Xueping Wan, Mo Zhang, Yuxiang Zhou, Mengwei Zang, Jingyan Han.

Station # 9

Objectives: Binge drinking has become the most common and deadly pattern of excessive alcohol use and is closely related to the increased risk of cardiovascular disease. Oxidative stress as a result of ethanol metabolism is the primary pathogenic factor for alcohol-induced end organ injury, but the role of protein S-glutathionylation—a reversible oxidative modification of protein cysteine thiol groups has not been explored.

Methods: To mimic the weekend binge drinking pattern in humans, ApoE deficient (*ApoE*^{-/-}) mice on the Lieber-DeCarli liquid diet received ethanol or isocaloric maltose gavages for a total of 6 weeks. The primary alcohol-target organs (liver, brain), and cardiovascular system (heart, aorta, lung) of these two groups of mice were assayed for the protein S-glutathionylation levels and its regulatory enzyme system [Glutaredoxin1(Grx1), glutathione reductase (GR), glutathione -S-transferase Pi (GST- π)], as well as aortic endothelial function and liver lipid accumulation.

Results: We found that binge drinking selectively stimulated protein S-glutathionylation in

aorta, liver, and brain, which coincided with altered glutathionylation regulatory enzyme system. Functionally, binge drinking induced fatty liver and damaged aortic endothelial cell function were reflected by increased permeability and reduced flow-mediated vasodilation. **Conclusion:** We conclude that the selective induction of protein S-glutathionylation in aorta and liver is associated with aortic endothelial dysfunction and fatty liver, which may be a potential redox mechanism for the increased risk of cardiovascular disease in binge-drinkers.

114 REDOX REGULATION OF VASCULAR SMOOTH MUSCLE SIRTUIN-1 IN AORTIC ANEURYSMS

Sandra Sulser Ponce de Leon, Enkhjargal Budbazar, Yuhao Huangfu, Hanxiao Liu, Francesca Seta.

Station # 10

Objectives: Vascular smooth muscle (VSM) sirtuin-1 (SirT1), a lysine deacetylase, is essential for vascular integrity. We previously found that decreased VSM SirT1 increases matrix metalloproteinases (MMPs) and promotes aortic dissections. Impaired SirT1 activity by oxidative stress leads to liver disease, however, SirT1 oxidative inactivation in the vasculature has never been studied. We hypothesized that SirT1 activity loss due to oxidative modifications is involved in the pathogenesis of aortic aneurysms (AA). Thus, we aim to (1) assess the role of VSM SirT1 in a mouse model prone to develop AA (mgR^{-/-}); (2) Develop an ELISA to measure SirT1 deacetylase activity; (3) Produce an adeno-associated virus (AAV) expressing an oxidant-resistant triple mutant (3M) SirT1 that can prevent MMPs activation and the development of AA.

Methods: MMPs activity in WT and mgR^{-/-} VSM cells and aortas was measured by in-gel zymography. We developed a colorimetric ELISA that measures acetylated and total p53 peptide fractions, as index of SirT1 deacetylase activity. We produced AAVs expressing a control or 3M SirT1 in VSM cells.

Results: MMPs activity increases in mgR^{-/-} mouse aortas (7.7 ± 0.3 ng in WT, n=6 vs 11.4 ± 1.1 ng in mgR^{-/-}, n=6; p=0.05) and VSMC (3.8 ± 0.4 ng in WT, n=4 vs 8.9 ± 1.4 ng in mgR^{-/-}, n=3; p=0.05). We completed the first stage of optimization of the ELISA. Control and SirT1 3M AAVs infected VSM cells to overexpress active SirT1.

Conclusion: Preliminary data indicates that SirT1 deacetylase activity is preserved in VSM cells infected with SirT1 3M AAV and under a pro-oxidant stimulus.

162 GLUTAREDOXIN-1 IN ENDOTHELIAL CELLS ATTENUATES STEATOSIS IN NON-ALCOHOLIC STEATOHEPATITIS (NASH)

Yuko Tsukahara, Beatriz Ferran, Brian Chong, Erika Minetti, Jingyan Han, Francesca Seta, Valerie Guoun-Evans, Reiko Matsui.

Station # 11

Objectives: Liver sinusoidal endothelial cells (LSECs) sustain liver blood flow and transfer nutrients and lipids to hepatocytes. LSECs function influences NASH progress and fibrosis, however, it is not elucidated how LSECs affect the development of NASH. Our previous studies show that glutaredoxin-1 (Glx) inhibits steatosis, angiogenesis, and protects EC from dysfunction. Glrx is an enzyme that controls redox signaling by reducing S-glutathionylated proteins. We aim to examine the role of Glrx in LSEC in the progress of NASH.

Methods: Endothelial cell-specific Glrx overexpression mice (EC-Glx) and littermate control were fed NASH diet (high fat/cholesterol/fructose) for 15-20 weeks. Lipid accumulation is evaluated by Oil red O staining and measurement of cholesterol and triglyceride levels. Human LSECs and HepG2 cells (hepatoma cell line) were used for *in vitro* study.

Results: NASH diet causes obesity and steatohepatitis. Although both control and EC-Glx mice showed similar increased body weight by NASH diet, lipid accumulation was dramatically reduced in EC-Glx mice. ALT/AST liver injury markers and ballooning damaged hepatocytes were ameliorated in EC-Glx mice, especially in male. Importantly, conditioned media from Glrx-overexpressing LSECs challenged with palmitic acid significantly inhibited lipid accumulation in HepG2 cells.

Conclusion: Glrx overexpression in ECs protected hepatocytes from lipotoxicity induced by NASH diet. *In vitro* study suggests Glrx regulates LSECs secreted factors that control lipid accumulation in hepatocytes. Identifying secretory factors may uncover a novel crosstalk between LSEC and hepatocytes leading to therapeutic intervention for NASH.

189 INUCTION OF VASCULAR PROTEIN S-GLUTATHIONYLATION IMPAIRS UNFOLDED PROTEIN RESPONSE IN AGING

Xueping Wan, Yuxiang Zhou, Tomoko Mori, Fangzhou Cheng, Kerstin Seidel, Jingyan Han.

Station # 12

Objectives: Vascular aging is associated with endoplasmic reticulum (ER) stress and oxidative stress, two cross-talk mechanisms that predispose the elderly to cardiovascular disease. Herein, we aim to understand how induction of vascular protein S-glutathionylation—a reversible oxidative modification mediating cellular responses to oxidative stress—regulates ER stress response also known as unfolded protein response (UPR) during vascular aging.

Methods: Both single-cell transcriptome analysis of aged murine and monkey aortae from publicly available datasets, and redox proteomics analysis of human aortic endothelial cells revealed cellular responses to oxidative stress and ER stress in aortic endothelial cells were significantly regulated with aging. Levels of glutathionylated proteins and UPR signaling in aorta from young (2-4 mo.) and aged (18-24 mo.) C57BL6 mice were assessed by immunoblotting and immunofluorescence analyses.

Results: In aged aorta, the PrS-SG levels, but not irreversible protein oxidation (e.g. 4-Hydroxynonenol adducts) were significantly increased; this induction of PrS-SG with age coincided with compromised UPR as reflected by diminished BiP chaperone protein and two pathways (PERK and IRE), but highly activated ATF6 signaling arm and apoptosis (p-JNK and cleaved caspase). These two aging-related processes were reversed by thiol reducing agent N-acetyl-L-cysteine administration for 6 weeks.

Conclusion: With aging, aortic proteins undergo S-glutathionylation thereby participating in regulation of UPR signaling in vascular endothelium.

85 ALPHA-1 ANTITRYPSIN DEFICIENCY ADULT CLINICAL AND GENETIC LINKAGE STUDY

Mark Dodge, Michelle Higgins, Nora Lee, Erica Menino, Grace (Qing) Zhao, Joseph Kaserman, Danielle Zimmerman, Andrew Wilson.

Station # 13

Objectives: Alpha-1 antitrypsin deficiency (AATD) is a monogenic disease resulting from homozygous inheritance of a single base pair mutation in the *SERPINA1* gene. While the lung disease associated with homozygosity of the mutant “Z” allele is highly penetrant, the penetrance of and risk factors associated with liver disease in ZZ patients have not been well defined.

Methods: We joined a multi-center observational cohort study to recruit ZZ participants and follow them over time. Study participants at each site are followed annually for a total of 4 years through a combination of questionnaires, physical examination, pulmonary function testing, liver elastography, blood tests, and liver biopsy (visits 1 and 4 only).

Results: Participant demographic and clinical data is entered into a database and linked to biospecimens, including serum, RNA, DNA, whole blood, reprogrammable blood cells for iPSC generation, and liver tissue. A total of 92 participants have been enrolled in the study including 25 participants at Boston University.

Conclusion: Liver biopsies performed in year 1 revealed a range of findings, including presence of inflammation, intrahepatic accumulation of AAT protein, and fibrotic injury.

194 ENDOCRINOLOGISTS' EXPERIENCES WITH TELEHEALTH: ORGANIZATIONAL AND LOGISTICAL ISSUES WITH IMPLEMENTATION

Denise Wong, Kailyn Sitter, Rendelle Bolton, Varsha Vimalananda.

Station # 14

Objectives: Due to the COVID public health emergency, there has been a drive to shift a large portion of routine general and specialist care to video and telephone visits, and the use of telehealth has skyrocketed over the past year. Our study examined endocrinologists' experiences with synchronous telehealth and identified factors that affect their experiences with its implementation.

Methods: We identified 26 endocrinologists located around the US using a snowball approach, and conducted semi-structured one-on-one video interviews. We used directed content analysis with a rapid qualitative analytic approach.

Results: Endocrinologists' experiences with telehealth were influenced by three main factors, as aligned with the human-organization-technology fit framework: 1) provider factors, including motivation to start and continue using telehealth, perceptions of telehealth, satisfaction, and perceived benefits; 2) organizational factors, including institutional structures to support use, changes to workflow, staff coordination, and system-level policies; and 3) aspects of technology, including ease of use and availability of technical support.

Conclusion: Endocrinologists reflected that their experiences of telehealth use thus far in the public health emergency have been varied and greatly impacted by provider factors, organizational factors, and aspects of technology. Further implementation strategies for telehealth should therefore address these three main issues to maximize success in telehealth adoption and use.

Session 2 – Floor 8 Thursday 10/7 10:30 am - 11:30 am

170 TRANSCRIPTOME-WIDE ANALYSIS OF DIFFERENT DEMENTIA TYPES IN HUMAN HIPPOCAMPUS

Oluwatosin Olayinka, Junming Hu, Nicholas O'Neill, Xiaoling Zhang, Irene Simkin, Thor Stein, Lindsay Farrer.

Station # 1

Objectives: Alzheimer's disease (AD) is a disease characterized by cognitive deterioration and the presence of extracellular amyloid beta deposits and neurofibrillary tangles in the brain. These may occur in tandem with markers of Lewy body (LB) and vascular (Va) dementia. Studying expression profiles for these provide an opportunity to learn more about factors shared between AD and other dementias.

Methods: Bulk RNA-sequencing was performed on 210 human postmortem hippocampal samples obtained from brains donated to the BU AD Research Center by 186 subjects with a diagnosis of AD and 21 controls. After quality checks, we analyzed 191 samples classified as AD+LB, AD+Va, AD alone, and controls. Analysis of expression differences between each of these AD groups and controls was performed using limma adjusting for age, sex, RNA quality, plate, and two surrogate variables to adjust for unknown variation. Gene sets from the Molecular Signatures Database (MSigDB), weighted gene coexpression network analysis (WGCNA), and gene set variation analysis (GSVA) were applied to identify set of coexpressed genes.

Results: 481 genes were differentially expressed between AD cases and controls. Upregulated genes in AD subjects were enriched for cilia function and morphological development and downregulated genes for mitochondrial energy production. GSVA analysis with MSigDB showed an involvement of complement and Rab genes in AD. A similar analysis with WGCNA modules showed an enrichment of several chaperone genes in AD+LB and cilia genes in AD+Va.

Conclusion: Our analysis revealed the involvement of different sets of co-expressed genes in AD hippocampi with and without hallmarks related to other forms of dementia.

113 USE OF A STANDARDIZED DISCHARGE TEMPLATE MAY IMPROVE POST-DISCHARGE TRANSITIONS OF CARE FOR DIALYSIS PATIENTS

Sophie Claudel, Christopher Valente, Hope Serafin, Mohamed Hassan Kamel, Sandeep Ghai.

Station # 2

Objectives: Patients with end-stage kidney disease requiring dialysis encounter high hospital readmission rates. One contributor is poor communication between hospitals and outpatient dialysis facilities. We hypothesized that improved communication may reduce 30-day readmissions for patients on dialysis.

Methods: We created a standardized discharge handoff tool that is easy to use and provides concise data for the dialysis center. Then, we measured the implementation and electronic facsimile (e-fax) rate of the tool, and its impact on patient outcomes. The handoff tool was a novel, electronic dot-phrase to be included in the discharge summary. Internal Medicine residents received instructions for the dot-phrase and e-faxing immediately prior to their Renal rotation. We collected 3 months of baseline and post-intervention data on discharges from the Renal service, identifying 82 and 84 index discharges in each respective study period.

Results: Patients were predominantly male (61.4%) and receiving hemodialysis (91.5%); a minority (9%) were homeless. The dot-phrase was used in 96.8% discharge summaries and 90.1% of discharge summaries were e-faxed within 24-hours of discharge. Renal discharges followed by a 30-day Renal readmission were not statistically lower post-intervention for the index discharge alone (**26.8% vs 21.4%, $p=0.21$**), but were for overall discharges (**51.2% vs 33.3%, $p=0.01$**).

Conclusion: There was high uptake of a standardized discharge handoff tool among Internal Medicine residents. Improving communication with outpatient dialysis centers through use of a handoff tool and e-faxing may reduce readmissions among some patients, but a more comprehensive approach is needed.

193 ROLE OF INTRAVASCULAR ULTRASOUND (IVUS) IN DETECTION AND CHARACTERIZATION OF VASCULAR STENOSIS IN PATIENTS WITH DIALYSIS ACCESS MALFUNCTION

Najia Idrees, Wenqing Yin, Joanna Mangio, Kevin Daley, Suvarnu Ganghuly, Jeffrey Syracuse, Alik Farber, Vipul Chitalia.

Station # 3

Objectives: Vascular access is the lifeline of patients with end stage kidney disease (ESKD). Its malfunction accounts for significant morbidity and resource utilization. Contrast venography is the standard-of-care for access stenosis evaluation, but suffers from several limitations. Venography underestimates the severity of stenosis and cannot determine the composition of these lesions. Alternatively, Intravascular ultrasound (IVUS) is known to detect stenotic lesions with greater accuracy and is able to discern the lesion topography and morphology. In this study, we assessed the role of IVUS in detection and characterization of vascular stenosis.

Methods: In this prospective study, we recruited thirty patients with ESKD and dialysis access malfunction, who underwent diagnostic venography followed by IVUS. A machine learning approach was adopted to discern the morphological details of the stenotic lesion.

Results: The thirty patients underwent consecutive IVUS study after venography without complications. IVUS displayed a wide variety of stenotic lesions including concentric and eccentric stenosis, calcification, thrombosis and struts of stents. Machine learning approach is underway with expert-based annotation being developed to discern the luminal boundary and the morphology of lesions.

Conclusion: IVUS represents a novel modality for assessment of dialysis access malfunction. Further analysis is needed to perform a head-to-head comparison of IVUS and venography for delineating vascular access lesions.

163 THE USE OF PLASMA BIOMARKER-DERIVED CLUSTERS FOR CLINICOPATHOLOGIC PHENOTYPING

Insa Schmidt, Prasad Patil, Steele Myrick, Ingrid Onul, Isaac Stillman, Anand Srivastava, Ragnar Palsson, Helmut Rennke, Sushrut Waikar.

Station # 4

Objectives: Protein biomarkers can provide insight into kidney disease pathology. Unbiased clustering analyses using multiple protein biomarkers may identify phenotypically distinct kidney disease categories.

Methods: We used unsupervised hierarchical clustering on 225 plasma biomarkers in 541 individuals enrolled into the Boston Kidney Biopsy Cohort, a prospective cohort study of individuals undergoing native kidney biopsy with adjudicated semiquantitative scores of histopathology. Chi-square tests were used to determine differences in clinicopathologic diagnoses by cluster membership. We examined contributions of biomarkers to each cluster and explored cluster-specific pathways using principal component analysis and pathway enrichment analysis, respectively.

Results: The biomarker-derived clusters partitioned subjects into 3 groups. The mean eGFR was 71.4 ± 29.2 , 72.5 ± 34.3 , and 39.3 ± 31.3 ml/min/1.73m² in Cluster 1, 2, and 3, respectively. Compared to Cluster 1, individuals in Cluster 3 were more likely to have tubulointerstitial disease ($p < 0.001$) and diabetic nephropathy ($p < 0.001$). The top-contributing biomarker in Cluster 1 was AXIN, a negative regulator of the Wnt signaling pathway. The top-contributing biomarker in Cluster 2 and 3 was Placental Growth Factor (PGF), a member of the VEGF

family. The top ranked pathways were tumor-necrosis factor receptor-related signaling and interleukin and cytokine signaling in Cluster 1, 2, and 3, respectively.

Conclusion: Plasma biomarkers can be used to identify distinct clusters of individuals with CKD and may uncover relevant pathways and biomarker candidates for clinicopathologic phenotyping of kidney diseases.

129 DIETARY SATURATED AND UNSATURATED FATS AND CARDIOMETABOLIC RISK IN THE FRAMINGHAM OFFSPRING STUDY

Ioanna Yiannakou, Mengjie Yuan, Martha Singer, Lynn Moore.

Station # 5

Objectives: Effects of dietary saturated fats on cardiometabolic risk (CMR) are controversial. We examined the prospective association between intakes of saturated (SFAs), polyunsaturated (PUFAs), and monounsaturated fatty acids and incident CMR among participants in the Framingham Offspring Study, ≥ 30 years old. A secondary goal was to assess separate effects of n-3 and n-6 PUFAs.

Methods: Dietary fats were derived from 3-day records (exams 3-5) and weight-adjusted based on the residual method. Multivariable Cox proportional-hazards and analysis of covariance models were used and adjusted for confounding.

Results: There were no adverse associations between moderate or higher (vs. lower) intakes of SFAs and risks of cardiovascular disease, type 2 diabetes or impaired fasting glucose in men and women. Further higher vs. lower intakes of SFAs (≥ 30 g vs. < 20 g) were associated with a 30% reduced risk (95% CI: 0.50-0.98) of total mortality and a lower adjusted mean %body fat ($p=0.009$), especially in men. No associations were seen with other dietary fats on obesity-related measures. Further, a higher intake of SFA was associated with a non-statistically significant larger LDL particle size (p -trend=0.058) and a lower VLDL concentration ($p=0.053$).

Conclusion: This study adds evidence that SFAs had no adverse effects on CMR, and, in fact, their higher intakes were associated with less body fat and lower total mortality in this cohort of Caucasian adults.

144 YOGURT INTAKE, WEIGHT GAIN, AND OBESITY RISK DURING THE MENOPAUSAL TRANSITION

Mengjie Yuan, Yanping Li, Howard Cabral, Frank Hu, Lynn Moore.

Station # 6

Objectives: Weight gain during the menopausal transition is common. Dairy intake may have beneficial effects on weight and different types of dairy may have different effects. We investigated effects of total dairy and yogurt on risk of obesity and menopausal weight gain among 116,429 women in the prospective Nurses' Health Study II cohort.

Methods: Weights were self-reported in biennial questionnaires. Diet was assessed with food frequency questionnaires every 4 years. Generalized estimating equations were used to assess repeated measures of weight change and proportional hazards models were used to estimate risk of obesity, controlling for confounding.

Results: Women with higher (≥ 2 srv/wk) yogurt intakes gained less weight per yr ($p < 0.01$) than women consuming < 1 srv/mo) over 12 years. Higher yogurt intakes reduced obesity risk by 29% (95% CI: 0.66 - 0.76). We explored possible effect modification by physical activity and Alternate Healthy Eating Index (AHEI) scores. Activity alone was associated with a 27% reduction (95% CI: 0.68-0.79) in risk of obesity. Yogurt intake in combination with activity led to a 49% reduced risk of obesity (95% CI: 0.47-0.57). In combination with higher scores on the AHEI, yogurt intake led to a 46% lower risk (95% CI: 0.49-0.59) of obesity.

Conclusion: Total dairy intakes had no impact on weight gain or obesity risk. Yogurt intake was associated with reduced weight gain and obesity risk in women during the menopausal transition.

108 INTERSECTION OF STRUCTURAL, INSTRUMENTAL, AND SYMBOLIC STIGMA AMONG PEOPLE WITH HIV WHO INJECT DRUGS: A QUALITATIVE STUDY IN ST. PETERSBURG, RUSSIA

Molly Zhao, Marina Vetrova, Olga Toussova, Olga Toussova, Nakul Vyas, Sarah Rossi, Elena Blokhina, Karsten Lunze.

Station # 7

Objectives: People with HIV (PWH) who inject drugs are stigmatized for both conditions. This qualitative study aimed to explore how HIV and substance use stigma interact and to assess the effect of intersectional stigma on health care for PWH who inject drugs in St. Petersburg.

Methods: We sampled PWH who inject drugs who had experiences with and insight into HIV and substance use stigma and recruited 15 individuals at addiction treatment and HIV clinics in St. Petersburg, Russia. We analyzed data from semi-structured interviews conducted from September through December 2017 on NVivo 1, guided by the *Health Stigma and Discrimination Framework*.

Results: PWH who inject drugs said that their healthcare providers viewed them as unreliable and unmotivated because of their substance use. This symbolic mistrust related to substance use and the instrumental fear of PWH related to the risk of HIV contagion, resulted in providers' intersectional stigma of PWH who inject drugs, and in structural stigma such as unofficial hospital policies that refuse or prescribe separate care protocols to PWH who inject drugs. In the absence of support, participants internalized symbolic and instrumental stigma, further exacerbating existing care barriers, which include requiring a myriad of medical tests and certificates to obtain free HIV and addiction treatments.

Conclusion: Among participants, intersectional HIV and substance use stigma originated from healthcare providers' mistrust of people who inject drugs (symbolic stigma) and fear of HIV (instrumental stigma), which led to discriminatory institutional policy (structural stigma) and affected individuals' internalization of these stigmatizing attitudes.

Session 3 – Floor 1 Thursday 10/7 11:30 am - 12:30 pm

92 UTILIZATION OF TECHNETIUM-99M PYROPHOSPHATE IMAGING FOR THE DIAGNOSIS OF TRANSTHYRETIN AMYLOID CARDIOMYOPATHY (ATTR-CM): A MULTI-CENTER, COMMUNITY HOSPITAL-BASED STUDY

Rabah Alreshq, Steven Sigman, Catherine Marti, Andrew Darlington, Arun Krishnamoorthy, Benjamin DeMoss, Frederick Ruberg.

Station # 1

Objectives: Technetium 99m pyrophosphate (Tc-PYP) scintigraphy can diagnose transthyretin amyloid cardiomyopathy (ATTR-CM) without confirmatory biopsy in the context of normal plasma cell testing. While widely employed at academic medical centers, community utilization of Tc-PYP is poorly defined. In this study, we report Tc-PYP utilization and diagnosis of ATTR-CM among community-based hospitals.

Methods: Multi-center, retrospective study of n=274 consecutive patients referred for Tc-PYP in metropolitan Atlanta, Georgia, from five community-based hospitals between Jan 2017 and Jul 2020. Clinical data was collected from the electronic health record. Tc-PYP was considered diagnostic for ATTR-CM with grade 2 or 3 cardiac uptake and/or a heart/contralateral ratio >1.5 at 1-hour post injection, in the absence of light chain abnormalities.

Results: Positive Tc-PYP was observed in n=79 (29% total scans) with plasma cell testing performed in 97%, and genotyping in 84%. Final amyloidosis diagnoses were wild type-ATTR-CM (39%), hereditary ATTR-CM owing to the Val122Ile variant (44%), ATTR-CM (13% pending genotype), and light-chain AL amyloidosis (4%). Mean age was 77.1±6.3 years, 76% were males, and 67% African American. Among those Black patients with a positive PYP scan, n=32 or 60% had the TTR variant pV142I, indicating hereditary ATTR

Conclusion: Approximately 30% of patients referred for PYP imaging in metropolitan Atlanta GA had unrecognized ATTR-CM. Of those referred patients who were Black, 60% had a hereditary form of ATTR-CM that has important implications for relatives and siblings. Identification of unrecognized ATTR-CM affords patients directed therapies such as tafamidis.

182 FACILITATORS AND BARRIERS TO CHRONIC CARE AMONG PATIENTS WITH HEART FAILURE IN RURAL HAITI A QUALITATIVE STUDY

Elizabeth Basow, Gene Kwan, Benito Isaac, Darius Fenelon, Eyrna Toussaint, Dawson Calixte, Michel Ibrahim, Lisa Hirschhorn, Mari-Lynn Drainoni, Alma Adler, Gene Bukhman.

Station # 2

Objectives: To investigate facilitators and barriers to accessing care for chronic heart failure in rural Haiti from patients' perspectives.

Methods: We conducted three group and one individual interview with thirteen patients with heart failure. We recruited patients after discharge from an NGO-supported academic hospital in rural Haiti. We employed thematic analysis using emergent coding and categorized themes using the socioecological model.

Results: Facilitators of chronic care included participants' knowledge about the importance of treatment for heart failure and engagement with health systems to manage symptoms. Strong social support networks helped participants access clinic visits. Participants reported low cost of care, good medication accessibility and trust in the healthcare system. Participants expressed strong spiritual beliefs, such that the healthcare system is an extension of God's influence. Barriers to chronic care included misconceptions about medication adherence and taking medications with food. Lack of social support networks limited clinic access and non-healthcare costs associated with clinic were prohibitive. Many patients also expressed low satisfaction regarding the clinic experience. The belief that heart disease caused by supernatural spirits is incurable was also a barrier to healthcare.

Conclusion: We identified several facilitators and barriers to chronic heart failure care with implications for management in rural Haiti. Future interventions should address misconceptions about heart failure management and foster patient support systems for visit and medication adherence. Leveraging spiritual beliefs may also promote care engagement.

15 EVALUATING FOR EQUITY AT A SAFETY NET HOSPITAL- SOCIOECONOMIC STATUS, ADHERENCE, AND OUTCOMES IN CARDIAC REHABILITATION

Joshua Gilman, Tulani Washington-Plasket, Na Wang, Stephanie Zombeck, Gary Balady. Station # 3

Objectives: Uncovering the racial/ethnic health disparities that exist within cardiovascular medicine offers potential to mitigate treatment gaps that might affect outcomes. Since race is a social construct, socioeconomic status (SES) may be a more appropriate underlying factor to assess. We sought to evaluate whether adherence and outcomes in cardiac rehabilitation are associated with SES in a safety net hospital.

Methods: The area deprivation index (ADI) reflects income, education, employment, and housing quality within a given 9-digit zip, where a higher ADI indicates more disadvantage (range 1-10). Home ADI's were obtained for 770 enrollees of the Cardiac Rehabilitation Program at Boston Medical Center from 2016-2020. Associations between ADI and adherence (attending > 70% of sessions) was evaluated while controlling for age, sex, race, education, diagnosis, smoking and transport times. Secondary outcomes included associations of ADI with change in exercise capacity, LDL, weight, quality of life, nutrition, and depression scores.

Results: Among the enrollees, 197 had missing covariates and 147 did not have a zip code with an associated ADI, leaving 426 patients for analysis. Enrollees had a mean age of 59.8 years, 34% were female, 44% self-reported as black and 9% as Hispanic. The ADI for patients varied (mean 5; median 6). The primary outcome after adjustment revealed no association for ADI with adherence (OR 1.03 95% CI: 0.99-1.07) or attendance rate (OR 0.98 95% CI: 0.96-1.004). Secondary outcomes improved among patients regardless of ADI.

Conclusion: In our safety net hospital that provides care without exception, we found equity in cardiac rehabilitation program outcomes despite SES.

96 ABNORMAL LIGHT-CHAIN TESTING AND DIAGNOSIS OF TRANSTHYRETIN AMYLOID CARDIOMYOPATHY (ATTR-CM) AMONG PATIENTS REFERRED FOR TECHNETIUM-99M PYROPHOSPHATE IMAGING

Matthew Cozzolino, Rabah Alreshq, Brian Lilleness, Alexandra Pipilas, Varsha Muralidhar, Eric Guardino, John Berk, Omar Siddiqi, Deepa Gopal, Vaishali Sanchorawala, Frederick Ruberg.

Station # 4

Objectives: Clinical algorithms stipulate that transthyretin amyloid cardiomyopathy (ATTR-CM), an important cause of heart failure, can be diagnosed non-invasively by Tc-99m pyrophosphate (PYP) imaging when normal markers of plasma cell dyscrasia (PCD) exclude light-chain (AL) amyloidosis. Among patients with a positive PYP scan and abnormal PCD markers, we sought to define the degree of light-chain abnormalities associated with a final diagnosis of ATTR-CM.

Methods: Retrospective, cohort study of 279 sequential patients with suspected ATTR-CM referred for PYP for suspected ATTR-CM from Oct 2014 to Jan 2019. PCD markers included serum free light-chain (FLC) assay and serum/urine immunofixation electrophoresis (IFE), with abnormal results in 100 (36%). After exclusions for incomplete data, the final study population was 82. Clinical characteristics were collected from the health record. Amyloidosis was determined by multi-disciplinary clinical assessment or biopsy. Wilcoxon rank-sum and Fisher's exact tests were employed.

Results: Among PYP-positive (PYP-pos, n=67), ATTR-CM was diagnosed in 62 (93%), confirmed by tissue biopsy in 39 (63%) including 23 cardiac biopsies. FLC ratio was abnormal in 59 (88%) and SIFE in 21 (31%), with 8 (12%) patients with normal FLC ratio and abnormal SIFE. FLC ratio was >1.65 and <3.1 in 55 (82%) among PYP-pos, of which 52 had confirmed ATTR-CM.

Conclusion: Among 67 patients referred for PYP imaging with abnormal PCD markers, 52 diagnosed with ATTR-CM had pos-PYP and an abnormal FLC ratio between 1.65 and 3.1, suggesting that invasive biopsy may be avoidable in these circumstances.

133 EVALUATION OF DIFFERENTIAL MICRO RNA EXPRESSION IN PERIPHERAL ARTERY DISEASE

Syed Husain Mustafa Rizvi, Rosa Bretón Romero, Robert M. Weisbrod, Naomi M. Hamburg.

Station # 5

Objectives: Peripheral artery disease (PAD) is one of the most common presentation of atherosclerosis in lower extremities resulting in ischemic limbs, disability and amputation. There are limited treatments to improve disease symptoms. Recently miRNAs have shown their potential in different physiological and pathological conditions including cardiovascular diseases. We aim to identify potential miRNA signatures related to PAD.

Methods: We collected adipose tissue from proximal and distal locations of ischemic limbs of patients with PAD at the time of revascularization surgery. Control adipose tissue were procured from the knee or hip replacement surgery patients. We performed miRNA sequencing for differential gene expression and *invitro* angiogenesis assay to see the angiogenesis potential in PAD fat.

Results: In miRNA sequencing data, a number of genes were significantly differentially expressed between PAD and control group, whether its PAD proximal or PAD distal fat tissue, as compared to between the two PAD groups. Pathway analysis revealed that miRNA candidates miR205-5p, miR182-5p, miR291a-3p and miR17-5p target angiogenesis, insulin and cell cycle signaling. *In vitro* angiogenesis assay revealed impaired angiogenesis potential in PAD fat tissue.

Conclusion: Overall, miRNA signature identified in PAD fat tissue can potentially provide insight into disease severity and mechanism behind the development of PAD.

95 LONG-TERM MORTALITY ASSOCIATED WITH USE OF CARVEDILOL VS METOPROLOL IN HEART FAILURE PATIENTS WITH AND WITHOUT TYPE 2 DIABETES- A DANISH NATIONWIDE COHORT STUDY

Brian Schwartz, Colin Pierce, Christian Madelaire, Morten Schou, Søren Lund Kristensen, Gunnar Gislason, Lars Køber, Christian Torp-Pedersen, Charlotte Andersson. Station # 6

Objectives: Carvedilol may have favorable glycemc properties compared with metoprolol, but it is unknown if carvedilol has mortality benefit over metoprolol in patients with type 2 diabetes (T2DM) and heart failure with reduced ejection fraction (HFrEF).

Methods: Using Danish nationwide databases between 2010-2018, we followed patients with new-onset HFrEF treated with either carvedilol or metoprolol for all-cause mortality until the end of 2018.

Results: There were 39,260 patients on carvedilol or metoprolol at baseline (mean age 70.8 years, 35% women), of which 9,355 (24%) had T2DM. Carvedilol was used in 2,989 (32%) patients with T2DM and 10,411 (35%) of patients without T2DM. Users of carvedilol had a lower prevalence of atrial fibrillation (20% vs. 35%), but other characteristics appeared well-balanced between the groups. Totally 11,306 (29%) were deceased by the end of follow-up. We observed no mortality differences between carvedilol and metoprolol, multivariable-adjusted hazards ratio 0.97 (0.90-1.05) in patients with T2DM versus 1.00 (0.95-1.05) for those without T2DM, p for difference =0.99. Rates of new-onset T2DM were lower in users of carvedilol vs. metoprolol; age, sex, and calendar year adjusted hazards ratio 0.83 (0.75-0.91), p<0.0001.

Conclusion: In a clinical cohort of HFrEF patients with and without T2DM, carvedilol was not associated with a reduction in long-term mortality compared to metoprolol. However, carvedilol was associated with lowered risk of new-onset T2DM supporting the assertion that carvedilol has a more favorable metabolic profile than metoprolol.

125 THE SHORT PHYSICAL PERFORMANCE BATTERY SCORE IS ASSOCIATED WITH QUALITY OF LIFE IN BLACK AND HISPANIC OUTPATIENTS WITH STABLE CONGESTIVE HEART FAILURE

Christopher Valente, Cody Chiuzan, Rabah Alreshq, Tori Blot, Denise Fine, Stephen Helmke, Carlos Rodriguez, Natalia Sabogal, Sergio Teruya, Morgan Winburn, Mathew Maurer, Frederick Ruberg.

Station # 7

Objectives: Functional status is associated with poor health outcomes, including quality of life. The Short Physical Performance Battery (SPPB) is commonly used to assess functional status. There are limited data describing quantifiable functional status limitations in Black and Hispanic patients with stable congestive heart failure. We hypothesized that in a Black and Hispanic outpatient population with heart failure, low functional capacity, as determined by low SPPB score, would be associated with worse quality of life.

Methods: The multicenter, prospective, Screening for Cardiac Amyloidosis in Minority Populations (SCAN-MP) study identified Black and Hispanic subjects with heart failure, collected baseline characteristics, and measured SPPB. Quality of life was measured by the Kansas City Cardiomyopathy Questionnaire (KCCQ). SPPB scores were stratified into severe functional deficit (0-6), mild functional deficit (7-9) and no functional deficit (10-12).

Results: Of 220 patients in the study, 201 (91.3%) completed the SPPB. Subjects with severe functional deficits scored lower on overall KCCQ score than those with no deficits (mean 56.2 vs. 75.6, p<0.001). Patients with low SPPB scores were more likely to be older, female, have higher BMI and NYHA class, less education, more comorbidities, and worse Six-Minute Walk Test (p<0.05).

Conclusion: Among Black and Hispanic outpatients with stable heart failure, stepwise decrements in functional status, as defined by the SPPB, are associated with overall KCCQ score, and scores across a variety of sub-domains. These findings suggest that targeted interventions to improve patients' functional status could broadly benefit quality of life.

13 CONTEMPORARY INCIDENCE AND OUTCOMES OF AORTIC DISSECTION DURING PREGNANCY AND PUERPERIUM IN THE UNITED STATES

Yunda (George) Wang, Kanhua Yin, Karl Karlson, Niloo Edwards, Nikola Dobrilovic.
Station # 8

Objectives: To investigate the incidence and in-hospital outcomes of aortic dissection during pregnancy and puerperium in a US national database.

Methods: The National Inpatient Sample, a large and publicly available all-payer inpatient care database, was queried to identify pregnancy-related AD hospitalizations using codes from the International Classification of Diseases (ICD-9 and ICD-10). Identified hospitalizations were stratified into Stanford type A AD (TAAD) and type B AD (TBAD) using the associated procedure codes. The weighted values of the hospitalizations were used to generate national estimates.

Results: From January 2002 to December 2017, a total of 471 pregnancy-related AD hospitalizations were identified, with 106 being TAAD and 365 being TBAD. The mean age of the entire cohort was 30.9 years; 52.1% were White, 20.6% were Hispanic, and 9.4% were Black. Marfan syndrome, primary hypertension, and pre-eclampsia and/or eclampsia were found in 21.9%, 11.3%, and 13.1%. In 18.0% of the entire cohort with ICD-10 trimester information, we found that 58.8% of AD occurred in the third trimester. Overall, the incidences of AD, TAAD, and TBAD were 0.66, 0.15, and 0.51 per 100,000 pregnancy-related hospitalizations. We observed a trend of increasing incidence for pregnancy-related AD during the 16-year study period - predominantly driven by TBAD. The in-hospital mortalities of AD, TAAD, and TBAD were 7.3%, 4.3%, and 8.1%.

Conclusion: For the first time, we quantified the population-level incidence and in-hospital outcomes of AD during pregnancy and puerperium in the US; while its incidence is increasing, its in-hospital mortality appears better than that of the general population.

86 UTILIZING GENOMIC MARKERS OF BRONCHIAL PREMALIGNANT LESION SEVERITY AND PROGRESSION TO PREDICT CANCER STATUS OF INDETERMINATE PULMONARY NODULES

Kelley Anderson, Gang Liu, Ehab Billatos, Marc Lenburg, Jennifer Beane.
Station # 9

Objectives: We have previously identified modules of co-expressed genes whose expression is associated with lung squamous premalignant lesion (PML) severity and progression/regression. The modules defined molecular subtypes of lesions. The "Proliferative" subtype was enriched with dysplastic lesions. A module associated with interferon signaling was decreased in progressive Proliferative lesions. We sought to determine if expression of these modules in the uninvolved airway are associated with cancer status in high-risk patients with indeterminate pulmonary nodules.

Methods: Bronchial and nasal brushings from patients undergoing bronchoscopy for suspicion of lung cancer (AEGIS: Bronchial n=938, Nasal n=505; DECAMP: Bronchial n=130, Nasal n=212) were profiled using microarray (AEGIS) or bulk RNA-seq (DECAMP). Gene set variation analysis (GSVA) was used to score samples for the expression of modules identified in PMLs. A nearest centroid predictor using module genes was used to predict if the nodule was benign or malignant.

Results: In both the nasal and bronchial epithelium, GSVA scores for immune-associated modules were significantly higher in benign versus malignant samples. Classifiers using the immune modules also predicted cancer status with the highest accuracy.

Conclusion: Our results suggest that genes related to immune pathways that are altered in patients with persistent or progressive PMLs are similarly altered throughout the airway in the presence of cancer. These immune alterations have value for detecting cancerous indeterminate pulmonary nodule, and also reinforce the role of the immune system in the continuum from premalignancy to malignancy.

62 PREDICTING MALIGNANCY IN INDETERMINATE PULMONARY NODULES USING MODELS INTEGRATING QUANTITATIVE CT IMAGING AND NASAL GENE EXPRESSION

Kate Bloch.
Station # 10

Objectives: There is a need for a non-invasive biomarker to differentiate between benign and malignant lung nodules detected by low dose CT screening. This would help to accelerate diagnosis in patients with cancer, and avoid more invasive diagnostic procedures in patients without disease. Here, we investigated the utility of combining quantitative radiomics with nasal gene expression to predict malignancy of small pulmonary nodules.

Methods: Data including cancer status, age, gender, smoking status, radiomics, and nasal gene expression from 213 patients from the Detection of Early Lung Cancer Among Military Personnel (DECAMP1) consortium were used in this study. DECAMP1 is a prospective study of 500 current or former smokers with indeterminate pulmonary nodules. For the prediction models, we have used various feature selection methods and machine learning algorithms including Random Forest, Gradient Boosting Machine and Support Vector Machine (SVM). Data was split into train and test set with tenfold cross-validation. To evaluate the performance of our models, we used the following metrics: Accuracy, Sensitivity, Specificity and AUC-ROC.

Results: Our results indicate that the best performance was achieved by the SVM Polynomial model using a combination of 6 radiomic features and 18 nasal genes with the AUC of 0.952.

Conclusion: In this study, we showed the potential of a minimally invasive radiogenomics biomarker to improve lung cancer prediction. For future work, we are planning to validate these findings in separate, independent cohorts and to compare the contributions of radiomic and genomic data to the overall model performance.

94 ENHANCED DECONVOLUTION AND PREDICTION OF MUTATIONAL SIGNATURES

Aaron Chevalier.

Station # 11

Objectives: Mutational signatures are patterns of somatic alterations in the genome caused by carcinogenic exposures or aberrant cellular processes. To provide a comprehensive workflow for preprocessing, analysis, and visualization of mutational signatures we created the Mutational Signature Comprehensive Analysis Toolkit (*musicatk*) package. *musicatk* enables users to select different schemas for counting mutation types and easily combine count tables from different schemas. Exploratory features include the ability to compare signatures to the COSMIC database, embed tumors in two dimensions with UMAP, cluster tumors into subgroups, identify differentially active exposures and plot exposure distributions across annotations such as tumor type. Overall, *musicatk* enables users to gain novel insights into the patterns of mutational signature observed in cancer cohorts.

Methods: *musicatk* supports both Latent Dirichlet Allocation (LDA) from the *topicmodels* package and Non-Negative Matrix Factorization (NMF) from the *NMF* package. We also implement a Bayesian algorithm based on LDA where exposures are estimated using a fixed set of signatures.

Results: *Musicatk* allows users to make the best use of COSMIC signatures and their own datasets. From individual clinical samples to large novel or well-researched public datasets, *musicatk* allows for simple processing and deep analysis.

Conclusion: In conclusion, the *musicatk* package provides a comprehensive set of preprocessing utilities, access to several discovery and prediction tools, and functions for downstream analysis of the patterns of mutational signatures in a cohort of tumors.

118 SUBCHONDRAL BONE LENGTH: A DEEP LEARNING DRIVEN IMAGING MEASURE FOR KNEE OSTEOARTHRITIS

Ray Jhun, Gary Chang, Lisa Park, Nina Le, Tejus Surendran, Joseph Lai, Hojoon Seo, Nuwapa Promchotchai, Grace Yoon, Jonathan Scalera, Terence Capellini, David Felson, Vijaya Kolachalama.

Station # 12

Objectives: Develop a measure reflecting extent of cartilage loss and bone flattening in knee osteoarthritis (OA) and test it against estimates of disease severity.

Methods: Cartilage and menisci of the tibia and the femur in 61 knees obtained from the Osteoarthritis Initiative (OAI) were annotated and learned by a deep neural network (U-Net), and its predictions compared with radiologist-driven annotations on an independent test set (27 knees). U-Net was applied to extract joint structures on the larger OAI dataset (9434 knees).

Subchondral bone length (SBL) was defined as a novel measure, which characterized the extent of cartilage and bone changes, and analyzed for its relationship with radiographic joint space narrowing (JSN), WOMAC pain and disability, and subsequent knee replacement (KR). **Results:** Mean SBL values for knees with and without JSN were consistently different. SBL was positively associated with greater pain and disability. For knees with medial or lateral JSN, odds ratios between lowest and highest SBL quartiles for future KR were 5.67 (95% CI:[3.89,8.26]) and 7.15 (95% CI:[3.69,13.87]), respectively.

Conclusion: SBL quantified OA status based on JSN severity. It has promise as an imaging marker in predicting clinical and structural OA outcomes.

25 CHARACTERIZING TRANSCRIPTOMIC PROFILES AND MICROBIAL ABUNDANCE OF ORAL POTENTIALLY MALIGNANT DISORDERS

Mohammed Muzamil Khan, JENNIFER FRUSTINO, ALESSANDRO VILLA, BACH-CUC NGUYEN, SOOK-BIN WOO, XARALABOS VARELAS, MARIA KUKURUZINSKA, STEFANO MONTI.

Station # 13

Objectives: Oral cancer (OC) is the 8th most common cancer among males in the United States. Within the oral cavity, oral potentially malignant disorders (OPMD) transform into OC through a multi-step process and are thought to progress through a series of well-defined clinical and histopathological stages. This study aims to characterize OPMDs using their transcriptomic and microbial profiles which could help in early detection and diagnosis.

Methods: We collected biopsy samples and performed total-RNA seq from a cohort of 77 patients which were grouped into five categories: (i) Control (23.4%); (ii) Inflammatory disorders(14.3%); (iii) hyperkeratosis, not reactive(HkNR) (22%); (iv) dysplasia (28.6%); (v) squamous cell carcinoma (SCC)(11.7%). Geneset enrichment analysis was carried out on multiple geneset compendia along with relevant signatures from published cancer studies.

Results: The differentially expressed markers across groups showed enrichment in pro-inflammatory pathways such as TNF- α , IFN- γ , and others, along with epithelial-to-mesenchymal transition (EMT) and partial-EMT processes, especially in the HkNR group. The host-microbe interaction model, considering only specific microbes, showed a significant positive association of certain genera, e.g., Fusobacterium with inflammatory response pathways' activity.

Conclusion: Enrichment analysis showed significant associations between the inflammatory, HkNR and dysplastic groups in various cancer and immune-related pathways indicating host-microbial relationships. These findings may help to advance our understanding of common biological mechanisms related to OPMDs and their progression towards malignancy.

66 VALIDATION OF BRONCHIAL GENE EXPRESSION ASSOCIATED WITH COPD IN BRONCHIAL AND NASAL BRUSHINGS PROFILED BY RNA-SEQ

Yusuke Koga, Melody Morris, Margaret Fleming, Joshua Campbell, Ehab Billatos, Marc Lenburg.

Station # 14

Objectives: Chronic Obstructive Pulmonary Disease (COPD) is a leading cause of death globally. Smoking creates a field-of-injury throughout the airways and lungs which includes molecular changes such as alterations in gene expression. A prior study identified a bronchial gene expression signature associated with COPD-related phenotypes using microarrays. The goal of this study is to validate this signature in airway epithelium samples from an independent cohort profiled using RNA-seq.

Methods: RNA-seq data was generated from 171 bronchial and 66 nasal brushings collected within the DECAMP consortium. Association of gene expression profiles with COPD phenotypes was assessed with a linear model controlling for smoking status, age and gender. Genes were ranked by their t-statistic for FEV1% predicted, and enrichment of the signature was determined with Gene Set Enrichment Analysis.

Results: The genes in the previous signature that were increasing ($n=54$) or decreasing ($n=44$) in expression in COPD were concordantly enriched with genes associated with COPD in bronchial and nasal samples from the DECAMP cohort (FDR $q<0.05$). A 375-gene signature associated with COPD was identified in the bronchial DECAMP samples (FDR $q<0.05$) and was concordantly enriched in the previous microarray cohort (FDR $q<0.05$).

Conclusion: These results demonstrate the robustness of the bronchial COPD signature across cohorts and suggest that it can be leveraged to further understand molecular changes associated with worse lung function in the airway.

145 IMMUNOPHENOTYPING OF PREMALIGNANCY IN A MURINE MODEL OF LUNG SQUAMOUS CELL CARCINOMA VIA IMAGING MASS CYTOMETRY

Tachira Pichardo, Roxanna Pfefferkorn, Chris Husted, Jennifer Beane, Sarah Mazzilli.
Station # 15

Objectives: Lung cancer (LC) is the leading cause of cancer death worldwide, taking more lives annually than breast, colon, and prostate cancers combined. Lung squamous cell carcinoma (LSCC), the second most common type of LC, is often preceded by the development of bronchial premalignant lesions (PMLs) and identifying strategies to intercept LC at this early stage may drastically reduce mortality. Prior work from our group and others identified early genomic alterations in PMLs associated with pro-inflammatory gene pathways.

Methods: Our study utilizes the murine N-nitrosotris-(2-chloroethyl)urea (NTCU) model of LSCC to explore how an inflammatory microenvironment (ME) contributes to PML progression. Dysplasia in the model is characterized by histological and transcriptomic alteration that resembles human bronchial preinvasive disease. We used imaging mass cytometry, a highly multiplexed imaging modality based on laser ablation of tissue stained with metal-conjugated antibodies, to immunophenotype the ME of NTCU-induced premalignancy.

Results: We found an increase in neutrophils in the direct vicinity of developing lesions and tumors, suggesting that an inflammatory niche is established early in LSCC carcinogenesis.

Conclusion: Given that late-stage LSCC is characterized by inflammation, which contributes to poor prognosis, an enhanced understanding of the role of the immune system in early LSCC tumorigenesis is critical for interception efforts that take advantage of the ongoing immunotherapy revolution.

Session 3 – Floor 2 Thursday 10/7 11:30 am - 12:30 pm

82 GENE EXPRESSION ASSOCIATED WITH VASCULAR INVASION IS PREDICTIVE OF TUMOR AGGRESSIVENESS IN STAGE I LUNG ADENOCARCINOMA

Dylan Steiner, Jiarui Zhang, Gang Liu, Avrum Spira, Eric Burks, Jennifer Beane, Marc Lenburg.
Station # 1

Objectives: In early-stage lung adenocarcinoma (LUAD), vascular invasion (VI) is strongly associated with recurrence and overall survival (OS) but can only be observed upon resection. There is a need for biomarkers to guide surgery and neoadjuvant therapy in stage I LUAD.

Methods: FFPE tumors from stage I LUAD patients (n=56) were profiled by RNA-seq. Genes associated with VI were identified with linear modeling. The association between the VI signature and tumor aggressiveness was tested in publicly available bulk and single cell lung tissue data and on components (n=32) of independent macro-dissected tumors to simulate pre-surgical biopsies.

Results: Genes increased with VI were enriched for MSigDB Hallmark EMT while decreased genes were associated with cell junction organization. In stage I LUAD tumors profiled by scRNA-seq (n=9), VI up genes were localized to CAFs while down genes were localized to alveolar epithelial cells. VI gene expression was significantly associated with 5-year OS in two cohorts of stage I LUAD tumors profiled by RNA-seq (n=53) and microarrays (n=182). In the latter VI genes were independently predictive of 5-year OS after controlling for age, chemotherapy, and a biomarker of aggressive histology. Finally, VI genes separated components from tumors with and without aggressive histology with an AUC of 0.89.

Conclusion: Our results show that VI-associated gene expression changes can be detected by bulk RNA-seq of FFPE tissue and suggest the potential to predict patient outcome from pre-resection biopsies.

155 POST-TRAUMATIC STRESS DISORDER IN COMBAT-EXPOSED VETERANS IS NOT ASSOCIATED WITH IRRITABLE BOWEL SYNDROME AND FUNCTIONAL DYSPEPSIA BUT GASTROESOPHAGEAL REFLUX DISEASE

Abishek Arokiadoss, Kelly Harper, Hassen Abdulkerim, Brian Marx, Terence Keane, Christian Weber.

Station # 2

Objectives: IBS is a highly prevalent functional bowel disorder characterized by abdominal pain and altered bowel habits. Depression and anxiety are significantly comorbid with IBS, but little is known about its association with PTSD. Therefore, we examined the large prospective Veterans After-discharge Longitudinal Registry (VALOR) cohort to test whether IBS is associated with PTSD.

Methods: Veterans enrolled in the VALOR registry with (N=1028) and without PTSD (N=619) were examined for the presence of IBS based on ICD codes at baseline (T1) and follow up (T4). PTSD diagnosis was made using the PTSD module of the Structured Clinical Interview for DSM-IV. Data analysis was performed using Chi-square test, T-test, and logistic regression analyses.

Results: Whereas overall IBS was present in VALOR subjects with (3.9%) and without PTSD (3.4%) in similar frequencies ($p=0.6$) at T1, subgroup analyses of veterans with re-experiencing symptoms of PTSD were more likely to have IBS. At T4 veterans with avoidant symptoms of PTSD were more likely to have IBS. We also determined that gastroesophageal reflux disease (GERD) was significantly more frequent in the PTSD group at T1 and T4 ($p=0.01$ and $p=0.001$) as compared to controls whereas functional dyspepsia (FD) occurred in similar frequencies ($p=0.5$ and $p=0.4$).

Conclusion: Our study in combat-exposed veterans showed that a diagnosis of PTSD per se did not result in risk of IBS; however, the presence of specific PTSD re-experiencing symptoms at baseline and avoidance symptoms were significantly associated with IBS diagnosis at baseline and long-term follow-up, respectively. Severity of each PTSD symptom cluster also incurred risk for GERD, but not FD.

188 RISK FACTORS ASSOCIATED WITH DELAY IN DIAGNOSIS OF EARLY-ONSET COLORECTAL CANCER IN A SAFETY-NET HOSPITAL POPULATION

Laura Chiu, Kevin Huang, Xixi Xu, Rubiya Rahman, Paul Schroy.

Station # 3

Objectives: The incidence of early-onset colorectal cancer (EOCRC) is increasing in the U.S. It is unclear why patients with EOCRC, particularly black patients, are at risk of presenting with more advanced disease at diagnosis. Thus, we investigated the characteristics of white and black EOCRC patients within our safety net hospital setting.

Methods: We performed a retrospective cohort study of patients diagnosed with primary colorectal cancer (CRC) before the age of 50 who received care at Boston Medical Center between 1/1/2000 and 5/1/2020 confirmed by endoscopic or surgical pathology. We excluded patients who were diagnosed through routine screening, had recurrent CRC, or had insufficient data. Descriptive analyses were conducted to examine patient, provider and system level associated with timing of diagnostic evaluation.

Results: A total of 106 subjects diagnosed with EOCRC were ultimately reviewed for this preliminary study, with 43 white subjects and 63 black subjects. Compared to white subjects, black subjects had a higher proportion of males, non-English speaking status, high school as their highest education level, and Medicaid/free care insurance status. Black subjects also had a higher proportion of high-grade disease histology and more advanced TNM staging. Additionally, despite a similar reported symptom duration (139 v. 137 days), black subjects had a longer workup duration (85 ± 136 v. 107 ± 180 days) and a higher number of medical visits for symptom evaluation prior to diagnosis.

Conclusion: The time to diagnosis for EOCRC between white and black subjects appears to differ. The cause of this potential difference is unclear. Further studies are warranted to confirm these findings.

120 PLANNING FOR THE FUTURE: DETECTING MISSED HIGH-RISK ADENOMAS AND COLORECTAL CANCERS DUE TO THE COVID-19 PANDEMIC

James Connolly, Heidi Ahmed, Enoch Chung, Howard Cabral, Arpan Mohanty.
Station # 4

Objectives: We estimate the number of missed high-risk adenomas (HRAs) and colorectal cancers (CRC) at Boston Medical Center due to postponed colonoscopies during the COVID-19 pandemic.

Methods: This observational study evaluates the number of HRAs (defined as ≥ 3 adenomas, adenoma ≥ 10 mm in size, villous histology, or high-grade dysplasia) and CRC diagnosed by elective colonoscopy in 2020 compared to 2017-19. Patients with a history of CRC or an indication of inflammatory bowel disease, therapeutic procedure (other than large polyp removal), or diarrhea were excluded. A Poisson regression model using data from 2017-19, adjusted for age, sex, race/ethnicity, and indication was used to predict expected HRAs and CRC per month in 2020. Predicted values were compared to actual values to estimate missed diagnoses.

Results: There were 41% fewer colonoscopies performed in 2020 compared to 2019, resulting in 40% fewer HRAs and 44% fewer CRC diagnosed. Given an average CRC detection rate of 6 per 1000 cases from 2017-19, 3000 additional colonoscopies will be needed to diagnose 10 missed CRC in our patient population. The HRA detection rate for patients who undergo colonoscopy for screening and positive fecal immunochemical test (+FIT) is 0.1 and 0.27, respectively. Assuming the same endoscopy capacity as 2019, the proportion of +FIT cases has to be increased from 7% to 28% to detect an estimated 195 missed HRAs.

Conclusion: The study provides one of the first real world estimates of missed HRAs and CRC due to cancellation of colonoscopies during the COVID-19 pandemic, with implications on screening strategies and endoscopy scheduling to increase detection of these high-risk lesions.

26 VACCINE HESITANCY TOWARDS COVID VACCINATION IN IBD PATIENTS IN A DIVERSE SAFETY NET HOSPITAL PATIENT POPULATION

Howard Herman, Max Rosenthaler, Venkata Satyam, Sharmeel Wasan.
Station # 5

Objectives: To identify concerns among IBD patients regarding COVID vaccination, particularly among an under-represented minority (URM) population.

Methods: Participants were recruited from 1265 adult patients with IBD at BMC. Patients were sent an electronic survey via Mychart assessing attitudes regarding Covid-19 vaccination. URM patients and those without access to MyChart completed the survey by phone. Subjects were defined as vaccine hesitant if they were not already vaccinated or planning to be as soon as possible. Analyses were performed to identify factors associated with vaccination intent. This study was approved by the IRB of BMC.

Results: 210 participants (159 electronic, 51 phone) completed the survey. The response rate was 16.6%. 11.9% of all patients were vaccine hesitant. while Spanish-speakers (25%, $p = 0.0102$) and Hispanic patients (27.8%, $p = 0.0001$) demonstrated significantly higher vaccine hesitancy. Multivariate regression including age, Hispanic ethnicity, and language revealed a significant association of age (OR 0.964, $p = 0.026$) and Hispanic ethnicity (OR 7.411, $p = 0.007$) with vaccine hesitancy.

Conclusion: COVID vaccination rates in the U.S. lag behind targets despite a surplus of supply. Our study demonstrates a significantly higher rate of vaccine hesitancy among Hispanic participants. Participants gave a variety of reasons for hesitancy and identified approaches that providers could take to address their concerns. Limitations include response bias and low response rates. Targeting outreach toward specific populations with tailored interventions may improve vaccination efforts.

37 THE PERFORMANCE OF FRACTURE RISK SCORES IN PATIENTS WITH IBD

Helen Lyo, Matthew Custodio, Alan Moss.
Station # 6

Objectives: ACG guidelines recommend risk-stratifying patients with IBD for risk of osteoporotic fractures. Fracture risk scores are preferred over universal bone density scans due

to the low fracture prevalence overall. We sought to compare two scoring systems in one cohort to quantify their test characteristics in identifying low bone mineral density in patients with IBD.

Methods: We identified patients with IBD who had risk assessment and DEXA scans from a safety net health network. We collected demographic, FRAX score, QFracture score and DEXA results. The primary outcome of interest was an abnormal DEXA scan (T-score <-1).

Results: A cohort of 72 patients with baseline and follow-up data were included. Demographic data showed mean age of 52, 76% females, 55% Caucasians, 5% with tobacco use, 42% with alcohol use, 4% with previous fractures, and 61% with exposure to steroids for longer than 3 months. Mean t-score from DXA scans was -1.1. Only 5/72 had a history of prior bone fractures. Based on DEXA scores, 47% had osteopenia, and 10% had osteoporosis. Mean FRAX score was 8.5 with 8% of patients having high risk of fractures.

The FRAX score (without BMD) had an AUC of 0.68 to predict a DEXA T-score <-1. In contrast, the QFracture score had an AUC of 0.58 for this outcome.

Conclusion: In an 'at-risk' cohort of patient with IBD, the test characteristics of risk scores was modest to predict DEXA results. A prospective study of risk factors and BMD quantification in patients would be required to identify an IBD-specific risk score.

179 PATTERNS OF ALCOHOL USE AND LIVER FIBROSIS IN THE FRAMINGHAM HEART STUDY

Brooke Rice, Michelle Long.
Station # 7

Objectives: To determine the relationship between specific alcohol use patterns and liver fibrosis in a community cohort, and specifically among moderate alcohol users.

Methods: We included Framingham Heart Study participants who completed alcohol use surveys and vibration-controlled transient elastography from 2016 to 2019. We defined fibrosis as liver stiffness measurement (LSM) ≥ 8.2 kPa. We defined heavy drinking by AASLD consensus guidelines (≥ 14 alcoholic drinks/wk for women, ≥ 21 for men) and risky weekly drinking as use in excess of US Dietary Guidelines (≤ 7 drinks/wk for women, ≤ 14 for men). We used logistic regression and adjusted for sociodemographic variables and components of the metabolic syndrome.

Results: Among 2911 participants (mean age 54.8, 53.8% women, mean BMI 28.5), mean LSM was 5.6 kPa and prevalence of fibrosis was 8.7%. Mean alcohol use was 5.3 drinks/wk. The prevalences of binge drinking, risky weekly drinking, and heavy drinking were 29.6%, 15%, and 5.1%. After adjustment, increased total number of drinks/wk (OR 1.16, 95% CI 1.04-1.30), frequency of drinking days (OR 1.07, 1.01-1.14), and risky weekly drinking (OR 1.5, 1.04-2.16) were significantly associated with fibrosis. Results were unchanged after excluding non-drinkers (n=15.3%). When excluding heavy drinkers, results were attenuated but trended toward significance for total drinks/wk (OR 1.13, 0.98-1.3) and risky weekly drinking (OR 1.47, 0.95-2.3).

Conclusion: In a community cohort with few heavy drinkers, increased weekly alcohol use, more frequent alcohol use, and risky weekly drinking were associated with significant liver fibrosis, suggesting that modest alcohol use may contribute to liver fibrosis.

150 LAXATIVE USE FOR PATIENTS WITH BOTH IMPAIRED COLONIC WAKE RESPONSE AND SLOW TRANSIT CONSTIPATION IS ASSOCIATED WITH IMPROVED CONSTIPATION SEVERITY SCORES BUT NOT LOWER ABDOMINAL PAIN OR DISCOMFORT

Brian Surjanhata, Ingrid Guerrero López, Jack Semler, Brad Kuo.
Station # 8

Objectives: Normal colonic motility includes sleep quiescence and heightened activity upon wakening. We prev showed an impaired wake response in slow transit constipation (STC) compared to healthy and normal colon transit (NCT) subjects with the wireless motility capsule (WMC). Only half of patients report satisfaction with constipation tx. We aim to assess the change in symptoms for subjects with an impaired wake response and use of laxatives.

Methods: Analysis of subjects that underwent WMC testing with subsequent management changes, including laxatives. A contraction count of < 64 was applied against the 20-minutes post-wake to identify subjects with an impaired response. Validated survey scores of lower

abdominal pain, lower abdominal discomfort, and constipation were assessed at baseline, 3 mo, and 6 mo. Subjects grouped by wake response (W), colonic transit, and laxative use (L). Median symptom scores at follow up vs baseline were compared using a Wilcoxon signed-rank test.

Results: STC (W-/L+) showed statistically significant improved constipation scores at 3 mo ($p = 0.02$) and 6 mo ($p = 0.006$). STC (W+/L+) and NCT (W-/L+) did not show significant changes in constipation scores over time ($p = \text{NS}$). No statistically sig changes in lower abdominal pain or discomfort over time were observed.

Conclusion: Only STC with impaired wake had constipation rating improvement assoc with laxative use from severe to moderate which was not seen in STC (W+/L+) nor NCT (W-/L+). This suggests that both STC and an impaired response may be a potential marker of severe dysmotility that may predict response to laxatives. Further study is required to understand if timed laxative with onset of wake would yield greater benefit.

49 INTERPROFESSIONAL COLLABORATION BETWEEN MINDFULNESS INSTRUCTORS AND PRIMARY CARE PROVIDERS

Dhanesh Binda, Janice Weinberg, Natalia Morone.

Station # 9

Objectives: We developed a survey assessing the 2016 Core Competencies for Interprofessional Collaborative Practice with the goal of understanding the attitudes of Primary Care Providers (PCPs) towards collaboration with instructors of the Mindfulness-Based Stress Reduction Program (MBSR), an evidence-based program for low back pain.

Methods: The 25 question survey was sent via email to providers at the UPMC General Internal Medicine Division, Pittsburgh, PA, the Piedmont Health Services Family Medicine Section, Chapel Hill, NC, the Boston Medical Center General Internal Medicine and Family Medicine Sections, Boston, MA, and the University of Massachusetts Family Medicine Section, Worcester, MA.

Results: Among 118 eligible respondents, 33 (28.0%) were male, 85 (72.0%) were female, mean age was approximately 41.5 ± 10.1 , and the majority (65.2%) were in medical practice ≤ 10 years. Of these PCPs, 83 (70.1%) reported familiarity with MBSR and 49 (59%) of them recommended patients to MBSR programs at least once a year. Of these, 8 (6.8%) reported collaboration with Mindfulness Instructors. All 8 found that communication increased the quality of patient care at least a little bit. Reasons for not referring to MBSR included lack of knowledge of the evidence-based guidelines and insurance coverage, perception of low patient acceptance, and availability/accessibility.

Conclusion: We found that the majority of PCPs had a general idea about MBSR programs and recommended it to their patients but had very little interaction with Mindfulness Instructors. Since the few providers who communicated with instructors found that it improved patient care, methods to augment communication should be considered.

165 METASTATIC MALIGNANT INSULINOMA WITH FAILURE OF INITIAL OCTREOTIDE THERAPY: A RARE MANAGEMENT COMPLICATION

Laura Burns.

Station # 10

Objectives: Pancreatic neuroendocrine tumors, or pNETS, represent a rare but clinically diverse subset of pancreatic neoplasms. One such pNET, the insulinoma, is found to be malignant in just 4% of cases. Due to the exceedingly rare nature of these tumors, little exists in the literature regarding evidence-based management. We therefore present the case of a 70-year-old male admitted with 3 months of episodic confusion.

Methods: Point-of-care glucose testing revealed profound hypoglycemia to the 30s when symptomatic. The patient underwent a monitored fast and was found to have inappropriately elevated endogenous insulin during an episode of hypoglycemia, suggestive of an underlying insulinoma. CT imaging revealed a pancreatic mass and nodules scattered throughout the liver, spleen, and lungs. An endoscopic biopsy of the liver and pancreas lesions confirmed the diagnosis of malignant insulinoma.

Results: The patient was initiated on octreotide therapy, which has been demonstrated in small case series to be effective in suppressing insulin secretion, thereby reducing symptom burden. Unfortunately, initial treatment with octreotide significantly worsened the severity of, and

decreased the time between, this patient's hypoglycemic episodes, representing a rare and clinically significant initial treatment side effect.

Conclusion: Ultimately, the patient was transitioned to diazoxide and octreotide was added back to his regimen without further exacerbation of hypoglycemic episodes.

21 ASSOCIATION BETWEEN CHANGE IN ALCOHOL CONSUMPTION AND D-DIMER OVER TIME AMONG PLHIV

Alexis Kiyanda, Samuel Mensah, Gregory Patts, Debbie Cheng, Wenqing Jiang, Jeffrey Samet, Kaku So-Armah.

Station # 11

Objectives: We assessed the association between change in alcohol consumption and change in D-dimer, a biomarker of altered coagulation associated with increased mortality risk in PWH.

Methods: ART-naive PWH were recruited in the 2012-2014 Russia ARCH study. Alcohol consumption (by biomarker PEth and by the self-reported 30 Day Timeline Follow Back) and D-dimer were recorded at baseline, 1 and 2 years. The primary analysis evaluated the association between the change in PEth and change in D-dimer over the same 1 year interval (contemporaneous). Secondary analyses included a) self-reported alcohol and b) associations of change in alcohol in prior year with change in D-dimer in the next year (lagged). Multivariable piecewise regression models were used to control for demographics and comorbidities.

Results: At baseline, the 349 participants had a mean age of 34, and 71% were male. No association was detected in the primary analysis of the contemporaneous change in PEth and change in D-dimer (beta= 0.05, 95% CI, [-0.05, 0.15]). No association was detected in the secondary analyses of change in self-reported alcohol use or in lagged analyses, except evidence of a nonlinear association in the lagged analyses of change in PEth and D-dimer.

Conclusion: We did not detect an association in the primary analysis and most secondary analyses. Future studies should include nonlinear models and explore lagged associations between alcohol and altered blood coagulation.

190 EFFECT OF ALCOHOL CONSUMPTION ON CD4 RECOVERY AFTER ANTIRETROVIRAL THERAPY (ART) INITIATION IN PEOPLE LIVING WITH HIV (PLWH)

A McLaughlin, N Lin, W Jiang, S Lodi, D Lioznov, G Patts, N Gnatenko, E Blokhina, S Bendiks, M Freiberg, H Tindle, E Krupitsky, J Samet, K So-Armah.

Station # 12

Objectives: This study evaluated alcohol's effect on CD4 recovery after initiating ART in PLWH.

Methods: In two cohorts in St. Petersburg, Russia, we selected participants with no ART >6 months who initiated ART in the 2-year study. Alcohol was assessed by phosphatidylethanol (PEth; an alcohol biomarker). PEth categories were undetectable (<8ng/mL) or detectable and below (medium) or above (high) the median. We used random effect models to estimate the slope of CD4 recovery by alcohol group.

Results: 60 PLWH met criteria. In the 3 groups pre-ART, mean PEth levels were 1, 31, and 345ng/mL and corresponding mean CD4 counts were 487, 457, and 381cells/mm³. There was a trend of slower post-ART CD4 recovery with alcohol consumption (Figure). With undetectable PEth, CD4 increased 0.45cells/mm³ per day. With medium and high PEth, CD4 increased 0.03 and 0.07cells/mm³. Rates were not statistically different from each other.

Conclusion: This suggests alcohol is associated with slower CD4 recovery after ART initiation but did not reach significance. Next steps include expanding to larger cohorts and evaluating the role of ART adherence.

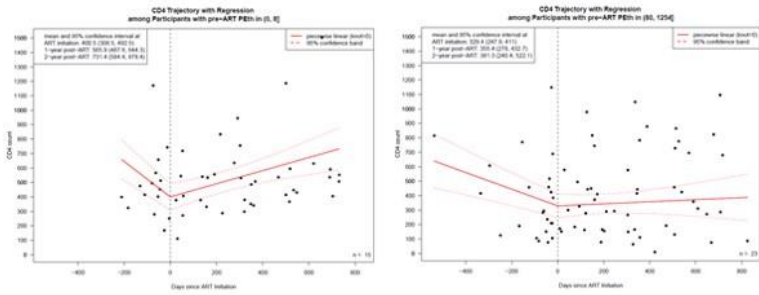


Fig 1. Change in CD4 after ART initiation in participants with PETH levels that were undetectable (left) and high (right). Time zero is time of ART initiation.

24 COVID-19 PANDEMIC-RELATED STRESS AND SUBSTANCE USE BEHAVIORS AMONG PEOPLE WITH HIV IN ST. PETERSBURG, RUSSIA

Sarah Rossi, Dmitry Lioznov, Debbie Cheng, Ve Truong, Sally Bendiks, Natalia Gnatenko, Sara Lodi, Elena Blokhina, Anita Raj, Lindsey Rateau, Yuliia Sereda, Evgeny Krupitsky, Jeffrey Samet, Karsten Lunze.

Station # 13

Objectives: This study describes the prevalence of pandemic-related stress and financial worry and its relation to substance use behavior among people with HIV (PWH) with a history of opioid use in St. Petersburg, Russia.

Methods: We analyzed data collected between May 2020 and March 2021 from a subsample of two RCTs. We used logistic regression to assess the relationships between pandemic-related stress and financial worry with decreased use of opioids (primary), cigarettes (secondary), and alcohol (exploratory) due to the pandemic, adjusting for gender and age.

Results: Among 114 participants, 4.4% reported a COVID-19 diagnosis and an additional 7.9% believed they were infected. 52.6% reported high financial worry and 30.7% reported high stress. Although a majority reported no change in their substance use due to the pandemic, 22.2% decreased opioid use, 18.3% smoking, and 10.8% alcohol. We detected an association between high financial worry and a decrease in opioid use (AOR 2.95; 95%CI: 1.02, 8.52; $p=0.05$), but not between high stress and decrease in opioid use (AOR 2.14; 95%CI: 0.79, 5.81; $p=0.14$). No associations were detected between high financial worry and high stress and decreases in smoking or alcohol use.

Conclusion: Pandemic restrictions might have exacerbated financial concerns due to temporary disruptions of labor markets and drug supply, which might have led to a decrease in opioid use.

91 THE ASSOCIATION OF PRESCRIBED OPIOIDS AND INCIDENT CARDIOVASCULAR DISEASE IN THE VETERANS AGING COHORT STUDY

Kaku So-Armah, Minhee Sung, Svetlana Eden, Chung-Chou Chang, Meredith Duncan, Suman Kundu, Kirsha Gordon, Robert Kerns, Steve Crystal, William Becker, Matthew Freiberg, Jennifer Edelman, Jennifer Edelman.

Station # 14

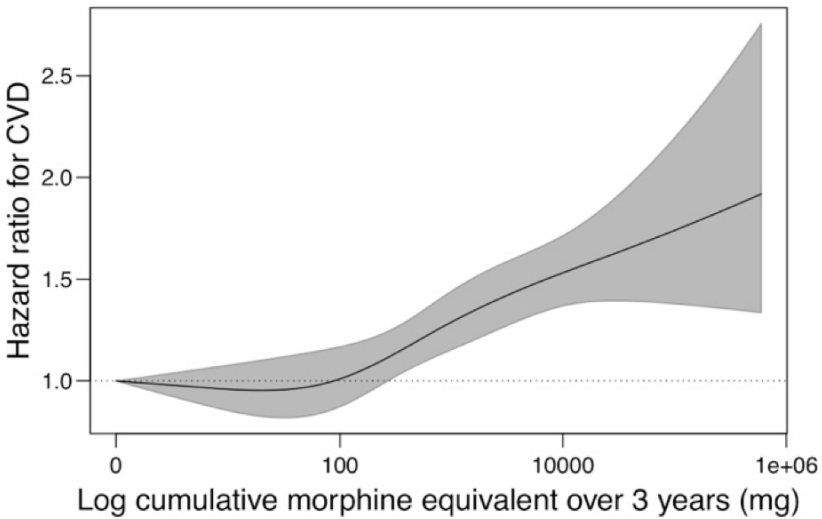
Objectives: We assessed the association of outpatient prescription opioid (PO) use with incident cardiovascular disease in the Veterans Aging Cohort Study (VACS).

Methods: PO receipt and total morphine-equivalent daily dose (MEDD), were determined over 3 years. Follow-up for incident CVD began at the end of the 3 year window among those free of CVD and cancer. We used Cox models to estimate hazard ratios (HR) with inverse probability weighting to balance confounders by probability of PO receipt. Models were adjusted for: CVD risk factors, HIV, pain intensity rating, VACS Index, hepatitis C, alcohol/cocaine use disorder, depression, antidepressants.

Results: Of 38,024 participants, 40% got PO in the 3 year period. Median age was 48 years; 97% male; 49% black, 48% current smokers. CVD incidence rates per 1000 person-years (18.8

[17.7-19.9] vs. 14.8 [14.0-15.7]) and risk (adjusted HR: 1.27 [1.16-1.37]) were higher among those with PO receipt than without. CVD risk increased with MEDD (Figure).

Conclusion: PO and higher MEDD are associated with increased CVD risk. Future studies will evaluate these effects by HIV status.



154 DIFFERENCES IN TREATMENT DELAY AMONG BREAST CANCER PATIENTS WITH ALCOHOL AND MARIJUANA COMPARED TO NARCOTIC SUBSTANCE USE DISORDERS

Anne Buck, Haley Urbach, Naomi Ko.

Station # 15

Objectives: Patients presenting for breast cancer treatment with concomitant substance use are a growing and vulnerable population, and one that necessitates further investigation due to the complexities of their care. We sought to investigate the differences between patients diagnosed with breast cancer who use commercially available substances such as alcohol and marijuana, versus illicit or prescription substances such as prescription opioids, heroin, fentanyl, cocaine, benzodiazepines.

Methods: This is a retrospective chart review of subjects diagnosed with breast cancer between January 1, 2005 and December 31, 2018 with underlying substance use. Data for this study was obtained from the hospital cancer registry and electronic medical record. Substance use was defined as any mention in the health record by a healthcare provider or ICD code with corresponding diagnosis. Treatment delay is defined as greater than 30 days. Demographic characteristics were analyzed descriptively, reporting frequencies and proportions while treatment delays were analyzed using Welch two sided t-test and Fishers exact t-test.

Results: The total number of subjects was 65 with 67% who only used commercially available substances- alcohol and marijuana. In the cohort of patients with SUD of illicit and prescription substances, time from diagnosis to initiation of treatment was a mean of 55 days compared to 74 days in those who have alcohol and/or marijuana SUD.

Conclusion: Subjects with SUD have significant delays to initiation of treatment following a breast cancer diagnosis. Future research on patients with SUD and barriers to initiation of treatment for their breast cancer diagnosis is warranted.

131 PERIPHERAL BLOOD MONOCYTE COUNT IS A DYNAMIC PROGNOSTIC MARKER FOR RISK STRATIFICATION IN MULTIPLE MYELOMA

Camille Edwards, Hamza Hassan, Grace Ferri, Karina Verma, Cenk Yildirim, Nathanael Fillmore, Nikhil Munshi.

Station # 1

Objectives: Tumor-associated macrophages, derived from peripheral blood monocytes, support multiple myeloma (MM) cell proliferation in bone marrow. We investigated the prognostic significance of absolute monocyte count (AMC) in MM.

Methods: Retrospective nationwide VA study of treatment naïve MM patients diagnosed from 2000-2019 without concomitant hematologic malignancies. We used AMC ($\times 10^3$) closest to & within 90 days prior to diagnosis & every 3 months from diagnosis up to 2.5 years. Patients were stratified to low (<0.2), normal (0.2 to <0.8), elevated (0.8 - 1.25) & severely elevated (>1.25) AMC groups. Cox models & Kaplan Meier with log-rank testing were performed.

Results: We analyzed 10,822 patients (median age 70 years [IQR 63-77]) with median follow up of 2.9 years (IQR 1.3-5.3). Patients with low, severely elevated, elevated, & normal AMC at diagnosis had median overall survival (OS) of 2.3, 2.7, 3.1, and 3.6 years ($p < 0.001$). Patients with normal AMC at diagnosis who developed abnormal AMC ≥ 1 year had inferior OS. Multivariable analysis (age, ISS, LDH) showed significant association of OS with AMC at diagnosis & up to 2.5 years after diagnosis. Hazard Ratios (HR) at diagnosis were 1.28 (95% confidence interval [CI] 1.06-1.41; $p < 0.001$), 1.10 (95% CI 1.04-1.17; $p = 0.002$), and 1.19 (95% CI 1.06-1.34; $p = 0.004$), and HRs at 2.5 years after diagnosis were 1.53 (95% CI 1.22-1.93; $p < 0.001$), 1.11 (95% CI 1.00-1.23; $p = 0.043$), 1.58 (95% CI 1.22-2.04; $p < 0.001$) for low, elevated & severely elevated AMC, respectively.

Conclusion: Abnormal AMC at diagnosis or follow up is significantly associated with inferior OS, independent of known risk factors suggesting that AMC may be included in MM risk stratification.

175 DEVELOPMENT OF A CLINICAL INFORMATION AND BIOSPECIMEN DATABASE IN THE HEMATOLOGY/ONCOLOGY OUTPATIENT CLINICS

Adrian Ilinski, Kiana Mahdavian, David Li, Nina Modanlo, Casey Simon-Plumb, Matthew Kulke.

Station # 2

Objectives: Developing cancer therapies increasingly depends on the characterization of tumors at the molecular level and understanding the associated tumor microenvironment and microbiome. Given this urgent need and our access to a unique patient population, we have developed a clinical information and biospecimen repository for patients evaluated in the Hematology/Oncology clinics at Boston Medical Center (BMC).

Methods: Our research protocol allows for patients seen in the clinics to consent to medical information, blood, tissue, and microbiome specimen collection and storage. Clinical research assistants embedded in the clinics work with providers to identify eligible patients for enrollment to the various research studies. The collected clinical data is linked to information obtained from biospecimen analysis.

Results: Since study initiation on February 2019, we have consented a total of 194 patients (consent rate of 66%). Lung cancers, breast, hepatocellular carcinomas and prostate cancer are the top represented cancers. Current translational studies leveraging biobank specimens and clinical data include but not limited to the investigation of biomarkers of response and resistance to immune checkpoint inhibition, heterogeneity of breast tumors and racial disparities, genomic alternations in circulating cell-free DNA in African American men with prostate cancer on androgen-deprivation therapies, and the serotonin metabolism in cholangiocarcinoma and gallbladder cancer.

Conclusion: With further growth, we anticipate that this biospecimen and clinical information database will become a valuable resource to advance translational research at BMC.

177 ASSESSMENT OF TRYPTOPHAN METABOLITES AS POTENTIAL BIOMARKERS OF RESPONSE TO IMMUNE CHECKPOINT INHIBITORS

David Li, Kiana Mahdavian, Lucas Schiffer, Nina Modanlo, Casey Simon-Plumb, Adrian Ilinski, Stephen Whelan, Norman Lee, Evan Johnson.

Station # 3

Objectives: Immune checkpoint inhibitors (ICIs) target inhibitory receptors on T cells and antigen-presenting cells, and have transformed cancer treatment. Because the efficacy of immune checkpoint inhibitors is dependent on T cell function, factors that affect the host immune environment can have a significant impact on treatment efficacy. Early studies have shown that levels of immunosuppressive metabolites of Tryptophan may play a role in predicting the efficacy of checkpoint inhibitors.

Methods: We studied the longitudinal associations of serum metabolite concentrations and progression-free cancer survival in 44 patients with different tumor types who have received ICI therapy at Boston Medical Center. Serum tryptophan metabolites were measured using API 4000 LC/MS before, and 6-8 weeks following ICI treatment initiation.

Results: Our targeted metabolomics data suggests that lower serum concentrations of indole 3 acetic acid, indoxyl acetate, kynurenine, and tryptophan at baseline and over time are associated with longer progression-free survival times among study participants.

Conclusion: Our data also suggests that the ratio of kynurenine to tryptophan changes significantly during the course of treatment and is associated with response to ICI therapy.

9 RACIAL DISPARITIES IN MYELOMA CLINICAL TRIALS: A SYSTEMATIC REVIEW AND POOLED ANALYSIS

Charles Milrod, David Hughes, Frances Blevins, J. Mark Sloan.

Station # 4

Objectives: Adverse events affecting Black patients, such as skin hyperpigmentation, may be overlooked using existing clinical trial data on immunomodulatory medications (IMiDs). The objective of this systematic review is to characterize the representation of Black participants and rate of skin hyperpigmentation in clinical trials.

Methods: A systematic search of ClinicalTrials.gov was performed from database inception to August 30, 2020. Phase 1-4 clinical trials that used lenalidomide in experimental treatment arms in participants with multiple myeloma were included. Sixty-eight studies were screened, of which 21 were included in the pooled analysis. Standard χ^2 tests were used for data analysis.

Results: In this systematic review and pooled analysis comprising 4539 participants, the proportion of Black participants in trials (6.9%, $n = 315$) was significantly less than the multiple myeloma population ($p < 0.001$). The rate of skin hyperpigmentation (0.066%, $n = 3$) was significantly less compared to a 40.8% incidence in a recent retrospective study ($p < 0.001$).

Conclusion: Among participants undergoing treatment with IMiDs for multiple myeloma, Black patients were underrepresented and the adverse event of skin hyperpigmentation was underreported. Fair representation of Black patients in clinical trials is needed to better describe this adverse event and other adverse events that may be underreported.

152 THE IMPACT OF DIABETES AND HYPERTENSION ON BREAST CANCER RECURRENCE IN PATIENTS AT BOSTON MEDICAL CENTER

Arthi Palani, Muhammad Qureshi, Naomi Ko, Tsion Fikre, Ariel Hirsch.

Station # 5

Objectives: The purpose of this study was to investigate disparities in breast cancer outcomes at an urban safety net hospital. This study examined the relationship of sociodemographic factors, hypertension and diabetes with recurrence rates in a cohort of patients with breast cancer.

Methods: A retrospective review was performed on patients who were diagnosed with breast cancer between 2009 and 2014. Data on patient demographics, endocrine treatment, diabetes, and hypertension were obtained from the BMC Clinical Data Warehouse. Analyses of variance and multivariable logistic regression models were performed to analyze the relationship of these factors with the incidence of breast cancer recurrence.

Results: 293 patients were identified and included in the preliminary analysis. There were 29 documented recurrences. In the complete adjusted case analysis there were no significant

findings across any of the factors. Patient comorbidities of diabetes and hypertension were associated with lower recurrence on odds ratio but this did not reach statistical significance.

Conclusion: In conclusion, there was no significant relationship between comorbidities and recurrence rates in the initial patient cohort. The association of comorbidity and lower recurrence on odds ratio may be explained by the regular hospital care received by these patients for their comorbidity. Another possibility could be the higher mortality rate associated with patients with comorbidities. The data set has since been expanded to include a larger sample size for analysis which may highlight statistical differences. We hope this study will help guide future research and identify disparities in breast cancer care at BMC.

185 TREATMENT DELAYS IN BREAST CANCER PATIENTS WITH SUBSTANCE USE DISORDER

Haley Urbach, Anne Buck, Naomi Ko.

Station # 6

Objectives: Patients presenting for breast cancer treatment with concomitant substance use are a population that necessitates further investigation due to the complexities of their care.

Methods: This is a descriptive study investigating treatment delay among breast cancer patients with substance use disorder (SUD) seeking cancer treatment at an urban safety net hospital. Breast cancer patients with substance use in their medical records were identified from the clinical data warehouse. We performed a retrospective chart review of subjects diagnosed with breast cancer and underlying substance use between January 1, 2005 and December 31, 2018. A chart abstraction tool was created in RedCAP and manually abstracted from the electronic medical record for all identified cases. Demographic characteristics and time to first treatment were collected. Treatment delay was defined as greater than 30 days. Predictors for delay were analyzed using chi-squared tests.

Results: The total number of subjects analyzed was 65. Among subjects in the cohort, 58.4% had documented history of substance use disorder and 47.7% had active substance use at the time of breast cancer diagnosis. The most frequently noted substances were alcohol (63.1%), marijuana (35.4%), cocaine (24.6%) and prescription opioids (12.3%). Of those analyzed 73.8% experienced a delay in treatment initiation and 12.3% experienced a delay in treatment completion.

Conclusion: Subjects with active substance use and SUD had higher rates of delay to first treatment than those with a past history of use. There are significant delays and difficulties in accessing breast cancer care for patients with substance use disorder.

198 IMPACT OF MASSHEALTH ON BREAST CANCER SURVIVORSHIP CARE DISPARITIES BETWEEN BLACK AND WHITE SURVIVORS AT AN URBAN SAFETY NET HOSPITAL

Preetha Velu, Tsion Fikre, Alexandra Fischman Han, Naomi Ko.

Station # 7

Objectives: Black breast cancer survivors (BCS) have the highest mortality when compared to all other races. Racial disparities in breast cancer are due in part to insurance coverage. The purpose of the study was to determine if the introduction of universal health care coverage (MassHealth) in 2006 improved health care delivery for Black BCS at an urban safety-net hospital.

Methods: We performed a retrospective chart review of patients diagnosed with breast cancer at Boston Medical Center in 2000 (n = 91) and 2014 (n = 106). Electronic medical records were examined for demographic characteristics, breast cancer subtype, and breast cancer survivorship care. Primary outcomes of survivorship care examined and analyzed included 1-year and 5-year annual mammography and annual endocrine therapy rates.

Results: The 1-year mammography and 1-year endocrine therapy rates improved for all BCS after MassHealth, with rates increasing from 37.4% to 47.2% for mammography (p = 0.213) and 27.5% to 35.8% for endocrine therapy (p = 0.27). In 2000, White BCS appear to have had higher rates of 1-year mammography than Black BCS (35.7% vs. 33.3%, p > 0.999), but lower rates for the other 3 categories. When compared to White BCS, Black BCS had a greater improvement in 1-year mammography and 1-year endocrine therapy rates after MassHealth, with rates improving from 33.3% to 57.8% for mammography and 25.9% to 40% for endocrine therapy.

Conclusion: In an urban safety-net hospital, Black BCS had improved mammography and endocrine therapy rates when comparing before and after MassHealth. Further studies identifying the cause of lower rates of survivorship care and interventions to improve care in an insured population are warranted.

64 RARE CASE OF HYPERAMMONEMIC ENCEPHALOPATHY IN NON-SECRETORY MULTIPLE MYELOMA

Karina Verma, Tina Zhang, David Mueller, Andrew Staron.

Station # 8

Objectives: The objective of this case report is to describe hyperammonemic encephalopathy (HE) as a rare poorly understood manifestation of non-secretory multiple myeloma (NSMM).

Methods: This is a case report of a single patient's clinical course.

Results: A 60-year-old man presented with back pain, hypercalcemia (14.8 mg/dL) and osteolytic lesions on CT. Protein electrophoresis with immunofixation detected no monoclonal protein; serum free light chains were <10 mg/dL; and bone marrow (BM) evaluation showed 80% plasma cells without light chain expression, consistent with NSMM. Cytogenetic analysis revealed translocation t(11;14). Despite normal liver function and correction of calcium, the patient developed HE (NH₃ >200 μmol/L), requiring brief extracorporeal dialysis and intubation. He was started on cyclophosphamide, bortezomib and dexamethasone. After adding daratumumab, a MAbs targeting CD38, he improved clinically and had partial response of his MM by BM re-assessment. After cycle 5 of therapy, the patient re-presented with HE and BM evidence of MM progression. He failed a trial of salvage chemotherapy. Thus, he was started on venetoclax, an oral selective BCL-2 inhibitor, leading to normalization of ammonia and clinical recovery.

Conclusion: Given no evident monoclonal protein production, this case of HE in NSMM contests the hypothesis that protein catabolism leads to hyperammonemia in MM. Clinical improvement on venetoclax parallels results from the BELLINI trial, showing improved progression-free survival in patients with MM harboring the t(11;14) translocation.

123 A MIXED-METHODS STUDY OF MINORITY ENROLLMENT IN CANCER BIOSPECIMEN RESEARCH

Tina Zhang, Nina Modanlo, David Li, Kiana Mahdaviani, Anish Parekh, Adrian Ilinski, Naomi Ko.

Station # 9

Objectives: Racial and ethnic minorities are underrepresented in cancer genomics research, and advancements in personalized medicine without inclusion of minority groups is likely to further exacerbate disparities in care and treatment outcomes. This study aims to intervene on barriers to enrollment.

Methods: Eligible participants for genomics studies were surveyed regarding reasons for consenting to biospecimen donation as well as barriers to participating among those who declined.

Results: Preliminary results include surveys from 30 participants. The majority of participants (73%) consented to specimen collection including 50% of Black participants, 92% of White participants, and 100% of Asian and other participants. Of eight respondents who did not consent to donation, seven were Black. Among nine participants who reported that the study was recommended by their provider, all but one consented to donation. Participants recommended including family members in the consent process. Some participants reported difficulty reading through the consent form and desire for more information "on the type of research" that would be conducted.

Conclusion: Our findings suggest that a majority of patients will consent to biospecimen collection, but Black patients are more likely to decline. Future work will include improving the consent process through greater physician engagement, inclusion of family members and caregivers, and patient-oriented presentation of information.

168 INVESTIGATION OF EFFECT OF CHRONIC OPIOID MISUSE ON HIV PATHOGENESIS AND LATENCY ESTABLISHMENT

Binita Basukala.

Station # 10

Objectives: Chronic opioid misuse potentially affects the host immune system and alters host's vulnerability to HIV infection. However, it is unclear how opioid misuse changes the course of HIV pathogenesis and latency. Latency is a barrier to curing HIV because latent reservoir of infected quiescent cells evade antiviral immune responses, are not targeted by ART, and allow HIV viremia to rebound upon treatment interruption.

Methods: To investigate how opioids alter the course of HIV infection and pathogenesis, we performed ddPCR assays on patient samples from different cohorts: ART treated and untreated HIV patients with or without opioid use disorder. We performed intact proviral DNA assay on patient samples using ddPCR platform to examine whether opioid usage alters persistent HIV reservoir. To look at effect of opioids on HIV transcriptional regulation, we performed a RT-ddPCR assay on patient samples which allows us to analyze blocks to transcription.

Results: No significant changes in the level of intact or defective provirus harbored by opioid dependent HIV patients compared to non users were observed indicating opioids did not alter the establishment of the persistent reservoir. Preliminary data suggests that there is a modest block to transcriptional elongation in opioid dependent HIV patients compared with HIV patients without any history of opioid use suggesting opioids users repress HIV transcription and potentially have a larger pool of latently infected cells.

Conclusion: Our data suggests that the systematic impact of opioids leaves a footprint on T cell subsets that influence HIV replication by repressing HIV transcriptional elongation and the maintenance of the latent reservoir.

8 BARRIERS TO ACCESSING TREATMENT FOR OPIOID USE DISORDER AFTER INPATIENT MANAGED WITHDRAWAL PROGRAM (DETOX): A QUALITATIVE STUDY

Allison David, Carlos Sian, Benjamin Linas, Jeffrey Samet, Judith Bernstein, Sabrina Assoumou.

Station # 11

Objectives: Despite the high death tolls from drug overdose in the United States in recent years, access to and uptake of evidence-based medication for opioid use disorder (MOUD) has been limited. The current study aims to determine barriers to MOUD uptake after inpatient detox and elicit potential solutions proposed by patients.

Methods: We conducted semi-structured interviews (N=24) at a detox center (2018-2019) and thematic analysis of coded data to identify patient perspectives about obstacles to treatment.

Results: Patients identified the following barriers: 1) care fragmentation; 2) lack of detox and residential treatment program beds; 3) unstable housing; and 4) lack of autonomy when choosing a treatment pathway. Solutions proposed by participants included: 1) increase low-barrier access to community-based MOUD; 2) add case managers at the detox center to establish continuity of care after discharge; 3) increase assistance with housing and other social determinants of health (SDOH); and 4) encourage patient participation in treatment decisions.

Conclusion: Patients identified care fragmentation, especially lack of care coordination, as a major barrier to substance use treatment. Increasing treatment utilization necessitates a multimodal approach to continuity of care, low-barrier access to MOUD, and support to address SDOH. Patients want care that incorporates attention to autonomy and respect for individualized preferences and needs.

98 RISK FACTORS AND CARDIOMETABOLIC IMPLICATIONS OF INTEGRASE INHIBITORS AMONG PEOPLE LIVING WITH HIV

Alex Olson, Archana Asundi, Carrie Coote, Wenqing Jiang, Laura White, Swati Patel, Manish Sagar, Nina Lin.

Station # 12

Objectives: Excessive weight gain associated with integrase strand transfer inhibitor (InSTI) antiretrovirals is an emerging issue for HIV treatment. Despite known associations between weight and cardiometabolic risk, implications of InSTI-associated weight gain remain unknown. Our objective was to evaluate InSTI-associated weight gain amongst a diverse, urban population and investigate potential risk factors and metabolic implications.

Methods: We obtained clinical data for ART-naïve adult HIV+ patients at Boston Medical Center between fiscal year (FY) 2007-17. We compared patients who initiated on an InSTI to those with an alternate regimen who remained on initial regimen for a minimum of 18 months.

We measured weight change (%) in the first 24 months of ART estimated by linear mixed effects model fit by restricted maximum likelihood. Our secondary outcomes were incident Diabetes mellitus (DM) diagnosis by Progression-free survival and changes in ASCVD scores during first 18 months of treatment.

Results: Overall, 139 patients were initiated on InSTIs and 1117 on alternative anchor regimens. Approximately, 33% were female and >75% were non-white. InSTI use in women was associated with increased weight gain in the first 24 months of ART compared to non-InSTIs (+9.57%, $p = 0.002$). Further, InSTI use was associated with more incident DM (HR = 3.27, $p = 0.014$).

Conclusion: Females have higher InSTI-associated weight gain which suggests they may be more susceptible to adverse metabolic issues. InSTI use is associated with an increased incidence of DM diagnoses following ART initiation. Further prospective studies will be necessary to describe the mechanism and refine clinical management of HIV.

11 CARDIAC MANIFESTATIONS OF CHAGAS DISEASE PATIENTS IDENTIFIED THROUGH COMMUNITY HEALTH SCREENING AND SEEN AT BOSTON MEDICAL CENTER TRAVEL MEDICINE CLINIC

Katherine Reifler, Samantha Hall, Davidson Hamer, Natasha Hochberg.

Station # 13

Objectives: There are limited data about cardiac manifestations of Chagas disease (CD) and screening in the United States. This study describes disease severity of Boston Medical Center CD patients by American Heart Association (AHA) stage and cardiac medication management.

Methods: This retrospective cohort analysis included patients identified by a community-based immigrant screening program and seen in infectious disease clinic January 2016-February 2021. We analyzed cardiac testing (electrocardiogram [EKG], echocardiogram, cardiac monitor, stress tests, and cardiac MRI) and medication management.

Results: Of the 63 patients, 34 (54%) were female, and the mean age was 45 years (range 22-73). Among the 4 patients who underwent cardiac MRI, 3 (75%) had late gadolinium enhancement findings suggestive of Chagas cardiomyopathy (CCM). Overall, 34 (54%) patients were AHA stage A (no EKG/echocardiographic changes), 22 (35%) were stage B1 (EKG or echocardiographic changes, normal ventricular function), 4 (6%) were stage B2 (ventricular dysfunction), and 2 (3%) were stage C (ventricular dysfunction and symptomatic heart failure). No patient was stage D (heart failure refractory to medical therapy) and 2 were unstageable due to limited data. After their cardiac workup, 4 patients were started on goal-directed therapy for heart failure, and 4 patients were started on anticoagulation (1=warfarin, 3=aspirin).

Conclusion: Almost half of patients had evidence of CCM and 10% had elevated 10-year mortality risk. We demonstrate that screening individuals from endemic countries in a community-based primary care setting identifies those at high risk and in need of medical therapy for cardiomyopathy.

104 THE IMPACTS OF THE COVID-19 PANDEMIC ON THE WELLBEING OF SYRINGE SERVICE PROGRAM STAFF

Andrea Wang, Raagini Jawa, Connor Buchholz, Angela Bazzi.

Station # 14

Objectives: Syringe service programs (SSPs) provide essential harm reduction services to people who inject drugs (PWID). During the COVID-19 pandemic, SSPs underwent unprecedented shifts in operational procedures (e.g., closures of physical sites, staff redeployment into COVID-related roles). We sought to explore the implications of these changes on SSP staff wellbeing.

Methods: From July-December 2020, we partnered with five SSPs across Massachusetts to interview staff members. Thematic analysis was used to identify common occupational experiences among participants. To aid in developing recommendations to advance SSP worker wellbeing, we considered how our findings aligned with the National Institute for Occupational Safety and Health (NIOSH) Total Worker Health framework.

Results: Among 18 participants, 3 (17%) were SSP directors, 6 (33%) were program coordinators, 12 (67%) were harm reduction specialists, and 2 (11%) had other roles. We identified uncertainty, powerlessness and abandonment as three challenges to wellbeing: staff

felt unable to help clients due to the closure of external services leading to low morale, and felt a lack of control over occupational COVID-19 exposure. Flexibility and dedication were two potentially protective factors; in particular, staff identified collaborative decision-making within the organization and a renewed sense of purpose to serve clients as positive aspects of work.

Conclusion: As essential public health workers in a prolonged emergency context, SSP staff may benefit from enhanced occupational supports that protect and promote their wellbeing.

174 ALKYLRESORCINOL, A BIOMARKER FOR WHOLE GRAIN INTAKE, IS NOT ASSOCIATION WITH OSTEOARTHRITIS: THE MOST STUDY

Juan-Pablo Zertuche, Gabriela Rabasa, Alice Lichtenstein, Nirupa Matthan, Michael Nevitt, James Torner, Cora Lewis, Devyani Misra, David Felson.

Station # 15

Objectives: Whole grains have been reported to protect against chronic disease, including incident symptomatic osteoarthritis. Alkylresorcinol (AR) (1,3-dihydroxy-5-n-alkylbenzene) homologues (C17:0, C19:0, C21:0, C23:0, C25:0) are found in whole grains. Plasma AR concentrations remain stable, making it a good biomarker of whole grain intake. We examined whether AR levels were associated with the development of knee OA.

Methods: Plasma of participants from the Multicenter Osteoarthritis study (MOST) was analyzed for AR homologues and total AR. We carried out two nested case-control studies, one for incident radiographic OA and one for incident symptomatic OA. We then examined the effect of AR levels.

Results: We found no significant nor suggestive associations of AR C19:0, AR C21:0 or the sum of AR homologues (AR C17:0 through AR C25:0) with incident radiographic OA (258 cases, 514 controls) or incident symptomatic OA (260 cases, 517 controls) (table 1).

Conclusion: Despite prior data describing benefits of fiber intake in OA, AR plasma levels were not associated with risk of symptomatic or radiographic knee OA.

Table 1: Cumulative incident radiographic(*) and symptomatic() OA up to 60 months by AR quartiles**

AR homologue	Quartile	Radiographic OA		Symptomatic OA	
		Adj OR (95% CI)	P test for trend	Adj OR (95% CI)	P test for trend
AR 19	Q4 vs. Q1	1.21 (0.78, 1.87)		1.16 (0.75, 1.78)	
	Q3 vs. Q1	1.16 (0.76, 1.80)		1.15 (0.75, 1.76)	
	Q2 vs. Q1	1.20 (0.77, 1.87)		0.91 (0.59, 1.40)	
	Test for trend	1 (referent)	0.45	1 (referent)	0.34
AR 21	Q4 vs. Q1	1.13 (0.72, 1.77)		1.56 (0.99, 2.43)	
	Q3 vs. Q1	1.69 (1.09, 2.63)		1.12 (0.73, 1.72)	
	Q2 vs. Q1	1.29 (0.83, 1.99)		1.38 (0.89, 2.15)	
	Test for trend	1 (referent)	0.39	1 (referent)	0.12
AR sum***	Q4 vs. Q1	0.94 (0.61, 1.47)		1.17 (0.74, 1.83)	
	Q3 vs. Q1	0.90 (0.74, 1.78)		1.33 (0.86, 2.06)	
	Q2 vs. Q1	1.15 (0.74, 1.78)		0.92 (0.60, 1.43)	
	Test for trend	1 (referent)	0.56	1 (referent)	0.25

* Adjusted for age, sex, BMI, race, physical activity at baseline, smoking status

** Adjusted for age, sex, BMI, race, physical activity at baseline, smoking status, depressive symptoms

*** AR sum: log of sum (C17:0, C19:0, C21:0, C23:0, C25:0)

Session 3 – Floor 4 Thursday 10/7 11:30 am - 12:30 pm

176 QUANTITATIVE PUPILLOMETRY FOLLOWING ANALGO-SEDATIVE ADMINISTRATION IN CRITICALLY ILL PATIENTS WITH NEUROLOGIC EMERGENCIES

Wang Pong Chan, Brenton Prescott, Emelia Benjamin, Stelios Smirnakis, Josee Dupuis, David Greer, Charlene Ong.

Station # 1

Objectives: The pupillary light reflex (PLR) exam is often used to monitor neurological status in critically ill patients. Understanding the effects of analgo-sedatives on the Neurological

Pupil Index™ (NPI), a measure of our PLR, will facilitate improved management of patient in the intensive care unit (ICU). Our primary objective was to determine the relation between dexmedetomidine and NPI in a heterogenous cohort of patients with neurologic emergencies.

Methods: We performed a two-center retrospective study of patients admitted to the ICU between 2016 and 2018. We excluded patients with a history of glaucoma, cataracts, or retinal detachment. Our primary outcome was average NPI between left and right pupils measured within 60 minutes of medication administration. Our primary exposure was dexmedetomidine. We tested our hypothesis using a mixed effects linear regression.

Results: Of our 225 patients, forty patients received at least one dose of dexmedetomidine during their ICU stay. Dexmedetomidine was associated with a significant increase in NPI (median with=4.48, median without=4.20, $p<0.001$). The relation remained significant after adjusting for confounders ($B=0.19$, $p<0.001$). Our exploratory analysis revealed significant relations between other analgo-sedatives and NPI, including acetaminophen ($B=0.05$, $p<0.005$).

Conclusion: Analgo-sedatives have significant effects on quantitative pupillometry. We found that NPI counterintuitively improved following dexmedetomidine administration. Familiarity with pupil changes following medication administration is important for accurate interpretation of pupil findings. Our findings warrant a larger prospective study.

41 EVALUATION OF LIPOSOMAL BUPIVACAINE INFILTRATION AT RECONSTRUCTIVE SKIN GRAFT DONOR SITES IN OLDER PEDIATRIC AND YOUNG ADULT BURN PATIENTS: A RETROSPECTIVE ANALYSIS

Matthew DePamphilis, Farzin Sadeq, Robert Dabek, Branko Bojovic, Gennadiy Fuzaylov, Daniel Driscoll.

Station # 2

Objectives: Opioids have been the main analgesics used to control postoperative donor site pain following reconstructive skin grafting. Prolonged opioid use, however, has many negative side effects such as dependence and respiratory distress. There is a critical need to explore and promote non-opioid, multimodal analgesics. Infiltration of the local anesthetic liposomal bupivacaine in pediatric burn patients has not been previously investigated. Therefore, the goal of this study is to evaluate infiltration of liposomal bupivacaine for postoperative donor site pain management in adolescent and young adult burn patients.

Methods: This retrospective review included patients aged 14 to 25 years, who had at least two reconstructive skin grafting procedures, one that received the standard treatment (bupivacaine hydrochloride) and one that received liposomal bupivacaine. The final sample included 30 patients with a total of 44 liposomal bupivacaine cases and 53 standard treatment cases analyzed.

Results: In the authors' five-year experience, donor site infiltration of liposomal bupivacaine compared to standard treatment was associated with significant decreases in 0 to 4 h postoperative pain scores (mean 1.4/10 vs. 2.3/10, $p=0.04$) and 0 to 24 h postoperative pain scores (mean 1.7/10 vs. 2.4/10, $p=0.02$). There were no associated significant differences in length of stay or inpatient postoperative opioid usage.

Conclusion: In this retrospective analysis, the authors report the first results that suggest liposomal bupivacaine donor site infiltration is associated with statistically improved patient outcomes in burn patients of at least 14 years of age undergoing reconstructive skin grafting.

158 EPITRANSCRIPTOMIC AND TRANSCRIPTOMIC CHANGES IN POSTMORTEM NUCLEUS ACCUMBENS OF SUBJECTS WITH ALCOHOL USE DISORDER, A PILOT STUDY

Yashrajsinh Jadeja, Yolpanhchana Lim, Huiping Zhang.

Station # 3

Objectives: N⁶-methyladenosine (m⁶A) is the most common RNA modification. Alcohol use may alter m⁶A RNA methylation in reward-related brain regions [e.g., the nucleus accumbens (NAc)], leading to altered RNA expression and increased risk of alcohol use disorder (AUD) and other substance use disorders. This study aimed to understand AUD-associated m⁶A epitranscriptomic and transcriptomic changes in the NAc and the function of differentially methylated (DM) and differentially expressed (DE) RNAs.

Methods: m⁶A epitranscriptome in postmortem NAc of 3 male AUD and 3 male control

Caucasian subjects were profiled using methylated RNA immunoprecipitation plus epitranscriptomic array. The transcriptomes of these samples were mapped by RNA-seq. AUD-associated RNA methylation and expression changes were analyzed by limma and limma-voom, respectively. Methylation and expression correlations in DM and DE RNAs were also examined.

Results: 60 DM mRNAs, 79 DM lncRNAs, and 15 DM miRNAs were identified in the NAc of AUD subjects ($|FC| > 1.3$ & $P < 0.05$). These DM mRNAs were enriched in pathways such as *Morphine Addiction*. Moreover, 90 DE mRNAs, 9 DE lncRNAs, and 2 DE miRNAs were identified in the NAc of AUD subjects ($|FC| > 2.0$ & $P < 0.005$). These DE mRNAs were enriched in pathways including *Morphine Addiction*, *Cocaine Addiction*, and *Amphetamine Addiction*. Additionally, methylation and expression levels of two DM and DE mRNAs (*COL5A2* and *SYTL2*) were significantly correlated.

Conclusion: This study demonstrated both epitranscriptomic and transcriptomic changes in the NAc of AUD subjects. It also showed that DM or DE genes in the NAc of AUD subjects are potentially involved in addiction-related pathways.

18 VALIDATION OF A CRISIS STANDARDS OF CARE MODEL FOR PRIORITIZATION OF LIMITED RESOURCES DURING THE CORONAVIRUS DISEASE 2019 CRISIS IN AN URBAN, SAFETY-NET, ACADEMIC MEDICAL CENTER

Albert Nadjarian, Jessica LeClair, Taylor Mahoney, Eric Awtry, Jasvinder Bhatia, Lisa Caruso, Alexis Clay, David Greer, Karan Hingorani, Lucas Horta, Michel Ibrahim, Michael Jeong, Thea James, Matthew Kulke, Remington Lim, Robert Lowe, James Moses, Jaime Murphy, Ala Nozari, Anuj Patel, Brent Silver, Arthur Theodore, Ryan Wang, Ellen Weinstein, Stephen Wilson, Anna Cervantes-Arslanian.

Station # 4

Objectives: The COVID-19 pandemic has overwhelmed healthcare resources even in wealthy nations, necessitating rationing of limited resources without previously established crisis standards of care protocols. In this study, we sought to retrospectively validate the Massachusetts triage protocol to cohorts of critically ill patients in BMC.

Methods: We applied our hospital-adopted guidelines, which defined severe and major chronic conditions as those associated with a greater than 50% likelihood of 1- and 5-year mortality, respectively, to a critically ill patient population. We investigated mortality for the same intervals.

Results: Of 365 admitted patients, 15.89% had one or more chronic life-limiting conditions. These patients had higher 1-year and 5-year mortality rates than those without underlying conditions. Irrespective of classification of disease severity, patients with metastatic cancer, congestive heart failure, end-stage renal disease, and neurodegenerative disease had greater than 50% 1-year mortality, whereas patients with chronic lung disease and cirrhosis had less than 50% 1-year mortality.

Conclusion: Patients with major and severe chronic medical conditions overall had higher mortality at 1 and 5 years, but mortality varied between conditions. Our findings support a crisis standards protocol which focuses on acute illness severity and only considers underlying conditions carrying a greater than 50% predicted likelihood of 1-year mortality. Modifications to the chronic lung disease, congestive heart failure, and cirrhosis criteria should be refined if they are to be included in future models.

187 ASSOCIATION BETWEEN CHANGE IN ALCOHOL USE AND CHANGE IN SCD14 IN PEOPLE WITH HIV (PWH)

Victoria Ontiveros.

Station # 5

Objectives: We assessed the relationship between the change in alcohol use and the change in levels of sCD14, a biomarker of monocyte activation associated with HIV disease progression and mortality.

Methods: PWH selected from the Russia ARCH study population were antiretroviral therapy naive. At baseline, year 1, and year 2, alcohol use was measured with a 30-Day Timeline Follow Back survey and a phosphatidyl ethanol (PEth) blood test; sCD14 levels were measured by ELISA. Primary analysis assessed the association between change in PEth and change in

sCD14 over two 1 year intervals; secondary analyses considered change in self reported alcohol and sCD14 over the same time interval as well as compared change in alcohol use in the first year compared to change in sCD14 in the next year in lagged analyses. We used piecewise linear regression models, adjusting for demographics and comorbidities.

Results: The 349 participants had a mean age of 34 and 71% were male. No association was detected between change in PEth and change in sCD14 levels (beta=47, CI 95%: -19, 112) in the primary analysis. The relationship between change in self reported alcohol use and the change in sCD14 over the same time interval was nonlinear. Lagged analyses fit linear models but did not reach statistical significance.

Conclusion: We did not detect a significant relationship between change in PEth and change in sCD14. Future studies should consider exploring the nonlinear relationship between the change in alcohol use and sCD14 levels.

29 BLOOD TRANSFUSION AT A HEMOGLOBIN THRESHOLD OF SEVEN G/DL IN CRITICALLY ILL PATIENTS: A TARGET TRIAL EMULATION

Nicholas Bosch.

Station # 6

Objectives: In critically ill patients, a hemoglobin transfusion threshold of <7.0 G/dl compared to <10.0 G/dl improves organ dysfunction. However, it is unclear if transfusion at a hemoglobin of <7.0 g/dL is superior to no transfusion. The objective was to emulate a clinical trial comparing transfusion to no transfusion at a hemoglobin threshold of <7.0 G/dl among critically ill patients.

Methods: We performed regression discontinuity analysis of hemoglobin measurements from adults admitted to seven intensive care units, estimating the change in organ dysfunction (modified sequential organ failure assessment score) in the 24-72-hour window following each hemoglobin measurement. We compared hemoglobin levels just above and below 7.0 g/dL using a ‘fuzzy’ discontinuity approach, based on the concept that measurement noise pseudorandomizes similar hemoglobin levels on either side of the transfusion threshold.

Results: Among 11,175 included patients, 56,375 hemoglobin measurements met eligibility. Hemoglobin measurements below the transfusion threshold did not differ in characteristics from those above the threshold, except that crossing below the threshold resulted in a 20.9% absolute increase in transfusion rates. Transfusion was associated with a 1.2 g/dL (95% CI 0.9-1.5, p<0.001) increase in hemoglobin level, and a 2.9-point increase (95% CI 0.7-5.0, p=0.009) in sequential organ failure assessment score, compared to no transfusion.

Conclusion: Transfusion was associated with increased organ dysfunction compared to no transfusion at a hemoglobin threshold of 7.0 g/dL, suggesting that evaluation of transfusion targets other than a hemoglobin threshold of 7.0 G/dl are needed.

63 PREVALENCE OF LUNG-RADS S CLASSIFICATIONS IN A NATIONAL COHORT OF US VETERANS SCREENED FOR LUNG CANCER

Caitlin Butler, Eduardo Nunez, Tanner Caverly, Sanqian Zhang, Mark Glickman, Shirley Qian, Jacqueline Boudreau, Donald Miller, Renda Wiener.

Station # 7

Objectives: The American College of Radiology’s Lung-RADS system is intended to standardize reporting of lung cancer screening (LCS) exams, with “S” modifiers used for significant incidental findings. Yet little is known about how “S” modifiers are applied in practice. We compared prevalence of extrapulmonary and intrapulmonary significant incidental findings with and without “S” modifiers in a national cohort of Veterans screened for lung cancer.

Methods: We assembled a retrospective cohort of veterans who underwent LCS in any VA facility from 2015-2019 and had a Lung-RADS categorization in the CT report. We drew a random sample of reports with and without “S” modifiers, matched by radiologist and year. We abstracted data from radiology reports on extrapulmonary and intrapulmonary findings.

Results: Overall, 37,908 veterans had LCS with Lung-RADS coding, and 2183 (5.8%) had a Lung-RADS “S” modifier. Use of Lung-RADS “S” modifiers varied across the 44 facilities where LCS occurred, ranging from 0% to 37% (Figure). On detailed review of radiology reports, we found a high percentage of LCS exams without S modifiers had significant incidental findings described in the report text, both intrapulmonary and extrapulmonary;

intrapulmonary represented a majority of significant incidental findings.

Conclusion: We found a lack of standardization in how “S” modifiers are applied, with most radiology reports describing both intrapulmonary and extrapulmonary significant incidental findings. Radiologists may need additional guidance on which LCS findings, both intrapulmonary and extrapulmonary, should be labeled with an “S” modifier.

74 VARIATION IN USE OF REPURPOSED MEDICATIONS AMONG PATIENTS WITH COVID-19

Michael Garcia, Shelsey Johnson, Nicholas Bosch, Emily Sisson, Christopher Sheldrick, Vishakha Kumar, Karen Boman, Scott Bolesta, Vikas Bansal, Neha Deo, Juan Domecq, Amos Lal, Ognjen Gajic, Rahul Kashyap, Allan Walkey.

Station # 8

Objectives: To describe variation and evolution in use of medications repurposed for management of patients hospitalized with COVID-19.

Methods: Observational cohort study of adults hospitalized with COVID-19 between February 15th 2020 and April 12th 2021 across 76 hospitals using the SCCM VIRUS COVID-19 registry. Repurposed medications were evaluated using multivariable adjusted random effects logistic regression models and unsupervised clustering.

Results: Contribution of hospital site to risk-adjusted variation was 46% for antivirals, 30% for corticosteroids, 48% for hydroxychloroquine, 46% for immunomodulators, and 19% for therapeutic dose anticoagulants. Compared to the early pandemic, the later pandemic period was associated with increased use of antivirals (OR 3.14, 95% CI 2.40,4.10), and corticosteroids (OR 5.43, 95% CI 4.23,6.97), with decreased use of hydroxychloroquine (OR 0.02, 95% CI 0.01,0.04) and immunomodulators (OR 0.49, 95% CI 0.34,0.70). There was no clinically significant change in the use of therapeutic dose anticoagulants (OR 1.01, 95% CI 1.01,1.02). Hospital practice phenotypes decreased from 9 to 2 clusters from early to later pandemic stages.

Conclusion: Hospital variation in use of repurposed medications for management of COVID-19 varied widely across hospitals early in the pandemic, and converged in the later stage with the emergence of randomized clinical trials.

56 HOSPITAL VARIATION IN MANAGEMENT OF ACUTE RESPIRATORY DISTRESS SYNDROME (ARDS) DUE TO CORONAVIRUS DISEASE-2019 (COVID-19) AND ASSOCIATED MORTALITY

Shelsey Johnson, Michael Garcia, Emily Sisson, Christopher Sheldrick, Vishakha Kumar, Karen Boman, Scott Bolesta, Juan Pablo Domecq Garces, Amos Lal, Ognjen Gajic, Rahul Kashyap, Allan Walkey.

Station # 9

Objectives: Adherence to guideline-recommended ventilator management of COVID-19 ARDS is unknown. We sought to evaluate variation in use of ‘guideline-based care’ and associated mortality for COVID-19 ARDS across 55 hospitals contributing to the Society of Critical Care Medicine VIRUS COVID-19 registry.

Methods: We used multivariable adjusted hierarchical random effects logistic regression to assess hospital-level, risk-adjusted use of ‘guideline-based care’ for ARDS, defined as low tidal volume (low Vt), plateau pressure (Pplat)<30 cmH₂O, and prone position for PaO₂:FiO₂<100.

Results: Among 2,021 patients with COVID-19 ARDS, 50% received care consistent with ARDS guidelines. After adjusting for demographic, geographic, time, and severity of illness characteristics, hospital of admission contributed to 20% of the risk-adjusted variation in ‘guideline-based care’; a patient treated at a hospital with high use of recommended therapies had 2.3 times (95% CI 1.3-4.3) the odds of receiving ‘guideline-based care’ as compared to a patient receiving care at a randomly selected hospital with lower use of evidence-based care. Mortality was non-significantly lower at hospitals within the highest-use quartile of ‘guideline-based care’ as compared to the lowest-use (risk-adjusted OR 0.5, 95% CI 0.2-1.1, p=0.06).

Conclusion: Only half of patients with COVID-19 ARDS received evidence-based ventilation strategies, with wide variation across hospitals. Given the significant mortality risk associated with COVID-19 ARDS, there is room for improvement in implementation of guideline-recommended ventilator strategies.

57 UNDERSTANDING VA SPECIALTY AND PRIMARY CARE CLINICIANS' PERSPECTIVES ON E-CONSULT REQUESTS

Ariella Krones, Ekaterina Anderson, Varsha Vimalananda, Sarah Cutrona, Jay Orlander, Judith Strymish, Seppo Rinne.

Station # 10

Objectives: Electronic consultations (e-consults) are an increasingly common aspect of virtual care that can improve quality, efficiency, and timeliness of health care. Prior literature demonstrates that initiating consults with a clear question is crucial for a meaningful answer, but also that specialists are frequently dissatisfied with the quality of the consult request. We sought to address this gap with respect to e-consults by analyzing the perspectives of VA providers on sub-optimal e-consult requests.

Methods: We conducted a qualitative study at the VA New England Healthcare System with 38 specialists and 35 primary care providers (PCPs). The interviews were analyzed using thematic analysis procedures and by applying sociotechnical systems theory to assess the results within the social and technological environments.

Results: Specialists and PCPs agreed that e-consult requests should be focused, precise, not require lengthy chart review, and include results of an adequate preliminary work up. At the same time, specialists felt that many requests were either too basic or too complex. Interviewees attributed the inappropriate e-consult requests to features of the e-consult interface, divergence between the areas of expertise, and ambiguous division of roles between PCPs and specialists.

Conclusion: There is a disconnect between the attributes of optimal e-consult requests and the perceived quality of actual e-consult requests. This difference relates to the issues with the interrelated technology, personnel, and organizational subsystems. Clear opportunities exist to address specific challenges that we noted with these sociotechnical challenges to improve e-consult systems.

22 A CLASSIFICATION AND REGRESSION TREE MODEL FOR RISK STRATIFYING PATIENTS FOR RIGHT HEART CATHETERIZATION IN SYSTEMIC SCLEROSIS

Justin Lui, Ruchika Sangani, Deepa Gopal, Marcin Trojanowski, Andreea Bujor, Michael LaValley, Renda Soylemez Wiener, Elizabeth Klings.

Station # 11

Objectives: Pulmonary hypertension (PH) occurs in 8% to 12% of patients with systemic sclerosis (SSc) and is a leading cause of mortality. An invasive right heart catheterization (RHC) is required for diagnosis often relying on an estimated pulmonary artery systolic pressure on echocardiography. Due to its poor specificity for PH, a greater number of patients than necessary are referred to RHC leading to possible complications. The development of improved prediction models for PH in SSc may inform decision-making for RHC.

Methods: We performed a retrospective analysis of patients with SSc with and without PH. A CART model was developed, incorporating structural findings on echocardiography and conduction abnormalities on electrocardiography. A validation method using a train-test split (2-to-1) assessed the prediction of our classification rule by calculating the sensitivity, specificity, and accuracy of our model. A receiver operating characteristic (ROC) curve was generated from the data.

Results: 213 SSc patients suspected of PH with at least one RHC, electrocardiogram, and echocardiogram were included in the present study; 167 (78%) were diagnosed with PH. Our model had a sensitivity of 31%, specificity of 95%, and accuracy of 80%. From our ROC analysis, the area under the curve was 0.81.

Conclusion: A CART model to identify PH in SSc patients was developed which may aid in risk stratifying patients for RHC. Assimilating data from both echocardiography and electrocardiography, our model had a specificity of 95% compared to 53% to 85% by echocardiography alone. There may be a role for this model in patients with SSc where echocardiography is not congruent with other clinical data.

126 FACTORS ASSOCIATED WITH DECLINING LUNG CANCER SCREENING AFTER SHARED DECISION MAKING IN A NATIONAL COHORT OF VETERANS

Eduardo Nunez, Tanner Caverly, Sanqian Zhang, Mark Glickman, Shirley Qian, Jacqueline Boudreau, Donald Miller, Renda Soylemez Wiener.

Station # 12

Objectives: Our objective was to characterize how often Veterans decline Lung Cancer Screening (LCS) after Shared Decision Making (SDM) discussion and identify patient and facility factors associated with declining LCS.

Methods: This was a retrospective study of Veterans eligible for LCS between 2013-2021. The primary outcome was the presence of a clinical reminder documenting a Veteran as declining LCS. We conducted hierarchical mixed effects logistic regression analyses, with VA facilities and providers as random effects, to determine factors associated with declining LCS.

Results: Overall, there were 30,577 Veterans eligible for LCS of which 20,757 (67.9%) agreed to screen while 9,820 (32.1%) declined screening after undergoing SDM. Veterans were more likely to agree to screen if they were younger, racially Black, ethnically Hispanic, or had more frequent outpatient visits. Veterans were more likely to decline screening if they were older, spent more days in skilled nursing facilities, had a history of congestive heart failure, stroke, schizophrenia or higher Elixhauser Comorbidity Index. Hospitals and providers were responsible for a large amount of the variation in the probability of declining LCS.

Conclusion: Older Veterans with serious comorbidities, who may have competing health demands that make LCS a lower priority, were more likely to decline LCS. Further action is needed to address barriers to LCS uptake and adherence among populations that would benefit from LCS. Additionally, interventions to standardize shared decision making across hospitals and providers would ensure high-quality LCS.

130 VARIATION IN THE INITIAL SEDATION GOAL FOR MECHANICALLY VENTILATED PATIENTS ACROSS UNITED STATES HOSPITALS

Justin Rucci, Nicholas Bosch, Wei Wang, Michael Harhay, Allan Walkey.

Station # 13

Objectives: Sedatives are critical in the care of mechanically ventilated patients, but sedation practices in US ICUs are not well described. We sought to quantify variation in sedation goals and associated outcomes among mechanically ventilated patients.

Methods: We used the eICU database (208 US hospitals, 2014-2015) to identify mechanically ventilated adults with documented RASS goals (scoring system [-5 to +4] to prescribe and monitor sedation level). We recorded initial RASS goals and factors at multiple levels of care that may influence sedation goals. A mixed effects ordinal regression model defined factors associated with initial RASS goal. Intraclass correlation coefficient showed the proportion of variance in RASS goal attributable to the admitting hospital. We used multivariable linear regression to assess the association between hospital-level RASS goals and duration of mechanical ventilation.

Results: 1,504 patients in 19 hospitals were included. Median age was 65 (IQR 54, 74); median SOFA 5 (IQR 3, 7). Hospital median initial RASS goals ranged from -3 (movement to voice, no eye opening) to 0 (alert, calm). In a mixed effects ordinal regression model, admission to MICU (vs mixed MICU/SICU) had the greatest effect on RASS goal (β -adjusted 1.6 [95% CI 1.1, 2.1]). The hospital of admission accounted for 11% of variation in risk-adjusted RASS goals. Multivariable linear regression showed hospitals with lower median RASS goals (deeper sedation) had longer durations of mechanical ventilation (β -adjusted in hours = -8.8 [95% CI -9.8, -7.7]).

Conclusion: Initial RASS goals vary across US hospitals. Hospitals that target deeper sedation levels have longer duration of mechanical ventilation.

36 THE IMPACT OF INTERSTITIAL LUNG DISEASE SEVERITY ON CLINICAL OUTCOMES IN SYSTEMIC SCLEROSIS-RELATED PULMONARY HYPERTENSION

Ruchika Sangani, Justin Lui, Kari Gillmeyer, Marcin Trojanowski, Andreea Bujor, Michael LaValley, Elizabeth Klings.

Station # 14

Objectives: While prognosis in patients with systemic sclerosis-related pulmonary hypertension (SSc-PH) is worsened by the presence of concomitant interstitial lung disease (ILD), little is known of how ILD severity affects outcomes in those with SSc-PH. We aimed to delineate clinical features of patients with SSc-PH and ILD and determine the association between ILD severity and mortality. We hypothesized that increasing ILD severity in patients with SSc-PH is associated with increased risk for all-cause mortality.

Methods: We conducted a retrospective study of patients with SSc-PH in which the presence of ILD was determined by computed tomography. ILD severity was classified by pulmonary function testing. Our primary outcome was survival from time of PH diagnosis. We calculated adjusted risks of time to mortality using Cox proportional hazards models.

Results: Of 161 patients with SSc-PH, 115 (71.4%) had concomitant ILD. Patients with severe ILD had less severe PH disease by cardiopulmonary hemodynamics compared to those with absent/mild ILD (mean pulmonary artery pressure 30.3 mmHg vs. 35.2 mmHg). However, 1-, 3-, and 5-year survival for patients with severe ILD were 88.9%, 22.2%, and 11.1%, respectively, compared to 86.0%, 79.7%, and 72.8% among those with absent/mild ILD. Patients with severe ILD had increased hazard for all-cause mortality (HR: 5.53; 95% CI: 2.29, 13.38) compared to those with absent/mild ILD.

Conclusion: Severe ILD confers a worse prognosis in patients with SSc-PH despite having less severe PH hemodynamically. These findings suggest the need for focusing therapies towards slowing ILD progression in patients with SSc-PH.

EVANS DEPARTMENT OF MEDICINE RESEARCH DAYS

INDEX OF ABSTRACTS

Abdulkerim, H.	155	Billatos, E.	66, 86
Acín-Pérez, R.	140	Binda, D. D.	49
Adeoye, B.	55	Blevins, F.	09
Adler, A.	182	Bloch, K.	62
Ahmed, H.	120	Blokhina, E.	24, 108, 190, 191
Alani, R.	58	Blot, T.	125
Alber, A. B.	69, 117	Blum, B.	140
Ali, F.	106	Bojovic, B.	41
Alreshq, R.	92, 96, 125	Bolesta, S.	56, 74
Altajar, S.	50	Bolton, R. E.	194
Alysandratos, K.	140	Boman, K.	56, 74
Anderson, E.	57	Bosch, N. A.	29, 74, 130
Anderson, K.	86	Bosmann, M.	12, 138
Andersson, C.	95	Boudreau, J.	63, 126
Arafa, E. I.	72	Buchholz, C.	104
Arokiadoss, A.	155	Buck, A.	185
Assoumou, S. A.	08	Buck, A. K.	154
Asundi, A.	98, 110	Budbazar, E.	114, 196
Au, R.	20, 119	Bujor, A.	36, 80
Avagyan, S.	19	Bujor, A. M.	22
Awtry, E. H.	18	Bukhman, G.	182
Ayyar, K. K.	142	Burgess, C.	39
Baird, L.	67, 124	Burks, E.	23, 44, 82, 88, 97, 127
Bais, M.	106	Burns, L. E.	165
Balachandra, A. R.	119	Butler, C.	63
Balady, G. J.	15	Cabral, H.	120, 144
Balazs, A.	109	Calixte, D.	182
Balazs, A. B.	99	Camassola Breda, J.	44
Bansal, V.	74	Campbell, J.	66, 88
Barker, K.	178	Campbell, J. D.	12, 17, 99, 132, 139
Barker, K. A.	72, 76	Capellini, T.	118
Barve, S.	184	Caporarello, N.	81, 156
Basow, E.	182	Carty, S.	61, 112, 172
Basukala, B.	168	Caruso, L. B.	18
Bazzi, A. R.	104	Casey, A.	171
Bean, D.	83	Caverly, T.	63, 126
Beane, J.	23, 44, 82, 86, 88, 103, 127, 145	Cervantes-Arslanian, A. M.	18
Beane, J. E.	97, 132	Chakraborty, A.	143
Becker, W.	91	Chambers, J. M.	90
Beeram, I.	93	Chan, W.	176
Beermann, M.	146	Chang, C.-C.H.	91
Beers, M.	140	Chang, G.	118
Belghasem, M.	54	Chatterjee, S.	71
Belkina, A.	109, 173, 178	Chaudhary, N.	12
Belkina, A. C.	72, 76, 99	Chen, F.	76
Bendiks, S.	190	Chen, G.	78, 166
Bendiks, S.	24, 191	Chen, J. G.	164
Benjamin, E.	176	Cheng, D.	21, 24, 191
Benson, G.	75	Cheng, F.	73, 189
Beral, A.	89, 146	Chevalier, A.	94
Berk, J. L.	96	Chin, S.	119
Bernstein, J. A.	08	Chitalia, V.	40, 46, 193
Bhatia, J. S.	18	Chitalia, V. C.	32, 35, 54
		Chiu, D. J.	88

Chiu, L.	188	Fan, X.	68
Chiuzan, C.	125	Farber, A.	193
Cho, M.	79	Farrer, L.	170
Chong, B. S.	162	Federico, A.	75, 122
Chung, E.	120	Felson, D.	118, 174
Claudel, S. E.	113	Fenelon, D.	182
Clay, A.	18	Ferran, B.	162
Clayton, S.	75	Ferri, G.	131
Cole, F.	140	Ferri, G. M.	14
Colucci, W.	90	Fetterman, J. L.	137
Connolly, J. J.	120	Fikre, T.	152, 198
Connor, K. K.	35	Fillmore, N.	131
Coote, C.	98	Fine, A.	16, 61, 112, 172
Cozzolino, M.	96	Fine, D.	125
Crossey, E.	16, 61, 112, 172	Fischman Han, A.	198
Croteau, D.	90	Fleming, M.	66
Crystal, S.	91	Flores, E.	151
Custodio, M.	37	Freeman, R.	19
Cutrona, S. L.	57	Freiberg, M.	91, 184, 190, 191
Dabek, R. J.	41	Frustino, J.	25
Daley, K.	193	Fuzaylov, G.	41
Dambal, V. Y.	143	Gajic, O.	56, 74
Darlington, A.	92	Ganghuly, S.	193
David, A. R.	08	Garcia, M. A.	56, 74
DeMoss, B.	92	Garcia-Beltran, W.	99
Denis, G.	160, 171, 173	Geyer, K. L.	17
Deo, N.	74	Ghai, S.	113
DePamphilis, M. A.	41	Gillmeyer, K.	36
Dey-Guha, I.	132	Gilman, J. P.	15
Dobrilovic, N.	13	Gindra, R.	127
Dodge, M. E.	85	Gislason, G. H.	95
Domecq, J. P.	74	Glickman, M.	63, 126
Domecq Garces, J.	56	Gnatienco, N.	24, 190, 191
Dowrey, T.	99	Gojanovich, A. D.	135
Dowrey, T. W.	101	Goltry, W.	139, 178
Drainoni, M.-L.	182	Goltry, W. N.	72, 76
Dries, R.	78, 99, 164, 166	Goodman, J.	40, 196
Driscoll, D. N.	41	Goodman, J. B.	183
Dudek, M.	138	Gopal, D. M.	22, 96
Duffy, E.	88	Gordon, K.	91
Duncan, M.	91	Gouon Evans, V.	59
Dupuis, J.	176	Gouon-Evans, V.	47, 52, 162
Ebbert, J.	58	Graham, M.	87
Edelman, J.	91, 91	Green, E.	97, 127
Eden, S.	91	Greer, D.	18
Edwards, C.	131	Greer, D. M.	176
Edwards, N. M.	13	Guan, J.	81, 156
El Adili, F.	80	Guardino, E.	96
Elsadawi, M.	46	Guerrero López, I.	150
El Zinad, N.	46	Gur, B.	58
Elzinad, N.	32, 35, 40, 54	Guttentag, S.	140
Emili, A.	140	Hagedorn, E.	19, 169
Enkhbayar, K.	19, 169	Hall, S.	11
Ennis, C.	78, 173	Hamburg, N.	133
Eshkind, L.	138	Hamburg, N. M.	137
Etesami, N. S.	72, 178	Hamer, D.	11
Everton, E.	52, 59	Hamilton, D.	77
Fan, H. J.	105	Hamvas, A.	140

Han, J.	121, 162, 189, 196	Jiang, W.	21, 98, 190
Hansen, U.	35	Jiang, Z. Y.	93
Haratianfar, M.	141	Johnson, E.	177
Harhay, M. O.	130	Johnson, R.	180
Harper, K.	155	Johnson, S. W.	56, 74
Harris, D.	135	Johnson, W. E.	105
Hassan, H.	131	Jones, D.	156
Hassan Kamel, M.	113	Jones, D. L.	81
Hawkins, F.	146	Jones, M.	67, 112, 124
Hayes, K.	30	Jones, M. R.	16, 61, 72, 76, 139, 172
Heaphy, C.	87	Karagiannis, T.	101
Heinze, D.	141	Karjadi, C.	20
Heinze, D. M.	148	Karlson, K. J.	13
Hekman, R.	140	Kaserman, J. E.	85, 157
Helmke, S.	125	Kashyap, R.	56, 74
Henao Vasquez, J.	16, 61	Keane, T.	155
Henao-Vasquez, J.	172	Kelley, E.	78, 164
Henault, E.	19, 169	Kenison-White, J.	107
Herman, H.	26	Kerns, R.	91
Herriges, M.	45	Khan, M.	25
Herriges, M. J.	70	Kim, C.	32, 40, 46, 54
Higgins, M. I.	85	Kim, Y.	124
Hinds, A.	172	Kirber, M.	40, 183
Hingorani, K. S.	18	Kiyanda, A.	21
Hirsch, A. E.	152	Klings, E.	36
Hirschhorn, L.	182	Klings, E. S.	22
Hix, O.	140	Ko, N.	123, 160, 185, 198
Hochberg, N.	11	Ko, N. Y.	152, 154
Hollenberg, A. N.	117	Køber, L.	95
Horta, L. F.	18	Koga, Y.	66
Hu, F. B.	144	Kolachalama, V.	54, 118, 119
Hu, J.	170	Kolachalama, V. B.	20, 127
Hu, T.	139	Kolla, M.	160, 171, 173
Huang, D.	77	Kook, S.	140
Huang, J.	60	Korkmaz, F.	67, 124
Huang, K.	188	Korkmaz, F. T.	76, 139
Huang, S. K.	81	Kotton, D.	39, 45, 60, 70, 79, 140, 146
Huangfu, Y.	114	Kotton, D. N.	43, 69, 117
Huggins, J.	17	Kramnik, I.	71
Hughes, D.	09	Krishnamoorthy, A.	92
Hulme, M.	58, 100	Kristensen, S.	95
Husted, C.	145	Kroehling, L.	75
Hutchison, A.	58	Krones, A.	57
Ibrahim, M.	18, 182	Krupitsky, E.	24, 190
Idrees, N.	193	Kukuruzinska, M.	25
Ieong, M. H.	18	Kulke, M.	175
Ikonomou, L.	69	Kulke, M. H.	18
Ilinski, A.	123, 175, 177	Kumar, S.	68, 99, 102
Isaac, B.	182	Kumar, V.	56
Jadeja, Y.	158	Kumar, V. K.	74
Jadick, M.	119	Kundu, S.	91
Jafari, N.	160, 171, 173	Kuo, B.	150
James, T.	18	Kurmann, A.	117
Janes, S. M.	132	Kwan, G.	182
Jawa, R.	104	Lachut, K.	164
Jayaraman, A.	12	Lai, J.	118
Jean, J.	140, 146	Lal, A.	56, 74
Jhun, R.	118		

Lam, E.	99	Marti, C. N.	92
Lara, B.	107	Martin, I. M.	72, 76, 139
Laudon, A. D.	102	Marx, B.	155
LaValley, M.	36	Matson, E. M.	136
LaValley, M. P.	22	Matsui, R.	162
Le, J.	32, 54	Matsuura, S.	153
Le, N.	118, 135	Matte, T.	99, 146
LeClair, J.	18	Matthan, N. R.	174
Lee, J.	81, 156	Maurer, M.	125
Lee, N.	177	Mazzeo, C.	160, 197
Lee, N. J.	85	Mazzilli, S.	23, 88, 127, 145
Lenburg, M.	66, 82, 86, 103	Mazzilli, S. A.	44, 97, 132
Lenburg, M. E.	44, 132	McCracken, A.	141, 148
Leshchik, A.	167	McLaughlin, A.	190
Le Suer, J. A.	115	Meeker, A.	87
LeSuer, J.	146	Melley, C.	164
Lewis, C. E.	174	Menino, E.	85
Li, D.	123, 159, 175, 177	Mensah, S.	21, 184
Li, M.	99	Mensah, S. O.	191
Li, Y.	144	Mercer, R.	135
Lichtenstein, A. H.	174	Merenstein, C.	44
Liesa, M.	140	Meridew, J.	81, 156
Ligresti, G.	81, 156	Meshulam, T.	171
Lilleness, B.	96	Miller, D.	63, 126
Lim, R.	18	Milo Rasouly, H.	68
Lim, Y.	158	Milrod, C. J.	09
Lin, N.	98, 110, 190	Minakin, K.	140
Linas, B. P.	08	Minetti, E.	162
Lindstrom-Vautrin, J.	45, 52, 69, 99, 109, 141, 146, 146, 157	Misra, D.	174
Lioznov, D.	24, 190, 191	Mithal, A.	30, 141, 148
Liu, G.	82, 86	Mizgerd, J.	67, 124, 178
Liu, H.	47, 114	Mizgerd, J. P.	12, 16, 61, 72, 76, 138, 139
Llevenes, P.	160, 173	Modanlo, N.	123, 175, 177
Lo, D.	35	Mohanty, A.	120
Lodi, S.	24, 190	Monroe, J.	83
Long, M.	50, 179	Monti, S.	25, 75, 101
Lotfollahzadeh, S.	32, 35, 40, 54	Moore, L. L.	129, 144
Lotfollahzadeh, S.	46	Moreau, Y.	55
Lowe, R. C.	18	Mori, T.	189
Lowery, L.	58, 100	Morone, N. E.	49
Lu, W.	68, 102	Morris, M.	66
Lui, J.	36	Moses, J. M.	18
Lui, J. K.	22	Moss, A.	37, 197
Lunze, K.	24, 108	Moss, A. C.	142
Luptak, I.	90	Mostoslavsky, G.	30, 99, 135, 141, 148, 151
Lyo, H.	37	Mueller, D.	64
Lyon De Ana, C.	72, 76, 178	Mühlberger, E.	151
Ma, L.	45, 69	Mulugeta, S.	140
Madelaire, C.	95	Munawar, A.	40
Maglione, P.	30	Munshi, N.	131
Maglione, P. J.	136	Murabito, J.	50
Mahdavian, K.	123, 160, 175, 177	Muralidhar, V.	96
Mahoney, T. F.	18	Murphy, G.	109, 141
Majid, S.	137	Murphy, G. J.	99, 101
Mangio, J. C.	193	Murphy, J.	18
Marden, G.	143, 156	Murray, L.	166
Marquez, H. A.	69		

Myrick, S.	163	Qin, F.	90
Na, E.	67, 124	Qiu, S.	119
Nadjarian, A.	18	Qiu, Y.	160, 171
Najem, M.	80	Quinton, L.	67, 124
Napoleon, M.	40	Quinton, L. J.	61, 72, 76, 139
Nelson, E.	87	Qureshi, M. M.	152
Nevitt, M.	174	Rabasa, G.	174
Nguyen, B.-C.	25	Ragoonanan, D.	19, 169
Nijhawan, D.	119	Rahimi, N.	32
Ning, B.	103	Rahman, R.	188
Nozari, A.	18	Raj, A.	24
Nunez, E.	63	Rateau, L.	24
Nunez, E. R.	126	Ravid, K.	153
Odom, A. R.	84	Reed, E.	75
Odom, C.	67, 124	Reid, M. C.	44
Odom, C. V.	76	Reid, M. E.	132
Olayinka, O.	75, 170	Reifler, K. A.	11
Olson, A.	55, 98	Rennke, H. G.	163
O'Neill, N.	170	Rice, B. A.	179
Ong, C. J.	176	Rigor, M.	93
Ontiveros, V. C.	187	Rinne, S.	57
Onul, I.	163	Rizvi, F.	52, 59
Orlander, J. D.	57	Rizvi, S.	133
Orrick, J.	32, 40, 46, 54	Rock, J.	43
Orrick, J. A.	35	Rodriguez, C.	125
Palani, A. A.	152	Rodriguez, L.	140
Palatkin, V.	191	Romano, M. F.	119
Palmer, J.	105	Romero, R.	133
Palsson, R.	163	Rosen, G.	100
Panchmatia, A.	143	Rosenthaler, M.	26
Parekh, A.	123	Rosenthaler, M. P.	50
Park, L.	118	Ross, C.	160
Park, S.	141	Rossi, S.	24, 108
Parsons, D.	99	Ruberg, F. L.	92, 96, 125
Paschalidis, I. C.	20	Rucci, J.	130
Patel, A. D.	18	Russo, S.	140
Patel, S.	98	Sabogal, N.	125
Patil, P.	163	Sadeq, F.	41
Patts, G.	21, 184, 190, 191	Saeed, D.	77
Perls, T.	101	Sagar, D.	77
Petcherski, A.	140	Sagar, M.	55, 83, 98
Petrick, J. L.	105	Salant, D.	68
Pfefferkorn, R.	23, 145	Samet, J.	184, 190
Pfefferkorn, R. M.	97	Samet, J. H.	08, 21, 24, 191
Pham, T.	156	Sanchorawala, V.	96
Pham, T. X.	81	Sangani, R. A.	22, 36
Pichardo, T. K.	145	Satyam, V.	26
Pickering, R.	110	Scalera, J.	118
Pierce, C.	95	Schaus, S.	35
Pihl, R.	42	Schiffer, L.	177
Pimentel, D.	90	Schingo, V. A.	148
Pipilas, A.	96	Schmidt, I. M.	163
Pompa, I.	160	Schou, M.	95
Ponce de Leon, S.	196	Schroy, P.	188
Posabella, A.	117	Schwartz, B.	95
Prescott, B.	176	Sebastiani, P.	101
Promchotichai, N.	118	Seidel, K.	121, 189
Qian, S.	63, 126	Semler, J.	150

Senegal, C.	16	Teruya, S.	125
Seo, H.	118	Thapa, B.	45
Serafin, H.	113	Thapa, B. R.	43
Sereda, Y.	24	Tharani, Y.	143
Seta, F.	114, 162, 183, 196	Theodore, A. C.	18
Shafraan, J.	171	Thompson, M.	88
Shah, R.	142	Tilston-Lunel, A.	140
Shao, F.	16, 61, 172	Tilton, B. R.	72
Shao, F.-Z.	076	Tindle, H.	190, 191
Sharma, R.	68	Torner, J.	174
Shaw, N.	42	Torp-Pedersen, C.	95
Shea, C. V.	132	Toussaint, E.	182
Sheldrick, C. R.	56, 74	Toussova, O.	108, 108
Shenoy, A.	178	Traber, K.	42, 67, 124
Shenoy, A. T.	72, 76, 139	Traber, K. E.	61, 139
Sherr, D.	107	Trojanowska, M.	80, 143, 156
Shi, L.	100	Trojanowski, M.	36
Shirihai, O.	140	Trojanowski, M. A.	22
Sian, C. R.	08	Truong, V.	24
Siddiqi, O. K.	96	Tschumperlin, D.	81, 156
Sigman, S. R.	92	Tsukahara, Y.	162, 196
Silver, B.	18	Undeutsch, H. J.	117
Simkin, I.	170	Urbach, H.	154, 185
Simon-Plumb, C.	175	Valente, C.	113, 125
Simon-Plumb, C. L.	177	Valisno, J.	183
Singer, M. S.	129	Vanuytsel, K.	99, 109
Singhal, R.	184	Varelas, X.	25, 39, 67, 140
Sisson, E.	74	Vargas, L.	183
Sisson, E. K.	56	Vbranac, V.	99
Sitter, K. E.	194	Vedaie, M.	140
Sloan, J.	09	Velu, P.	198
Smimakis, S. M.	176	Venkatraman, D.	127
Smith, A. R.	47	Verma, K.	64, 131
Snyder, M.	107	Vetrova, M.	108
So-Armah, K.	21, 91, 184, 190, 191	Villa, A.	25
Soden, K.	110	Villacorta Martin, C.	101, 146
Soucy, A. M.	139	Villacorta-Martin, C.	39, 45, 52, 60, 69, 70, 99, 109, 140, 141, 157
Soylemez Wiener, R.	22, 126	Vimalananda, V. G.	57, 194
Spira, A.	82, 132	Vrbanac, V.	109
Spira, A. E.	44	Vyas, N.	108
Srivastava, A.	163	Wagaman, J.	169
Staron, A.	64	Waikar, S. S.	163
Stein, T.	170	Walachowski, S.	138
Steiner, D.	82	Walkey, A. J.	56, 74, 130
Stevenson, C.	44	Wambach, J.	140
Stillman, I. E.	163	Wan, X.	121, 189
Stojanova, M.	87	Wang, A.	104
Strymish, J. L.	57	Wang, F.	157
Sulser Ponce de Leon, S.	114	Wang, H.	19, 169
Sung, M.	91	Wang, N.	15, 50
Surendran, T.	118	Wang, R. S.	18
Surjanhata, B. C.	150	Wang, W.	130
Syracuse, J.	193	Wang, Y.	13, 93, 134, 196
Tabor, S.	183	Wang, Z.	99, 107
Taddeo, E.	140	Wasan, S.	26
Tan, Q.	81	Washington-Plasket, T.	15
Tandon, S.	184, 191	Watanabe, S.	197
Tansi, V.	138		

Weber, C.	155
Wei, Y.	78, 164
Weinberg, J. M.	49
Weinstein, E.	18
Weisbrod, R.	133
Weisbrod, R. M.	137
Werder, R. B.	79
Whelan, S.	177
White, L.	98
Wiener, R.	63
Wilson, A.	79, 157
Wilson, A. A.	85
Wilson, S. A.	18
Winburn, M.	125
Wong, D. H.	194
Woo, S.-B.	25
Xi, Z.	23
Xu, X.	188
Xue, C.	20
Yabaji, S. M.	71
Yajima, M.	17
Yamashita, T.	156
Yang, C.	100
Yang, K.	107
Yang, X.	153
Yeung, A.	109
Yiannakou, I.	129
Yildirim, C.	131
Yin, K.	13
Yin, W.	32, 54, 193
Yoon, G.	118
Young, L.	140
Ysasi, A.	172
Yuan, J.	16, 61, 172
Yuan, M.	129, 144
Zang, M.	121
Zeng, M.	172
Zertuche, J.-P.	174
Zhang, H.	158
Zhang, J.	82
Zhang, M.	32, 35, 46, 54, 121
Zhang, S.	63, 126
Zhang, T.	64, 123
Zhang, W.	40
Zhang, X.	170
Zhang, Y.	54
Zhao, G.	85
Zhao, M.	108
Zhao, R.	164
Zheng, A.	77
Zhou, Q.	93
Zhou, X.	79, 119
Zhou, Y.	121, 189
Zimmerman, D.	85
Zombeck, S.	15